Spinal Cord Stimulation in Mononeuropathic Pain

From Clinical Outcomes to Exploratory Somatosensory Analysis: A Pilot Study

TM30004: Master Thesis Project

A.W. (Anne) Veenhuizen

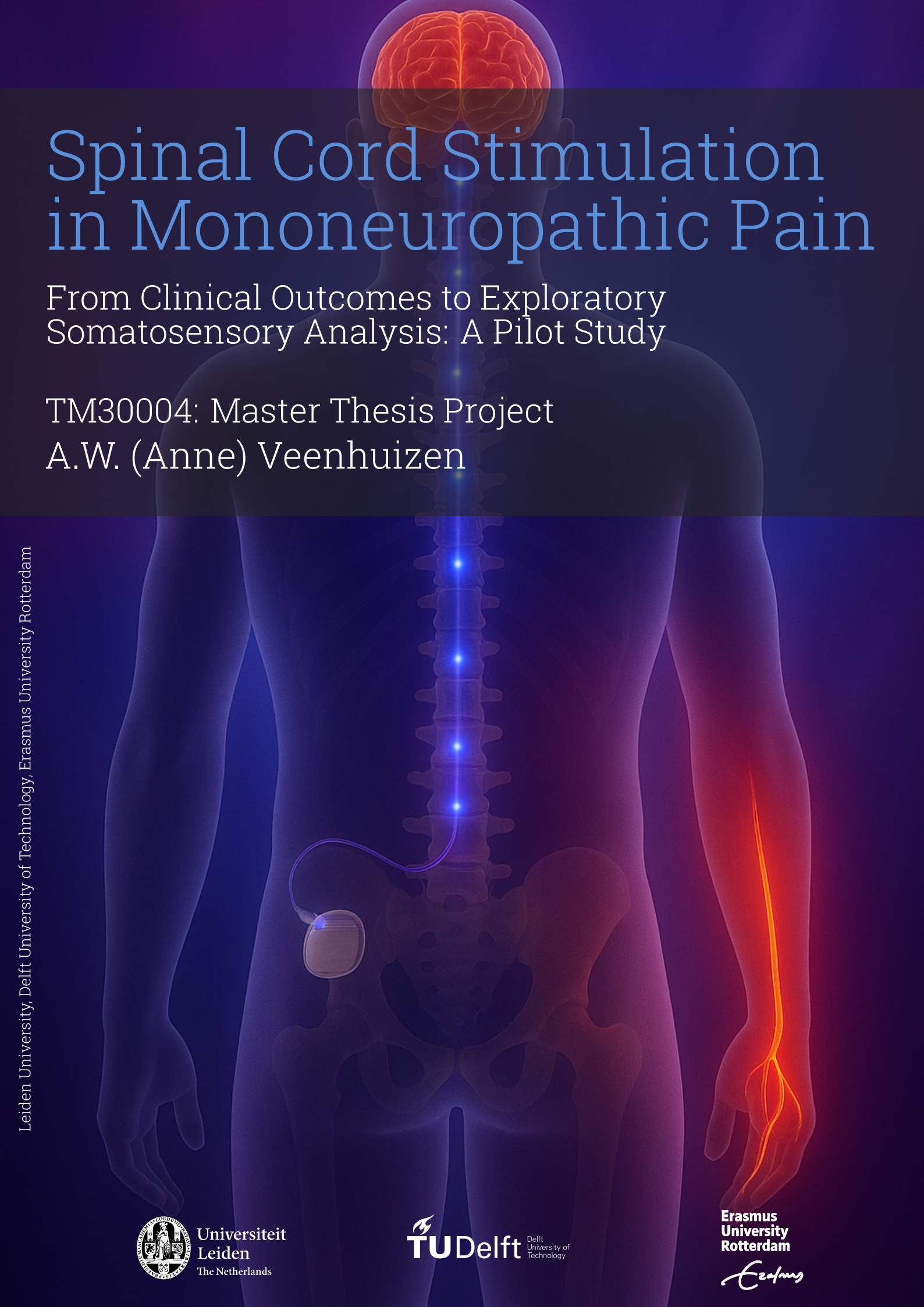

Leiden University, Delft University of Technology, Erasmus University Rotterdam

Universiteit Leiden
The Netherlands

TU Delft
Delft University of Technology

Erasmus University Rotterdam

SCIMONO: Spinal Cord stimulation for Intractable MONOneuropathy

A pilot study

A.W. Veenhuizen

Student number: 5022924

April 24, 2026

Thesis in partial fulfilment of the requirements for the joint degree of

Master of Science in Technical Medicine

Leiden University; Delft University of Technology; Erasmus University Rotterdam

Master thesis project (TM30004; 35 ECTS)
Dept. of Biomechanical Engineering, TU Delft
September 01, 2025 – April 24, 2026

Supervisor(s):
Dr. Ir. C.C. (Cecile) de Vos
Prof. Dr. F.J.P.M. (Frank) Huygen

Thesis committee members:
Dr. ir. Cecile de Vos, Erasmus MC (chair)
Prof. Dr. Frank Huygen, Erasmus MC
Dr. Monique van Velzen, LUMC

An electronic version of this thesis is available at
`http://repository.tudelft.nl/`

Universiteit Leiden

TU Delft

Erasmus University Rotterdam

Preface

When Cecile asked me nearly a year ago whether I wanted to take on this project, despite not being the strongest when it comes to making decisions, I did not have to think long. Neurostimulation had already captivated me during the first lecture, and even more so during my internship at the Centre for Pain department in my second master's year. The opportunity to carry out this research independently, and the sense that your work genuinely matters, made the choice easier. That last conviction only grew stronger when I got to know the people who participated in the study. They had been struggling with severe pain for years following trauma or surgery and had already tried countless other treatments. Their willingness to participate in a pilot study, with all the uncertainty that entails, left a lasting impression on me. And what perhaps stays with me most: even when stimulation yielded less than hoped, they kept looking for the positive.

Of course, there were also moments when things did not go as planned. Logistical hurdles, results that fell short of expectations, or a phone call to a patient asking them to come in one more time. The feeling of being in the middle of a puzzle with the box nowhere to be found is familiar to most researchers. Fortunately, there was usually someone, a supervisor or a NA-17 member, who came up with a good idea at just the right moment and made the picture a little clearer. One of the things I take away from this past three quarters of a year is that not every day has to feel productive; the reading, the thinking, the doubt, it all feeds into the work, even when it does not feel that way at the time.

I leave here with the sense that I have learned an enormous amount, while at the same time still aware of how much I do not yet know. I had perhaps underestimated the literature review: after working through a large body of articles, I came away feeling like I knew less than before rather than more. But reading those same articles now, I notice how much more easily I follow them and how they are slowly falling into place. What continues to fascinate me most is the question of how spinal cord stimulation actually works. So many different mechanisms have been described and every theory remains at least partly a hypothesis. Why does the pain largely disappear in one patient while another barely notices a difference? No one has a definitive answer yet, and I remain curious. Hopefully future research will bring more clarity.

Through all of it, the people around me made it both better and more enjoyable.

Thanks to Cecile for her day-to-day supervision, all the feedback, and the countless moments of clarity when I needed them most, and to Frank for his oversight and involvement throughout the project. Both always made me feel that their goal was not just to guide the research, but to genuinely teach me something and broaden my thinking along the way. Thanks also to the researchers and pain consultants on the department: for listening, for the discussions, and for the good company. Dorine, thank you for your help with the sensory testing. Daan and Jan, thank you for arranging the blood samples and EMGs. Gosse-Jacob, thank you for your involvement and the valuable conversations about the research. And Mathilde, thank you for the foundation you laid.

Finally, to my housemates, friends, and my parents: thank you for the distraction, the conversations, and the good times. It would have been a lot less enjoyable without you.

A.W. (Anne) Veenhuizen
Delft, April 2026

Summary

Peripheral mononeuropathy is a focal form of neuropathic pain in which a single nerve is affected, typically following trauma or surgery. Despite the availability of pharmacological and non-pharmacological treatments, less than 50% of patients with neuropathic pain achieve satisfactory relief with first-line treatment, and approximately 15–30% of patients with common mononeuropathies develop persistent symptoms for which therapeutic options are limited. Spinal cord stimulation (SCS) has demonstrated sustained analgesic efficacy in painful diabetic polyneuropathy and complex regional pain syndrome, but prospective evidence in refractory peripheral mononeuropathic pain was previously lacking.

This thesis presents the SCIMONO pilot study (NCT06546371), a prospective single-center exploratory study at Erasmus Medical Centre evaluating the clinical effects of SCS in patients with refractory peripheral mononeuropathic pain. Complementary exploratory analyses characterize multivariate somatosensory profiles at baseline and assess longitudinal changes following SCS, alongside descriptive assessment of endogenous pain modulation before and after treatment. 12 adults with electromyography (EMG)-confirmed peripheral mononeuropathy refractory to at least six months of conventional medical management were enrolled. After a two-week trial phase, patients achieving ≥30% pain reduction proceeded to permanent implantation. A three-month comparison phase evaluated four stimulation paradigms (tonic, fast, burst (delivered as microburst), and contour) in counterbalanced order, followed by a three-month preference phase. The primary outcome was change in pain intensity (NRS) from baseline to six months. Secondary outcomes included health-related quality of life (EQ-5D), emotional functioning (HADS), and pain-related functional interference (BPI). Quantitative sensory testing (QST) and conditioned pain modulation (CPM) were assessed at baseline and six-month follow-up to characterize the multivariate somatosensory profile of the cohort and to explore whether these dimensions change following SCS, thereby generating mechanistic hypotheses alongside the clinical outcome evaluation.

Of the 12 enrolled patients, 10 completed six-month follow-up and were included in the final analysis. One patient had not yet reached six-month follow-up at the time of analysis, and one patient withdrew during follow-up due to headache. Median NRS decreased significantly from 7.0 (IQR 6.1–7.4) at baseline to 3.8 (IQR 2.4–5.0) at six months, with a median within-patient reduction of −3.3 points ($p = 0.01$), exceeding the minimal clinically important difference of 2 points. Eight patients (80%) achieved ≥30%, of whom five achieved ≥50% pain reduction. EQ-5D and BPI scores improved significantly and exceeded their respective minimal clinically important differences. HADS scores did not change significantly. Differences between the four stimulation paradigms were not statistically significant and paradigm preferences varied across patients. No serious adverse events occurred.

Exploratory somatosensory analysis of baseline QST scores in this cohort revealed heterogeneous sensory profiles, varying continuously along dimensions of sensory loss and mechanical sensitization. The single non-responder showed marked vibration detection loss at baseline, indicative of impaired large-fiber afferent integrity. This was accompanied by virtually no reduction in somatosensory asymmetry and a qualitatively distinct pattern of somatosensory change following SCS, generating the hypothesis that large-fiber afferent integrity may be a relevant determinant of SCS efficacy. At the group level among participants with complete six-month follow-up data (n=10), no individual QST parameter changed significantly after Holm correction. Baseline CPM was heterogeneous with no consistent association with treatment response. A preliminary increase in inhibitory PPT-based CPM responses at six-month follow-up compared to baseline suggests that SCS may engage descending inhibitory pathways in the central nervous system, though this observation remains hypothesis-generating.

These findings provide the first prospective evidence supporting the feasibility of SCS in refractory peripheral mononeuropathic pain and inform the design of a future sham-controlled randomized trial. The exploratory somatosensory analyses suggest that pre-implantation multivariate QST profiling may carry predictive value for SCS response beyond current selection criteria, warranting prospective investigation in adequately powered studies.

Contents

Abbreviations

Abbreviation	Definition
BPI	Brief Pain Inventory
CDT	Cold Detection Threshold
CI	Confidence Interval
CPM	Conditioned Pain Modulation
CPT	Cold Pain Threshold
DFNS	German Research Network on Neuropathic Pain
EMG	Electromyography
EPT	Electrical Pain Threshold
EPTT	Electrical Pain Tolerance Threshold
EQ-5D	EuroQol 5-Dimension questionnaire
FAST	Fast-Acting Sub-perception Therapy
HADS	Hospital Anxiety and Depression Scale
HPT	Heat Pain Threshold
IASP	International Association for the Study of Pain
IQR	Interquartile Range
MDT	Mechanical Detection Threshold
MPS	Mechanical Pain Sensitivity
MPT	Mechanical Pain Threshold
NeuPSIG	Neuropathic Pain Special Interest Group
NRS	Numeric Rating Scale
PCA	Principal Component Analysis
PPT	Pressure Pain Threshold
QoL	Quality of Life
QST	Quantitative Sensory Testing
RCT	Randomized Controlled Trial
SCS	Spinal Cord Stimulation
TSL	Thermal Sensory Limen
VDT	Vibration Detection Threshold
WDT	Warm Detection Threshold
WUR	Wind-Up Ratio
Time points	
T0	Baseline assessment
T1A, T1B	Trial phase (week 1 and week 2)
T2A-T2D	Comparison phase (blocks 1-4, 3 weeks each)
T3	Six-month follow-up

1

Thesis Introduction

1.1. Background and Scientific Context

Neuropathic pain, defined as pain caused by a lesion or disease of the somatosensory system [1], remains difficult to treat despite advances in pharmacological and interventional pain management. Fewer than 50% of patients achieve satisfactory long-term relief with first-line treatments [2], and a substantial proportion develops persistent symptoms that significantly impair quality of life (QoL) and daily functioning [3].

Peripheral mononeuropathy represents a focal form of peripheral neuropathic pain in which a single nerve is affected. Although anatomically localized, refractory peripheral mononeuropathic pain can lead to severe and persistent pain that remains insufficiently controlled despite optimized conservative and surgical treatment. For this subgroup of patients, therapeutic options are limited.

Spinal cord stimulation (SCS) has demonstrated clinically meaningful and sustained analgesic effects in several chronic neuropathic pain conditions, including painful diabetic polyneuropathy and complex regional pain syndrome [4, 5]. SCS is thought to exert its analgesic effects primarily through activation of large myelinated Aβ-fibers in the dorsal column, which activate inhibitory interneurons in the dorsal horn and thereby attenuate nociceptive transmission via the lateral spinothalamic tract (Figure 1.1) [6–8]. However, evidence supporting SCS in refractory mononeuropathy is scarce and largely limited to small observational studies [9, 10]. Prospective data are lacking to inform effect size estimation, inter-individual variability, and the design of future randomized controlled trials in this specific population.

Beyond establishing clinical efficacy, a key challenge in SCS and in neuropathic pain treatment more broadly is that patients with the same diagnosis may have fundamentally different underlying pain mechanisms, including peripheral nociceptive signaling, central sensitization, or impaired endogenous pain inhibition. Standard electrophysiological assessment such as electromyography captures large-fiber nerve conduction but does not evaluate small-fiber function or central pain processing. Quantitative sensory testing (QST) and conditioned pain modulation (CPM) address this gap by characterizing the somatosensory phenotype across multiple afferent fiber populations and assessing the functional state of descending inhibitory pathways, respectively [11, 12]. Phenotype-based patient stratification may reduce the current reliance on trial-and-error treatment selection and improve the proportion of patients achieving meaningful benefit [13, 14]. In the present thesis, QST and CPM are applied both as phenotyping tools to characterize baseline somatosensory organization and as exploratory outcome measures to examine whether these dimensions change following SCS, with the aim of generating mechanistic hypotheses alongside the clinical outcome evaluation.

This thesis presents a prospective exploratory pilot study (NCT06546371) in 12 patients with refractory mononeuropathy undergoing SCS, of whom 10 were included in the six-month analyses. By combining clinical outcome evaluation with quantitative sensory assessment in a single prospective cohort, it aims to provide preliminary evidence on the effects of SCS in refractory mononeuropathy and to inform the design of future adequately powered studies.

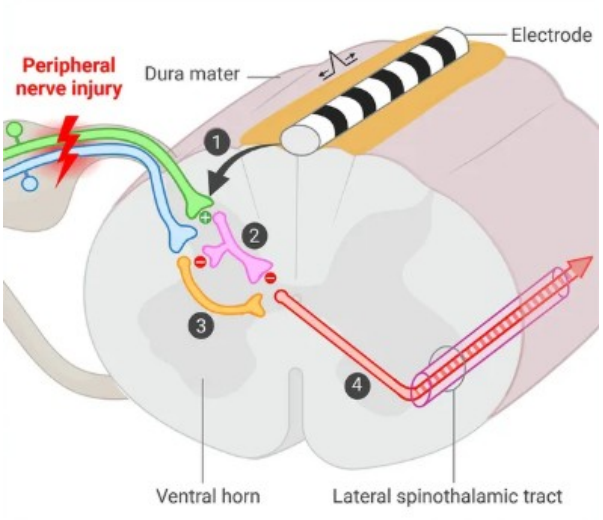

Figure 1.1: Proposed mechanism of action of spinal cord stimulation (SCS) in peripheral neuropathic pain. Following peripheral nerve injury, aberrant nociceptive signalling is transmitted via Aδ/C-fibers to the dorsal horn. SCS activates low-threshold Aβ-fibers in the dorsal column (1), which activate inhibitory interneurons (2) that attenuate excitatory interneuron input (3) and reduce activation of the lateral spinothalamic tract (4). Adapted from Kollenburg et al. [8].

1.2. Structure of the Thesis

Four complementary components are presented. Chapter 2 presents a scientific manuscript prepared in the format of a peer-reviewed medical journal, reporting the results of the SCIMONO pilot study. It evaluates the clinical effects of SCS in patients with refractory peripheral mononeuropathic pain, including the clinical rationale, study design, primary and secondary outcome analyses, and a discussion of clinical findings. Chapter 3 extends these analyses through exploratory multivariate somatosensory profiling at baseline, assessment of longitudinal changes in somatosensory organization following SCS, univariate analysis of within-patient QST change, and descriptive analysis of endogenous pain modulation using CPM, addressing questions that fall outside the scope of a conventional medical manuscript. These analyses are explicitly hypothesis-generating and aim to contextualize the clinical findings and inform future study design. Chapter 4 synthesizes the findings of both components in an overarching discussion and Chapter 5 presents the main conclusions of the thesis.

1.3. Objectives of the Thesis

The overarching aim of this thesis is to evaluate the clinical potential of SCS in patients with refractory peripheral mononeuropathic pain and to generate mechanistic hypotheses through exploratory quantitative sensory analyses to guide future research.

Objectives addressed in the research article

- To quantify changes in pain intensity (NRS) after six months of SCS in mononeuropathy
- To assess changes in quality of life, emotional functioning, and pain-related interference after six months of SCS in mononeuropathy
- To compare pain relief across different SCS stimulation paradigms (tonic, FAST, burst (delivered as microburst) and contour)
- To describe responder rates and stimulation preferences in patients with mononeuropathy treated with SCS

Objectives addressed in the technical chapter

- To characterize the dominant structure of somatosensory organization in mononeuropathy using Principal Component Analysis (PCA) of baseline QST data
- To explore longitudinal changes in somatosensory organization following SCS by projecting six-month QST data onto the baseline PCA space

- To examine whether individual QST parameters changed systematically and whether shared dimensions of somatosensory change exist between baseline and six months, using univariate and multivariate analysis of within-patient QST change
- To descriptively assess endogenous pain modulation at baseline and after six months with CPM data
- To descriptively examine whether baseline somatosensory profile, longitudinal somatosensory change, and CPM profile differ between responders and the non-responder

2

Research Article

Abstract

Background: Refractory peripheral mononeuropathic pain is associated with substantial impairment in quality of life (QoL) and frequently responds insufficiently to conventional treatment. While spinal cord stimulation (SCS) has demonstrated efficacy in other neuropathic pain conditions, prospective evidence in peripheral mononeuropathic pain remains limited. This prospective exploratory pilot study evaluates the clinical effects of SCS in patients with refractory peripheral mononeuropathic pain.

Methods: Adult patients with electromyography-confirmed peripheral mononeuropathy and persistent neuropathic pain refractory to at least six months of conventional management were included. After baseline assessment, patients underwent a two-week counterbalanced trial phase comparing tonic and fast-acting sub-perception therapy (FAST) stimulation. Patients achieving clinically meaningful pain reduction proceeded to permanent SCS implantation. During a three-month comparison phase, four stimulation paradigms (tonic, FAST, burst (delivered as microburst), and contour) were tested in counterbalanced order, followed by a three-month preference phase. The primary outcome was change in pain intensity (Numeric Rating Scale, NRS) from baseline to six months. Secondary outcomes included health-related quality of life (EQ-5D), emotional functioning (HADS), pain-related interference (BPI) and responder rates (≥30% and ≥50% reduction in NRS).

Results: 12 patients were enrolled and underwent trial stimulation; 10 completed six-month follow-up and were included in the final analysis. 1 patient withdrew during follow-up due to headache, and 1 patient had not yet completed follow-up at the time of writing. Median NRS decreased significantly from 7.0 (IQR 6.1 to 7.4) at baseline to 3.8 (IQR 2.4 to 5.0) at six months, corresponding to a median within-patient change of −3.3 points (IQR -4.8 to -2.5; $p = 0.01$). 8 patients (80%) achieved ≥30% pain reduction and 5 patients (50%) achieved ≥50% pain reduction at six months. Significant improvements were observed in EQ-5D and BPI at six months. HADS scores decreased, but not significantly. Pain reduction observed during the comparison phase was maintained at six months. Differences in pain intensity between stimulation paradigms were not statistically significant ($p = 0.09$). Concomitant analgesic medication was reduced during follow-up in 5 of the 6 patients who used medication at baseline. No serious adverse events occurred. Additionally, quantitative sensory testing (QST) was assessed at baseline and six-month follow-up to characterize the somatosensory profile of the cohort and to explore whether these dimensions change following SCS.

Conclusions: In this exploratory pilot study, SCS was associated with sustained reductions in pain intensity and improvements in QoL in patients with refractory peripheral mononeuropathic pain. These findings support further investigation in adequately powered controlled trials.

2.1. Introduction

Neuropathic pain is a form of chronic pain caused by a lesion or disease of the somatosensory system, as defined by the International Association for the Study of Pain (IASP) [1]. It is characterized by spontaneous pain, hyperalgesia and allodynia. Peripheral neuropathic pain can arise from focal nerve lesions such as mononeuropathies, as well as from polyneuropathies or radiculopathies [15]. In mononeuropathy, a single nerve is affected often after trauma or surgery [3, 16]. Although pathologically it is a localised condition, the pain can be severe and patients often experience marked limitations in daily functioning, sleep disturbance and psychosocial distress. These lead to a markedly decreased quality of life (QoL) and indirect healthcare costs [3]. Epidemiological studies suggest that mononeuropathies occur with an annual incidence in the order of approximately 2-4 per 1,000 persons in the general population, underscoring their clinical relevance [16–18].

Management of peripheral neuropathic pain typically includes first-line pharmacological treatments such as gabapentinoids and antidepressants [2, 19]. These are frequently complemented by non-pharmacological interventions such as transcutaneous electrical nerve stimulation and rehabilitative therapies to improve pain and function [20–22]. Despite available therapies, fewer than 50% of patients with neuropathic pain achieve satisfactory relief, and outcome studies in common mononeuropathies report persistent symptoms in approximately 15-30% of cases [2, 23, 24]. In this subset of patients, pain persists despite optimized treatment, resulting in refractory mononeuropathy. For these patients, current treatments are often insufficient. This therapeutic gap has led to increasing interest in interventional treatment strategies, including nerve blocks and neuromodulation techniques such as spinal cord stimulation (SCS) for treatment-resistant neuropathic pain [22].

SCS is an established therapy and has demonstrated clinically meaningful and sustained analgesic effects in other chronic neuropathic pain conditions, including painful diabetic polyneuropathy and complex regional pain syndrome beyond five-year follow-up [4, 25–27]. Mechanistically, SCS is thought to modulate dorsal column pathways and activate descending inhibitory circuits involved in nociceptive transmission [6]. This thereby reduces central sensitization and aberrant pain transmission. These mechanisms suggest that SCS may also be applicable to more focal neuropathic pain conditions, including mononeuropathic pain.

Despite this theoretical rationale, evidence supporting the use of SCS in mononeuropathy remains limited [9, 28]. Case reports and small observational studies have suggested potential benefit of SCS in selected focal neuropathic pain syndromes following peripheral nerve injury, including causalgic pain and median nerve injury [9, 28, 29]. In addition, dorsal root ganglion stimulation has shown promising results in focal and mononeuropathic-like neuropathic pain conditions, including pain following peripheral nerve injury [30, 31]. This supports the plausibility of neuromodulation in this population. However, robust prospective data on SCS in refractory mononeuropathy are scarce [10].

Therefore, there is a clear need for higher-quality evidence to evaluate the potential efficacy of SCS in patients with refractory mononeuropathy. Before conducting a randomized controlled trial, exploratory data are required to inform effect size estimation, assess within-patient variability, and optimize study design.

The present prospective exploratory pilot study aims to investigate the effects of SCS in patients with refractory peripheral mononeuropathic pain. The primary outcome is the change in pain intensity on the Numeric Rating Scale (NRS) between baseline and six-month follow-up. Secondary outcomes include changes in QoL, emotional functioning, pain-related interference, medication use and comparative effects of different stimulation paradigms.

2.2. Methods

This single-center, prospective exploratory pilot study enrolled patients with refractory peripheral mononeuropathic pain treated with SCS at Erasmus Medical Centre. The study design consisted of a baseline assessment, a 2-week trial phase, a three-month comparison phase evaluating four stimulation paradigms (tonic, FAST, burst (delivered as microburst), and contour) in counterbalanced order, and a three-month preference phase, as illustrated in Figure 2.1. The study was approved by the Medical Ethics Review Committee of Erasmus Medical Centre and was prospectively registered at ClinicalTrials.gov (NCT06546371).

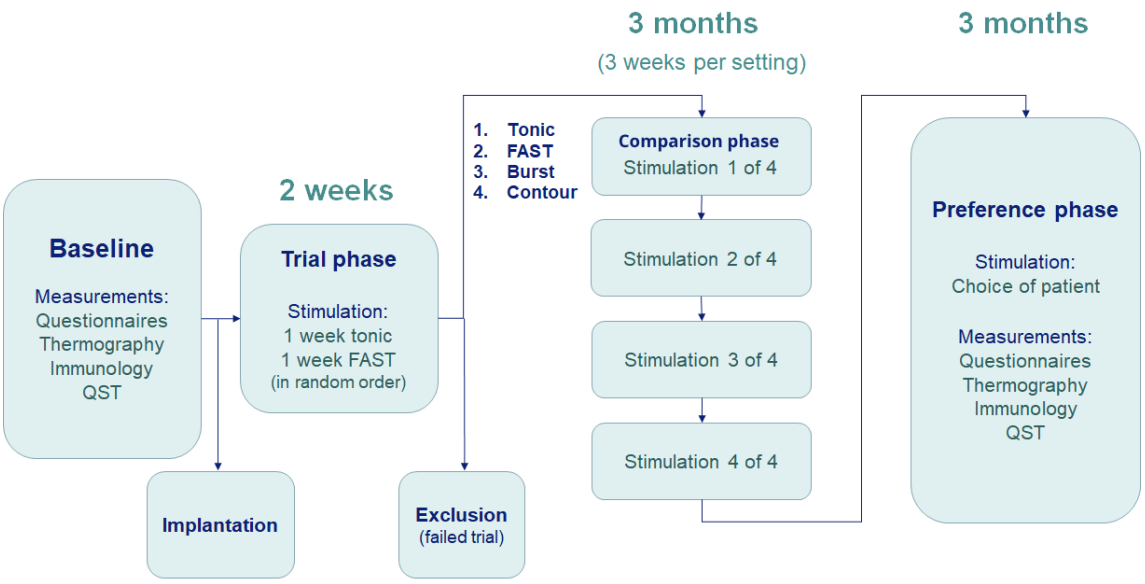

Figure 2.1: Study design and timeline. Overview of the study phases, including baseline assessment, the 2-week trial phase, the 3-month comparison phase with four stimulation paradigms applied in a counterbalanced order (3 weeks per setting), and the 3-month preference phase using the patient-selected stimulation paradigm. Questionnaires, quantitative sensory testing (QST), thermography, and immunological assessments were performed at baseline and at 6 months.

2.2.1. In- and exclusion criteria

Eligible participants were adults (≥18 years) with painful peripheral mononeuropathy of a distal extremity, preferably post-traumatic or post-surgical, fulfilling criteria for definite neuropathic pain according to the NeuPSIG grading system [15, 32], as confirmed by electromyography (EMG). Additional inclusion criteria were symptoms refractory to ≥six months of conventional medical management, an average pain score ≥5 on the 0-10 NRS in the week before baseline, and stable or no concomitant analgesic medication. Exclusion criteria included mononeuropathy of the head or torso, brachial plexus avulsion, life expectancy <1 year, clinically relevant coagulation disorders or anticoagulant therapy, immunodeficiency, pregnancy, anticipated non-compliance, or untreated psychological or addiction disorders. All participants provided written informed consent.

2.2.2. Surgical procedure and trial stimulation

Percutaneous octopolar epidural leads (one or two) were implanted under fluoroscopic guidance according to standard clinical practice and connected to an external pulse generator for the trial period. Intraoperative test stimulation was used to optimize lead placement. All patients underwent a two-week trial period consisting of one week of tonic stimulation and one week of fast-acting sub-perception therapy (FAST) in alternating order between patients. Participants were blinded to the specific paradigms and informed only whether stimulation was paresthesia-based or sub-perception. Patients who reported $\geq$30% pain reduction to at least one paradigm received a permanently implanted pulse generator (waveWriter Alpha, Boston Scientific, Valencia, CA, USA) connected to the existing lead(s).

2.2.3. Paradigm comparison and follow-up

During the subsequent three-month comparison phase, four stimulation paradigms (tonic, FAST, burst and contour) were programmed in counterbalanced order in three-week blocks to minimize period effects. After each block, participants completed pain diaries and standardized questionnaires. After completing all paradigms, at three months, participants selected their preferred paradigm, which was then used continuously during the three-month preference phase. The final evaluation was performed at six months. Concomitant analgesic medication was kept stable during the trial and comparison phase. During the preference phase, medication adjustments were permitted at the discretion of the treating physician but were not yet actively encouraged. Stimulation parameters per paradigm as defined in the protocol are summarized in Appendix A. Procedure- and device-related adverse events

were recorded throughout follow-up.

2.2.4. Outcomes

The primary outcome was change in pain intensity (0–10 NRS), derived from the Brief Pain Inventory (BPI; item 5: average pain over the last two weeks), between baseline (T0) and six-month follow-up (T3).

Secondary outcomes included changes in health-related quality of life (EuroQol 5-Dimension questionnaire, EQ-5D [33]), emotional functioning (Hospital Anxiety and Depression Scale, HADS [34]), and pain-related functional interference (Brief Pain Inventory interference score, BPI [35]).

For contextual interpretation of the primary and secondary outcomes, the following reference values were applied: a minimal clinically important difference of 2 points on the 0–10 NRS [36], a minimal clinically important difference of 0.074 for the EQ-5D index [37] and a minimal important change of 2 points for the BPI interference score [38]. For the HADS, a score of $\geq$8 on either subscale was used as the clinical threshold for possible anxiety or depression [34] and minimal clinically important differences of 2.1 points for the anxiety subscale and 2.5 points for the depression subscale were applied [39].

Additional analyses included (i) change in pain intensity during the comparison phase, defined as the lowest observed NRS score across the four stimulation paradigms (T2A–T2D), and (ii) within-patient differences in pain intensity between stimulation paradigms (Tonic, FAST, Burst, Contour) during the comparison phase.

Responder rates were defined as the proportion of patients achieving $\geq$30% and $\geq$50% reduction in NRS from baseline to six months.

Quantitative sensory testing (QST) and biomarker assessments (sIL-1β and sCD163) were performed at baseline and at six-month follow-up.

2.2.5. Statistical analysis

Given the exploratory nature of this pilot study, no formal sample size calculation was performed. A sample of 12 participants is methodologically consistent with recommendations for feasibility studies aimed at estimating variability and informing subsequent power calculations [40]. The statistical analysis plan was developed in consultation with S. Baart, statistician at Erasmus Medical Centre.

Outcome analyses were performed on patients who completed six-month follow-up (per-protocol population). 1 patient who withdrew during follow-up was excluded from outcome analyses but is depicted in the longitudinal NRS figure up to the last available time point. Missing data were not imputed.

Continuous variables are reported as medians with interquartile ranges (IQR). Values were rounded as follows: NRS scores to 1 decimal place; BPI interference scores (calculated as the mean of seven items) to 1 decimal place; HADS total scores to whole integers; and EQ-5D index values to 3 decimal places, consistent with conventional reporting standards. All analyses were performed on paired data and all statistical tests were two-sided with a significance level of $\alpha = 0.05$.

The primary outcome, change in NRS from T0 to T3, was analyzed using the Wilcoxon signed-rank test. Secondary outcomes (EQ-5D, BPI interference score, HADS-Anxiety and HADS-Depression) were analyzed using the same test. For all outcomes, the median within-patient difference with IQR was reported as the measure of effect magnitude. Responder rates (≥30% and ≥50% NRS reduction from baseline to six months) were calculated as proportions.

Pain reduction during the comparison phase was assessed by comparing baseline NRS to the lowest observed NRS across the four stimulation paradigms (T2A–T2D) per patient (best T2), analyzed using the Wilcoxon signed-rank test. Differences in pain intensity between paradigms (Tonic, FAST, Burst, Contour) were analyzed using the Friedman test, with effect size expressed as Kendall's W, followed by post-hoc pairwise Wilcoxon signed-rank tests with Holm correction. To assess potential period effects, a linear mixed model was fitted with NRS as outcome, stimulation paradigm and time as fixed effects, and patient as a random effect.

2.3. Results

2.3.1. Patient characteristics

After screening, 12 patients (7 females) with refractory peripheral mononeuropathic pain were enrolled and underwent trial stimulation. All patients showed a clinically meaningful response during the trial phase and subsequently received a permanent implant. 1 patient had not yet completed six-month follow-up at the time of analysis and was therefore excluded from the present report. Of the remaining 11 patients, 10 completed six-month follow-up and were included in the final analysis. 1 patient withdrew during follow-up due to headache and was excluded from outcome analyses. Available data up to withdrawal are depicted in the longitudinal NRS figure.

Baseline characteristics of the 11 included patients are summarized in Table 2.1. Median age was 53 years (IQR 42–63), and 7 patients (64%) were female. Median pain duration was 48 months (IQR 45–66). The majority of neuropathies were post-traumatic (64%). Most affected nerves were located in the lower limb (73%). The median NRS pain score was 7.0 (IQR 6.3–7.3). Patient-specific data can be found in Appendix B.

Table 2.1: Baseline Clinical and Demographic Characteristics

Characteristic	**Total Population (N=11)** *n (%) or Median (IQR)*
Age (years)	53 (42-63)
Sex, female	7 (64%)
Pain duration (months)	48 (45-66)
Etiology	
Post-traumatic	7 (64%)
Post-surgical	4 (36%)
Affected nerve/location	
Upper limb	*3 (27%)*
Ulnar nerve	3
Lower limb	*8 (73%)*
Peroneal nerve	4
Saphenous nerve	2
Sural nerve	2
NRS pain score (0-10)	7.0 (6.3-7.3)
BPI interference score	7.0 (5.3-7.7)
HADS-Anxiety	6 (4-8)
HADS-Depression	6 (5-10)
EQ-5D index	0.514 (0.454-0.578)

2.3.2. Primary outcome

Median NRS pain intensity decreased significantly (p = 0.01) from 7.0 (IQR 6.1 to 7.4) at baseline to 3.8 (IQR 2.4 to 5.0) at six months $(n = 10)$ (Figure 2.2). The median within-patient change was −3.3 points (IQR -4.8 to -2.5) and exceeds the threshold of 2 points for clinically meaningful pain reduction on the NRS [36]. 8 patients (80%) achieved ≥30% pain reduction, of whom 5 patients achieved ≥50% pain reduction at six months. Pain intensity remained consistently lower than baseline throughout the follow-up period, although the magnitude of reduction varied across time points. Individual patient trajectories are shown in Appendix Figure C.1.

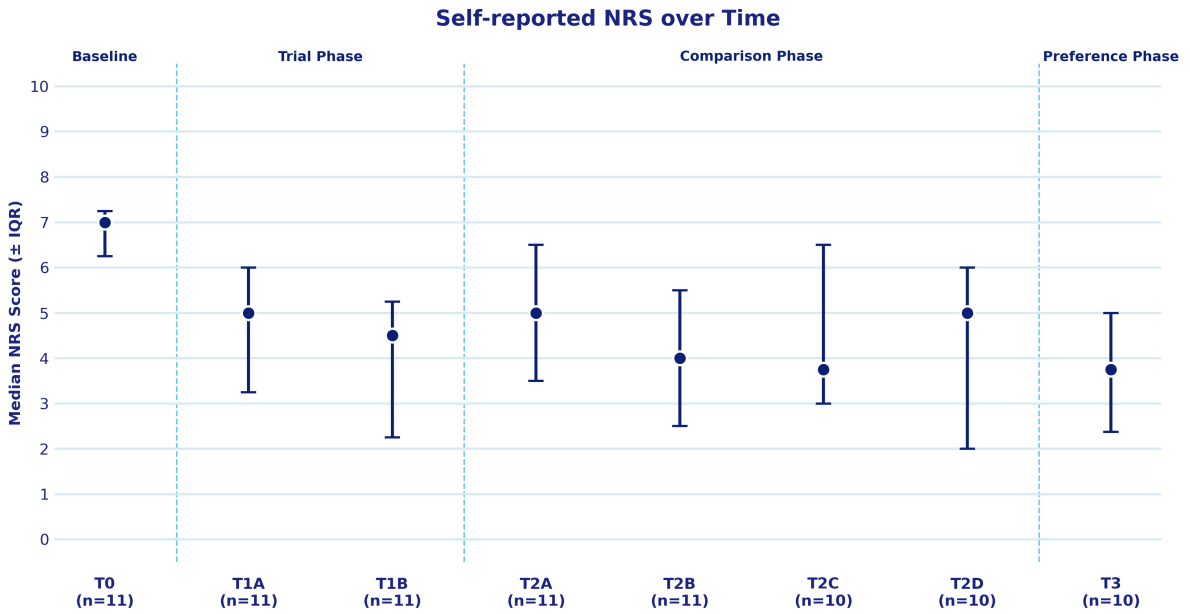

Figure 2.2: Pain intensity (NRS) over the course of the study from baseline (T0) through six-month follow-up (T3). Group medians are shown with whiskers representing the interquartile range (IQR). Data from 1 patient who withdrew at 2 months are included up to the last available time point (n=11 at baseline, n=10 at six months).

2.3.3. Secondary outcomes

QoL improved during the study period (Figure 2.3a). Median EQ-5D increased significantly from 0.514 (0.454 to 0.578) at baseline to 0.679 (IQR 0.619 to 0.857) at six months (p = 0.01; $n = 10$). Resulting in a median within-patient change of 0.165, exceeding the reported minimal clinically important difference of 0.074.

Functional interference (BPI interference score) decreased significantly from 7.1 (IQR 5.8 to 7.8) at baseline to 3.8 (IQR 1.4 to 4.7) at follow-up (p = 0.01; $n = 10$) (Figure 2.3b). Resulting in a median within-patient change of 3.3 points, exceeding the recommended minimal important change of 2 points.

HADS-Anxiety scores decreased non-significantly from 6 (IQR 4 to 8) to 3 (IQR 3 to 7) (p = 0.68; $n = 10$), with a median within-patient change of 0.5 points, not meeting the minimal clinically important difference of 2.1 points. HADS-Depression scores also decreased non-significantly from 7 (IQR 5 to 10) to 3 (IQR 2 to 8) (p = 0.16; $n = 10$), with a median within-patient change of 1.5 points, not meeting the minimal clinically important difference of 2.5 points (Figure 2.3c). At baseline, 3 of 10 patients scored $\geq$8 for anxiety and 5 of 10 for depression, indicating possible clinically relevant symptoms. At six months, these numbers were 2 and 3 respectively.

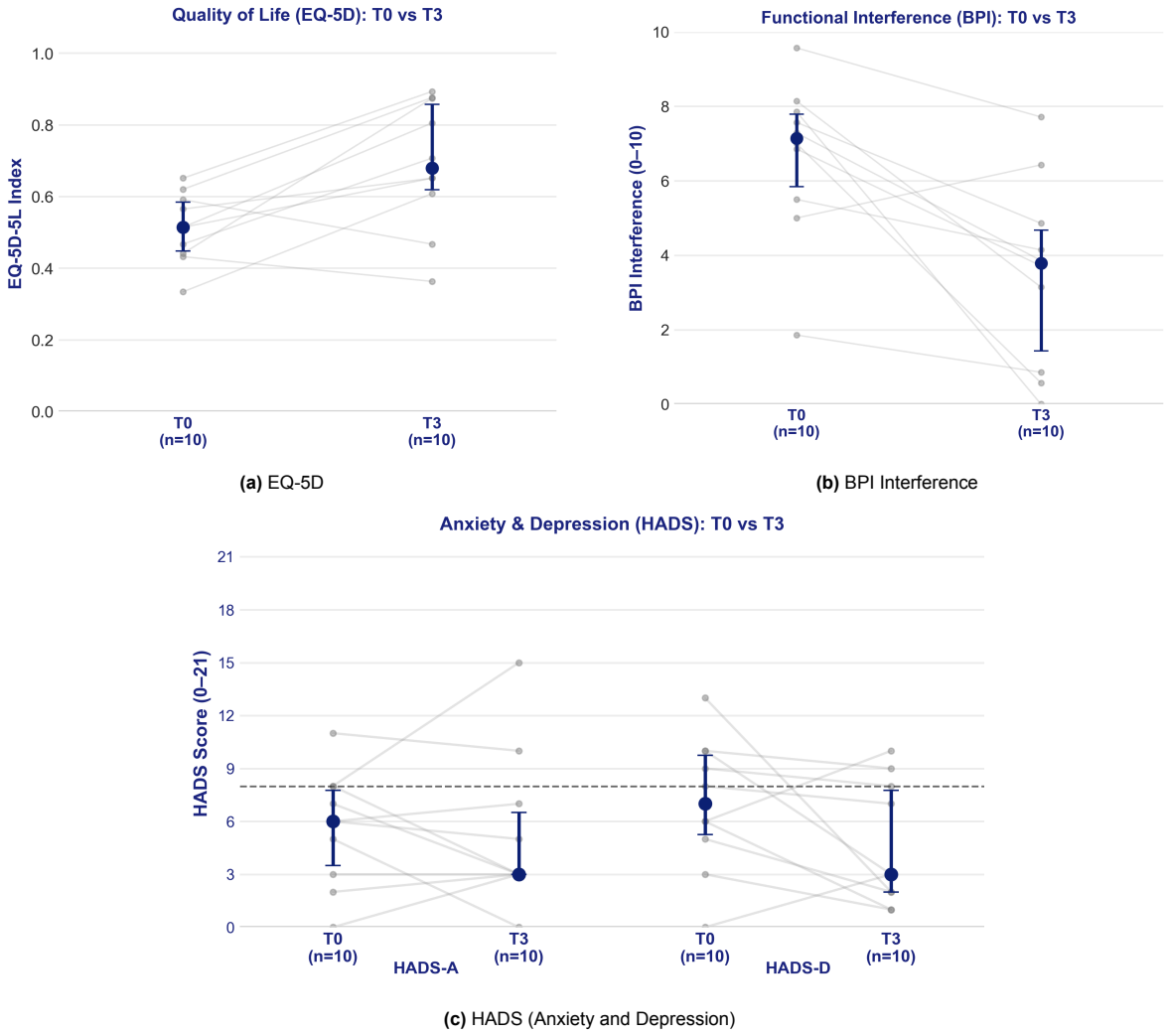

(a) EQ-5D

(b) BPI Interference

(c) HADS (Anxiety and Depression)

Figure 2.3: Changes in secondary outcomes between baseline (T0) and six-month follow-up (T3). (A) EQ-5D index values, (B) BPI interference scores, and (C) HADS anxiety and depression scores. Individual patient trajectories are depicted with paired points connected by thin grey lines. Group medians are shown as dark blue markers with whiskers representing the interquartile range (IQR).

Pain reduction during comparison phase

During the comparison phase, the lowest observed NRS score across stimulation paradigms (best T2) was 3.5 (IQR 1.3 to 5.0), compared to 7.0 (IQR 6.1 to 7.4) at baseline. The median reduction was −3.5 points. This reduction was statistically significant ($p = 0.002$).

Comparison between stimulation paradigms

Pain intensity during the comparison phase differed numerically between stimulation paradigms (Figure 2.4). Median NRS scores were:

- Tonic: 4.5 (IQR 1.8–6.5)
- FAST: 3.8 (IQR 2.0–5.8)
- Burst: 5.5 (IQR 3.3–6.0)
- Contour: 4.5 (IQR 3.0–6.0)

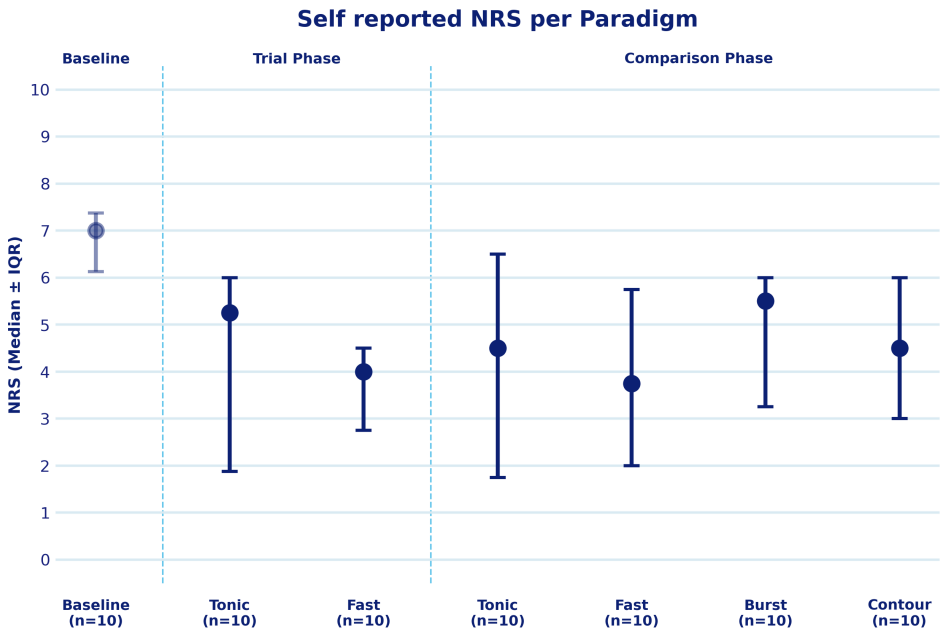

Figure 2.4: Pain intensity scores (NRS) during the trial and comparison phase according to stimulation paradigm (Tonic, FAST, Burst, and Contour). Group medians are displayed with whiskers representing the interquartile range (IQR).

Overall differences between paradigms were not statistically significant ($\chi^2(3) = 6.57$, $p = 0.09$; Kendall's $W = 0.22$). Post-hoc pairwise comparisons with Holm correction did not reveal significant differences between specific paradigms.

A linear mixed model did not demonstrate a significant period effect, and effect sizes for paradigm differences remained comparable to those obtained from the Friedman test, supporting the robustness of the primary paradigm comparison.

At six months, the preferred stimulation paradigm was FAST in 6 patients, Tonic in 2 patients, Burst in 1 patient, and Contour in 1 patient.

Quantitative Sensory Testing, biomarkers & medication use

Quantitative sensory testing performed at baseline and six-month follow-up demonstrated heterogeneous outcomes across individuals. Some patients showed a reduction in side-to-side sensory asymmetry at six months, whereas others showed no consistent change. Serum concentrations of IL-1β and sCD163 did not differ systematically between baseline and six-month follow-up. Of the 10 patients included in the final analysis, 4 were not using concomitant analgesic medication at baseline. Of the remaining 6, 5 reduced their medication during follow-up, though this number should be interpreted in light of the fact that medication adjustments were not permitted during the comparison phase and not actively encouraged during the preference phase.

Safety

1 patient withdrew during follow-up due to headache, which is addressed in the discussion. 1 other patient experienced procedure- and device-related complaints, including anchor site discomfort, tunneling site pain, and implantable pulse generator pocket pain, which together necessitated a revision procedure. This patient completed six-month follow-up and was included in the primary analysis, with a reported NRS score of 8.0. However, this score should be interpreted with caution as the patient was unable to distinguish the treated mononeuropathic pain from procedure-related pain. The revision procedure was performed after the six-month follow-up visit, and its outcome was not yet available at the time of writing. No serious adverse events occurred.

2.4. Discussion

2.4.1. Principal findings

This prospective exploratory pilot study is, to my knowledge, the first to prospectively evaluate the clinical effects of SCS in patients with refractory peripheral mononeuropathic pain. SCS was associated with a clinically meaningful and statistically significant reduction in pain intensity, with a median NRS decrease of 3.3 points from baseline to six-month follow-up, exceeding the established minimal clinically important difference of 2 points [36]. This was accompanied by significant improvements in health-related QoL (EQ-5D) and pain-related functional interference (BPI). A responder rate of 80% for $\geq$ 30% pain reduction and 50% for $\geq$ 50% pain reduction was observed at six months. No serious adverse events occurred.

2.4.2. Clinical implications

The present findings extend the limited prospective evidence base for SCS in refractory peripheral mononeuropathic pain, which was previously restricted to case series and small retrospective analyses in mixed neuropathic pain populations [9, 28]. SCS has previously demonstrated sustained analgesic efficacy in painful diabetic polyneuropathy and complex regional pain syndrome [4, 5, 41], and the present findings are broadly consistent with effects reported in these established indications. The magnitude of NRS reduction observed in this cohort (7.0 to 3.8) is comparable to that reported by Slangen et al. in a randomized controlled trial of SCS in painful diabetic polyneuropathy (7.1 to 4.0), both at six months [41]. Improvements in EQ-5D and BPI interference are consistent with quality of life and functional gains reported across these indications [4, 5], supporting the clinical relevance of these effects beyond pain intensity alone.

Prior evidence in adjacent populations includes the ACCURATE trial, which reported treatment success in 53.3% of patients with causalgia at three months [30]. However, causalgia is distinguished from peripheral mononeuropathy by the presence of autonomic and vasomotor features and is classified separately under established neuropathic pain criteria [32], limiting direct comparison. A recent retrospective study in traumatic and iatrogenic peripheral neuropathic pain reported an average NRS decrease from 8.1 to 3.0 with a responder rate of 63% at a mean follow-up of ten years [8]. Direct comparison is similarly limited by the inclusion of patients with multiple nerve involvement, retrospective design, and absence of a standardized follow-up interval. More broadly, differences in outcome measures, follow-up duration, and responder definitions preclude direct comparison of responder rates across studies.

Changes in HADS scores did not reach statistical significance and median within-patient reductions of 0.5 points for anxiety and 1.5 points for depression did not meet the minimal clinically important differences of 2.1 and 2.5 points respectively. This may be explained by the relatively low baseline scores: at baseline, only 3 of 10 patients scored $\geq$8 for anxiety and 5 of 10 for depression [34], leaving limited room for measurable improvement.

The high trial success rate, all 12 patients proceeded to permanent implantation, warrants cautious interpretation. Trial success rates in SCS studies for established neuropathic pain conditions typically range from 67-86% [42–44], though these studies generally apply a $\geq$50% pain reduction criterion for trial success, compared to the $\geq$30% threshold used in the present study. The comparatively lower threshold, combined with the stringent inclusion criteria requiring EMG-confirmed mononeuropathy, may have contributed to the high rate of progression to permanent implantation. Whether this selection profile is reproducible in larger cohorts and translates to favorable long-term outcomes remains to be established.

2.4.3. Mechanistic considerations

SCS is thought to exert its analgesic effects primarily through activation of large myelinated Aβ-fibers in the dorsal columns, modulating nociceptive transmission at the dorsal horn via inhibitory interneurons and activating descending inhibitory circuits [6, 45]. In peripheral mononeuropathy, focal nerve injury drives aberrant peripheral and central nociceptive signalling, which represents a principal target of SCS-mediated dorsal horn modulation [3]. The sustained pain reductions observed here, maintained from the comparison phase through the six-month preference phase, are consistent with a persistent modulatory effect on central nociceptive processing rather than a transient response. Differences in

pain intensity between the four stimulation paradigms were not statistically significant and individual paradigm preferences varied across patients, consistent with the broader literature [10]. This supports a personalized rather than fixed-paradigm approach to paradigm selection.

Although differences between paradigms were not statistically significant, 60% of the patients selected FAST as their preferred paradigm. A possible mechanistic explanation for this preference is the surround inhibition mechanism proposed for FAST, whereby sparse activation of dorsal column axons maximally inhibits dorsal horn neurons via segmental GABAergic pathways [46]. This may be particularly relevant in mononeuropathic pain, in which focal nerve injury drives central sensitization representing a principal target of dorsal horn modulation [3, 6].

2.4.4. Strengths and limitations

The principal strengths of this study are its prospective design, the diagnostic homogeneity of the study population of definitive mononeuropathy and the structured counterbalanced paradigm comparison phase, which minimizes period effects. The principal limitation is sample size: with ten patients in the final analysis, the study was underpowered for secondary analyses and definitive conclusions regarding paradigm superiority. The absence of a control condition means that spontaneous improvement, regression to the mean, and placebo effects cannot be excluded as contributors to the observed pain reductions. The latter is particularly relevant in neuromodulation research, where non-specific effects of an implanted device and associated clinical attention may contribute meaningfully to perceived benefit. The single-center design and predominantly post-traumatic etiology limit generalizability to other mononeuropathy subtypes and clinical settings. The absence of a washout period between paradigms carries the possibility of carryover effects, although no significant period effect was identified.

1 patient withdrew during follow-up reporting headache that she noted decreased when the stimulator was turned off and subsequently chose to discontinue stimulation. Neurological evaluation did not identify a cause attributable to the SCS system and the headache was considered likely attributable to a non-device-related etiology. This event was therefore not classified as a device-related serious adverse event, though a causal relationship cannot be definitively excluded. Furthermore, pain scores at six months for one patient who underwent a revision procedure may be confounded by procedure-related discomfort rather than the underlying mononeuropathic pain. As this patient showed no improvement from baseline, inclusion of these data likely yields a conservative estimate of the overall treatment effect of SCS in this cohort.

2.4.5. Future research

The present data provide the first prospective evidence to inform effect size estimation and power calculations for a randomized controlled trial of SCS in refractory peripheral mononeuropathic pain. This directly addresses a key barrier identified in the literature [10]. A future trial should incorporate a sham control arm to disentangle specific analgesic effects from non-specific and placebo effects. Furthermore, adequate follow-up beyond six months and sufficient sample size are needed to evaluate durability, paradigm effects, and responder predictors. The individual variation in paradigm preference observed in this cohort underscores the importance of incorporating personalized paradigm selection into future trial designs, rather than mandating a fixed stimulation paradigm, as this may be essential for accurately estimating the true analgesic potential of SCS in this population.

2.5. Conclusion

In this prospective exploratory pilot study, SCS was associated with sustained and clinically meaningful reductions in pain intensity and improvements in quality of life and functional interference in patients with refractory peripheral mononeuropathic pain, with no serious adverse events. These findings provide the first prospective evidence supporting the feasibility of SCS in this population and inform the design of future adequately powered randomized controlled trials. Given the exploratory nature of this study and the absence of a control condition, definitive conclusions regarding efficacy cannot be drawn. Larger prospective studies with sham and active comparator arms are warranted to establish the role of SCS in the management of refractory peripheral mononeuropathic pain.

3

Exploratory somatosensory profiling and endogenous pain modulation

3.1. Introduction

Neuropathic pain is characterized by substantial heterogeneity in both clinical presentation and underlying pathophysiology. It arises from a lesion or disease of the somatosensory system and can manifest as spontaneous pain, hyperalgesia, and allodynia through a range of distinct peripheral and central mechanisms [1]. Spinal cord stimulation (SCS) is an established interventional treatment for refractory neuropathic pain conditions, yet treatment response varies considerably between patients: some achieve substantial and sustained pain relief whereas others respond only partially or not at all [10]. Understanding what distinguishes these patients at the level of somatosensory function may provide mechanistic insight into this variability and inform patient selection in future studies.

3.1.1. Somatosensory profiling using quantitative sensory testing

Quantitative sensory testing (QST) enables standardized assessment of somatosensory function across multiple modalities, including thermal detection thresholds, thermal and mechanical pain thresholds, and dynamic pain processing [47]. Applied according to the protocol of the German Research Network on Neuropathic Pain (DFNS), QST generates 11 parameters per patient that together characterize the somatosensory profile of the affected region, capturing both signs of sensory loss and signs of sensitization across small and large nerve fiber populations. In patients with unilateral neuropathic pain, these parameters can be expressed as side-to-side differences between the affected and contralateral limb, isolating the deviation attributable to the focal nerve injury from general inter-individual variability.

However, these parameters are interrelated and difficult to interpret in isolation when the question concerns the overall profile of somatosensory function within a cohort. Analyzing each parameter separately does not capture the shared structure across modalities, and in small samples, univariate approaches carry limited statistical power and risk of false-positive findings when applied across 11 parameters simultaneously. A multivariate approach that summarizes the shared structure across parameters is therefore preferable when the aim is to characterize dominant patterns of sensory organization rather than to test individual parameters.

Principal component analysis (PCA) is such an approach: it identifies the dominant axes of variation within a dataset by computing which combinations of parameters vary together across patients and how much of the total variability those combinations explain [48]. The result is a small number of components, each a weighted combination of the original parameters, that together capture the dominant structure of somatosensory organization within the cohort. This allows individual patients to be positioned within a multivariate sensory space and compared descriptively [13]. Importantly, PCA characterizes the overall somatosensory organization within a cohort but is not designed to test whether individual parameters change systematically over time. A separate univariate analysis is therefore reported alongside the PCA to address that complementary question.

3.1.2. Conditioned pain modulation as a complementary assessment dimension

In addition to static somatosensory profiling, chronic pain conditions are frequently associated with alterations in endogenous descending pain modulation [14]. Conditioned pain modulation (CPM) provides a functional measure of this inhibitory capacity. By applying a conditioning stimulus at one site while measuring pain thresholds at another, CPM quantifies the degree to which the central nervous system suppresses incoming nociceptive signals [49]. Given that SCS is thought to modulate nociceptive processing at both spinal and supraspinal levels [7], individual differences in descending inhibitory function may represent a mechanistically relevant dimension in patients undergoing SCS.

3.1.3. Gaps in current knowledge and aims of this chapter

Taken together, multivariate somatosensory structure and endogenous inhibitory capacity represent complementary dimensions of nociceptive organization that may both contribute to variability in SCS response. Yet, how these dimensions coexist in patients undergoing SCS remains poorly characterized. Plantaz et al. assessed longitudinal changes in individual sensory thresholds in patients with persistent spinal pain syndrome treated with SCS, without performing multivariate sensory profiling or assessing endogenous pain modulation [50]. Nurmikko et al. concluded that sensory phenotyping combining QST results across multiple modalities has not yet been applied in SCS trials [51]. To my knowledge, combined multivariate sensory profiling using PCA of the full DFNS QST battery and CPM assessment has not previously been reported in patients with refractory mononeuropathy treated with SCS. Although QST and CPM are primarily applied as phenotyping tools to characterize somatosensory mechanisms prior to treatment, their repeated assessment before and after SCS also allows exploration of whether somatosensory organization and endogenous inhibitory capacity change following neuromodulation, providing exploratory mechanistic insight alongside the phenotypic characterization. More broadly, whether baseline somatosensory organization, longitudinal somatosensory change, and CPM profile differ between responders and non-responders has not yet been examined in this population.

This chapter therefore reports exploratory analyses in the SCIMONO cohort described in Chapter 2. The analyses address the following aims:

1. **Baseline multivariate sensory profiling (Aim 1).**
   Objective: To characterize the dominant structure of somatosensory organization within the cohort using PCA of baseline side-to-side QST z-scores ($n = 12$).
   Hypothesis: Heterogeneous somatosensory profiles are expected, as focal nerve injury can selectively affect different afferent fiber populations depending on the type and severity of the lesion [47, 52, 53]. This aim is distinct from testing whether individual QST parameters change following SCS, which is addressed in Aim 3.
2. **Longitudinal changes in somatosensory organization (Aim 2).**
   Objective: To explore whether somatosensory organization changed following SCS by projecting six-month QST data onto the baseline PCA space ($n = 10$).
   Hypothesis: A shift toward reduced somatosensory asymmetry is expected in clinical responders, based on evidence that pain-related QST parameters can normalize following successful neuromodulation [50, 54, 55].
3. **Univariate analysis of QST change (Aim 3).**
   Objective: To examine whether individual QST parameters changed systematically following SCS using within-patient Δ z-scores ($\Delta Z = Z_{T3} - Z_{T0}$) for participants with complete paired data ($n = 10$).
   Hypothesis: Selective changes are expected in parameters reflecting dynamic pain processing and central sensitization, such as WUR and mechanical pain thresholds, over static thermal detection thresholds, based on the proposed mechanism of SCS via Aβ-fiber activation in the dorsal columns [6, 7, 45]. Given the inconsistency of the broader literature [51], results are interpreted descriptively.
4. **Endogenous pain modulation at baseline and follow-up (Aim 4).**
   Objective: To descriptively assess endogenous pain modulation using CPM at baseline ($n = 12$) and six-month follow-up ($n = 10$) via a cold pressor conditioning paradigm.
   Hypothesis: Baseline CPM is expected to be variable and potentially impaired [14], and CPM efficiency is expected to improve following SCS based on evidence that SCS activates descending

inhibitory pathways [45, 54].

5. **Integration with treatment response (Aim 5).**
   Objective: To descriptively examine whether baseline somatosensory profile, longitudinal somatosensory change, and CPM profile differ between responders and the non-responder ($\geq$30% NRS reduction at six months, $n = 10$) [36].
   Hypotheses: Lower baseline CPM efficiency is expected to be associated with greater pain reduction following SCS, based on evidence that lower baseline CPM predicted greater pain reduction in chronic pain patients treated with SCS [56]. Regarding somatosensory organization, two mechanistic hypotheses are considered [6]: patients with preserved large-fiber function (VDT, MDT) may benefit more from SCS via intact Aβ-afferent input, whereas patients with a sensitization-dominated profile (elevated WUR, mechanical pain sensitivity) may also benefit more given the modulatory effect of SCS on dorsal horn hyperexcitability. Both remain speculative and are evaluated descriptively.

3.2. Methods

3.2.1. Analytical framework

This exploratory analysis was conducted within the SCIMONO cohort of patients with refractory peripheral mononeuropathic pain treated with SCS, as described in Chapter 2. QST and CPM assessments were performed at baseline prior to implantation (T0) and at six-month follow-up (T3). The following analyses were performed, with procedures described in the subsections below:

1. Baseline multivariate sensory profiling using PCA of side-to-side QST z-scores ($n = 12$; Section 3.2.3)
2. Longitudinal changes in somatosensory organization by projection of T3 QST data onto the baseline PCA space ($n = 10$; Section 3.2.3)
3. Univariate analysis of within-patient QST change using ΔZ-scores ($n = 10$; Section 3.2.4)
4. Descriptive assessment of CPM at baseline ($n = 12$) and six-month follow-up ($n = 10$; Section 3.2.5)
5. Exploratory integration of multivariate somatosensory profile, CPM, and treatment response ($n = 10$; Section 3.2.6)

Given the limited sample size, no predictive modeling, clustering validation, or confirmatory statistical inference was performed. All analyses are descriptive and hypothesis-generating.

3.2.2. Quantitative Sensory Testing z-score computation

This subsection describes the shared z-score pipeline underlying Analyses 1-3. Baseline QST was performed according to the standardized protocol of the DFNS [47]. All QST parameters were expressed as standardized side-to-side z-scores prior to further analysis which is explained in 3.2.2. The DFNS protocol includes 11 QST parameters: cold detection threshold (CDT), warm detection threshold (WDT), thermal sensory limen (TSL), cold pain threshold (CPT), heat pain threshold (HPT), mechanical detection threshold (MDT), vibration detection threshold (VDT), mechanical pain threshold (MPT), mechanical pain sensitivity (MPS), pressure pain threshold (PPT), and wind-up ratio (WUR). These parameters span five somatosensory domains: thermal detection (CDT, WDT, TSL), thermal pain (CPT, HPT), mechanical detection (MDT, VDT), mechanical pain (MPT, MPS, PPT), and dynamic pain modulation (WUR).

All QST parameters were computed according to the DFNS protocol. Deviations from or additions to the standard procedure are described where applicable.

Wind-up ratio computation

The Wind-up ratio (WUR) quantifies the degree to which repetitive painful stimulation leads to progressively increasing pain ratings, reflecting central sensitization mechanisms in the dorsal horn. It was calculated as the ratio of mean pain ratings during repetitive stimulation to mean ratings during single-stimulus application.

Because single-stimulus ratings occasionally equaled zero, direct computation of the ratio would result in undefined values and disproportionate inflation of ratio estimates. This issue has been acknowledged in the DFNS literature, where affected observations are typically excluded rather than corrected [47]. As no standardized correction method has been described for this specific problem, an empirical approach was adopted. A constant offset was added to both numerator and denominator for all observations:

$$\text{WUR}^* = \frac{\overline{\text{series}} + c}{\overline{\text{single}} + c}$$

Several offset values (e.g. $c = 0.1$, 0.5, 1.0, 1.5 and 2.0) were evaluated by comparing the resulting z-score distributions in both the SCIMONO cohort and an independent dataset of patients with complex regional pain syndrome from Eline van Lange to assess consistency across samples. Smaller constants produced disproportionate z-score inflation when denominators approached zero in both datasets. An offset of $c = 1$ resulted in the smallest overall distortion of z-score distributions across both samples and was therefore selected. The correction was applied uniformly across all observations when at least one participant had a mean single stimulus rating of zero to ensure internal consistency of the transformation.

Side-to-side standardization

Rather than comparing patient values to a healthy reference population, QST outcomes were expressed as side-to-side differences using the contralateral limb as an internal control:

$$\Delta X = X_{\text{affected}} - X_{\text{contralateral}}$$

This approach was chosen because, in unilateral neuropathic pain, comparing the affected side directly to the contralateral side isolates the deviation attributable to the focal nerve injury. This is possible because within-subject symmetry between sides is high in healthy individuals, with no systematic left-right differences [47]. In contrast, absolute QST values vary substantially between individuals due to factors such as age, sex, and body site, meaning that a population-based reference cannot account for these individual baseline differences. Using the contralateral limb as a patient-specific internal control therefore eliminates this source of inter-individual variability and increases sensitivity for detecting clinically meaningful sensory deviations on the affected side.

Side-to-side differences were standardized using the reference standard deviations for right-left differences in healthy individuals reported in Table 3 of Rolke et al. (2006) [47]. These values represent the expected within-subject variability across sides under normal conditions and are therefore the appropriate reference for side-to-side z-scores. This is in contrast to the between-subject standard deviations in Table 1 of the same publication, which are not appropriate for within-subject comparisons.

Several DFNS parameters are right-skewed in healthy individuals, and their reference statistics were therefore derived from log-transformed data [47]. To ensure compatibility with these reference values, the patient data from this cohort must be expressed on the same scale prior to standardization. For parameters where log-transformation was applied in the DFNS protocol (CDT, WDT, TSL, MDT, MPT, MPS, WUR, PPT), base-10 logarithmic transformation was applied to both the affected and contralateral values prior to subtraction:

$$Z = \frac{\log_{10}(X_{\text{affected}}) - \log_{10}(X_{\text{contralateral}})}{\sigma_{\text{reference}}}$$

CDT and WDT require an additional transformation before log-transformation. Per the DFNS protocol, CDT is expressed as the temperature drop from the 32°C thermode baseline ($32 - \text{CDT}_{\text{measured}}$) and WDT as the temperature rise above baseline ($\text{WDT}_{\text{measured}} - 32$). This step is necessary because the DFNS reference values for these parameters were derived from log-transformed differential values rather than absolute temperatures [47].

For parameters not log-transformed in the DFNS protocol (CPT, HPT, VDT), z-scores were calculated directly from raw values:

$$Z = \frac{X_{\text{affected}} - X_{\text{contralateral}}}{\sigma_{\text{reference}}}$$

For log-transformed parameters where any participant had a value of zero, a minimal offset of 0.1 was applied to all observations for that parameter prior to log-transformation to avoid undefined values, following the approach described by Mücke et al. (2016) [57].

Variable scaling

Prior to PCA, all QST z-scores were standardized to zero mean and unit variance using a z-transformation (StandardScaler, scikit-learn). Although the z-scores are already expressed in units of standard deviation relative to a healthy reference population, the spread of z-scores across parameters within a small clinical cohort may differ substantially. A parameter with z-scores ranging from -3 to $+3$ would otherwise contribute more to the principal components than a parameter with z-scores ranging from -1 to $+1$, regardless of clinical relevance. Standardization ensures equal statistical weighting across all 11 parameters and was chosen deliberately given the exploratory nature of the analysis and the small sample size, in which a single parameter with disproportionately high variance could otherwise dominate the component structure. It is acknowledged that this procedure abstracts from the clinical magnitude of absolute z-score deviations, which is discussed as a methodological limitation in Section 3.4.

Because the clinical direction of z-score deviations is parameter-dependent, a positive z-score indicates sensory loss for detection threshold parameters (CDT, WDT, TSL, MDT, VDT, MPT, PPT, CPT, HPT) but greater sensitization for pain sensitivity parameters (MPS, WUR), PCA component scores and loadings cannot be assigned a uniform clinical meaning without consulting the interpretation of each contributing parameter individually. No sign transformation was applied prior to PCA; the standard DFNS z-score convention is retained throughout. Component interpretation therefore requires explicit reference to the loading direction and the clinical meaning of each parameter, as described in the results.

3.2.3. Baseline PCA and longitudinal projection

PCA procedure

PCA was applied to baseline standardized QST z-scores from all participants with complete baseline data ($n = 12$) to identify dominant axes of sensory variance and to position individual patients within a multivariate sensory space, rather than to evaluate isolated parameters.

No rotational transformation was applied, as the objective was to describe the dominant variance structure in its natural form rather than to optimize the presentation of results.

Component retention

Component retention was based on the proportion of variance explained and the interpretability of loading patterns; the scree plot (Appendix E) was inspected as a supplementary check. Loading patterns refer to the weights assigned to each QST parameter within a component, indicating how strongly and in which direction each parameter contributes to that component. Parameters with high absolute loadings are the primary contributors and allow the component to be interpreted in terms of recognizable somatosensory dimensions.

Automated retention methods such as the Kaiser criterion and parallel analysis were not used as primary criteria: the Kaiser criterion is known to be unreliable in practice [58], and parallel analysis is sensitive to sampling variability at the observation-to-variable ratio present in this cohort ($n = 12$, 11 variables). PC1 and PC2 were retained for descriptive interpretation based on the criteria described above. Subsequent components were not interpreted further.

Longitudinal projection

To explore whether somatosensory organization changed following SCS, six-month QST data from participants with complete follow-up assessments were projected onto the baseline PCA space ($n = 10$, excluding two participants without T3 QST data: SCI-007 and SCI-012). This approach was preferred over fitting a joint PCA to the combined T0 and T3 data, because inter-individual variability in QST z-scores substantially exceeds within-patient change over time in this cohort. A joint PCA would therefore be dominated by between-patient differences, suppressing the within-patient longitudinal change that

is the dimension of interest for this aim. Instead, the component structure derived from baseline data was used as a fixed reference frame onto which follow-up data were projected, preserving the baseline sensory dimensions and respecting the paired structure of the data.

To quantify the magnitude of individual trajectories, two distance measures were calculated, both based on the Euclidean distance, that is, the straight-line distance between two points in the PC1-PC2 space. First, the distance from the origin was calculated for each participant at T0 and T3, where the origin represents the absence of side-to-side asymmetry; a decrease in this distance indicates movement toward somatosensory symmetry, regardless of the direction of displacement. Second, the distance between T0 and T3 positions was calculated as the magnitude of the within-patient shift in the PCA space, irrespective of its direction relative to the origin.

Visualization

Results are presented as a biplot of the PC1-PC2 space. Each participant is represented as a point, with loading vectors displayed as arrows indicating the direction and magnitude of each QST parameter's contribution to the components. Points are color-coded by responder status ($\geq$30% NRS reduction at six months) [36]. For the longitudinal analysis, T0 and T3 positions are distinguished by symbol and color, with paired observations connected by lines per participant.

3.2.4. Univariate analysis of QST change

ΔZ-score computation

To examine whether individual QST parameters changed systematically following SCS, within-patient ΔZ-scores were computed as $\Delta Z = Z_{T3} - Z_{T0}$ for each of the 11 parameters separately. Only participants with complete paired T0 and T3 data were included ($n = 10$).

Because z-scores reflect the deviation of the affected side from the contralateral side, a ΔZ moving toward zero indicates a reduction in side-to-side asymmetry following SCS, regardless of the direction of the baseline deviation. A ΔZ moving away from zero indicates an increase in asymmetry.

Statistical testing

For each parameter, a Wilcoxon signed-rank test was used to assess whether the median ΔZ differed from zero. This non-parametric test was chosen given the small sample size and the absence of assumptions about the distribution of ΔZ. The median ΔZ with IQR is reported as the primary effect measure, as it directly quantifies the magnitude of change in somatosensory asymmetry in units of the reference standard deviation. Holm correction was applied across the 11 parameters to control the type I error rate across multiple comparisons, and was preferred over Bonferroni correction as it is uniformly more powerful while providing equivalent familywise error control [59]. Given the small sample size and the resulting limited statistical power, non-significant results should not be interpreted as evidence of absence of change. Both uncorrected and Holm-corrected p-values are reported in the Appendix.

ΔZ-score PCA

To explore whether changes in individual QST parameters following SCS were correlated across patients, suggesting shared underlying dimensions of somatosensory change, PCA was additionally applied to the matrix of ΔZ scores ($n = 10$ participants $\times$ 11 parameters). Prior to PCA, ΔZ scores were standardized using the same procedure described in Section 3.2.2.

The same component retention criteria were applied as described for the baseline PCA (Section 3.2.3). It is noted that PCA maximizes variance across participants and therefore describes how patients differ in their pattern of somatosensory change, rather than identifying parameters that change uniformly across the cohort. The latter question is addressed by the Wilcoxon analysis described above.

Visualization

Results of the univariate analysis are presented as a forest plot with one row per QST parameter, showing individual patient trajectories as thin lines and the group median ΔZ with interquartile range as a filled marker with whiskers. A vertical reference line at zero indicates no change. Parameters are color-coded by somatosensory domain. Results of the ΔZ PCA are presented as a biplot of the PC1-PC2 space, with loading vectors as arrows and participants color-coded by responder status.

3.2.5. Conditioned Pain Modulation analysis

CPM protocol

CPM was assessed using a cold pressor test. The conditioning stimulus consisted of immersion of a non-symptomatic limb segment on the affected side in cold water maintained between 1-4°C for a maximum duration of 120 seconds or until intolerance. Test stimuli were applied at the index finger of the non-affected hand and included electrical pain threshold (EPT), electrical pain tolerance threshold (EPTT), and pressure pain threshold (PPT), applied sequentially in that order (Figure 3.1).

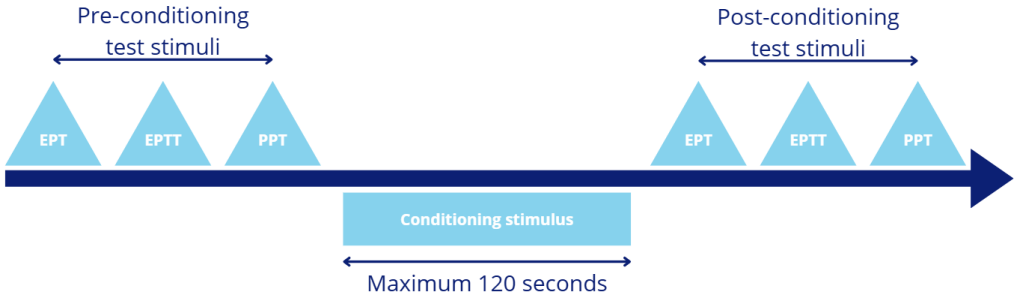

Figure 3.1: Schematic overview of the conditioned pain modulation protocol. Three baseline test stimuli (EPT, EPTT, PPT) were applied prior to the conditioning stimulus, consisting of cold water immersion for a maximum of 120 seconds. Three post-conditioning test stimuli were applied immediately following offset of the conditioning stimulus. EPT = electrical pain threshold, EPTT = electrical pain tolerance threshold and PPT = pressure pain threshold.

Applying test stimuli to the non-affected side while conditioning on the affected side avoids direct interaction with the symptomatic region while still capturing central inhibitory modulation, which operates systemically rather than locally.

For each modality, three baseline measurements were obtained before conditioning and three repeated measurements were obtained immediately following the conditioning stimulus. Mean pre- and post-conditioning values were used for analysis.

CPM effect quantification

The magnitude of the CPM effect was calculated as:

$$\Delta T = \overline{T}_{\text{post}} - \overline{T}_{\text{pre}}$$

where T represents the respective pain threshold (EPT, EPTT, or PPT). A positive ΔT indicates an increase in threshold during conditioning and is interpreted as inhibitory modulation, whereas a negative value reflects facilitation.

To assess whether the observed change exceeded within-session measurement variability, a 95% confidence interval for ΔT was calculated per individual using a Welch-adjusted standard error. This approach was preferred over percentage-based thresholds because it accounts for within-session variability and heterogeneity in variance between the pre- and post-conditioning series without requiring an arbitrary cutoff. In cases where repeated measurements within a series were identical (as with SCI-010 at T0 and SCI-002 at T3), the standard deviation of that series equalled zero. When this occurred in both series simultaneously, ΔT was computed as the difference between the two means. A confidence interval of [0, 0] was assigned, resulting in classification as uncertain.

Classification, visualization and statistical testing

CPM was classified as inhibitory when the confidence interval lay entirely above zero, facilitatory when entirely below zero, and uncertain when crossing zero. Group-level CPM effects were summarized descriptively. Longitudinal changes between baseline and six-month follow-up were evaluated descriptively at the individual level.

Results are presented as a forest plot displaying individual 95% confidence intervals for ΔT per participant and modality, with a vertical reference line at zero. A summary diamond below the individual confidence intervals represents the median of the individual ΔT point estimates, and the left and right

tips represent the IQR. This diamond serves as a descriptive visual reference only and should not be interpreted as a confidence interval around the median. Separate panels are shown for baseline and six-month follow-up to facilitate longitudinal comparison.

Paired Wilcoxon signed-rank tests were applied to ΔT values per modality to assess whether CPM effects changed significantly between baseline and six-month follow-up ($n = 10$). Holm correction was applied across the three modalities, consistent with the approach used for the univariate QST analysis in Section 3.2.4.

3.2.6. Integration with treatment response

Aim 5 did not require a separate analytical procedure. Findings from the analyses from aims 1–4 were integrated descriptively by comparing baseline somatosensory profile, longitudinal somatosensory change, and CPM classification between responders and the non-responder.

3.3. Results

The following results address the five aims described in Section 3.2.1, in the order in which the analyses were performed.

3.3.1. Baseline multivariate somatosensory structure

Explained variance and component structure

PCA performed on baseline QST data ($n = 12$) demonstrated that PC1 explained 31.7% of total variance and PC2 explained 22.7%, together accounting for 54.4% of the variance within the dataset. This indicates structured but multidimensional sensory variability within the cohort. Loading patterns are shown in Appendix D (FigureD.1).

PC1: sensory loss versus thermal asymmetry and mechanical sensitization

Inspection of loading patterns (Appendix D) showed that PC1 was characterized by opposing contributions of two parameter groups. Positive loadings were observed for PPT, VDT, CPT and MPT, whereas CDT, WDT, MDT, MPS, and WUR loaded negatively. In the DFNS convention, positive z-scores for PPT, VDT, and MPT indicate elevated thresholds on the affected side, reflecting sensory loss, whereas positive z-scores for MPS and WUR indicate greater pain sensitivity, reflecting sensitization. PC1 therefore represents a dominant axis opposing a profile in which the affected side shows elevated detection and pain thresholds, consistent with sensory loss, against a profile characterized by thermal detection asymmetry and mechanical sensitization. Positive PC1 scores reflect relatively elevated thresholds on the affected side (PPT, VDT, MPT), whereas negative PC1 scores reflect relatively greater thermal asymmetry and mechanical sensitization (CDT, WDT, MDT, MPS, WUR).

PC2: thermal sensory loss versus mechanical sensitization

PC2 was primarily driven by strong positive loadings for TSL, WDT, CPT and HPT. In the DFNS convention, positive z-scores for these parameters indicate elevated thermal detection and heat pain thresholds on the affected side, reflecting thermal sensory loss. Mechanical and dynamic pain measures including MPS, WUR, VDT and MPT contributed negatively to PC2. PC2 therefore captures a dimension differentiating profiles dominated by thermal sensory loss from profiles characterized by mechanical sensitization.

As principal components represent linear combinations of correlated variables, these axes should be interpreted as dimensions of shared variance rather than discrete clinical phenotypes.

Distribution of participants in the PC1-PC2 space

The distribution of participants within the PC1-PC2 space is shown in Figure 3.2. Individuals were distributed continuously without evidence of discrete clustering, supporting a dimensional rather than categorical organization of sensory heterogeneity. Most participants clustered around the origin, indicating broadly comparable multivariate sensory configurations, whereas several individuals demonstrated peripheral positioning relative to this central distribution.

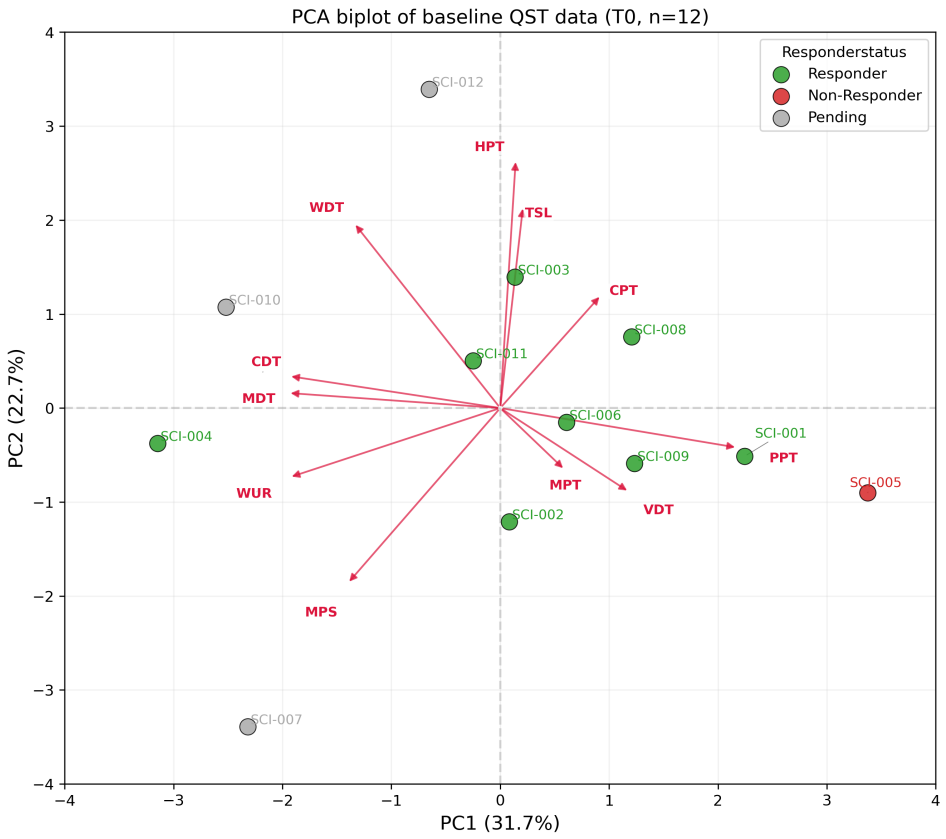

Figure 3.2: PCA biplot of baseline QST data (T0, $n = 12$). Each point represents an individual participant positioned according to PC1 and PC2 scores, color-coded by responder status ($\geq$30% NRS reduction at six months) [36]. Arrows indicate variable loadings. PC1 explained 31.7% and PC2 explained 22.7% of total variance. Loading directions should be interpreted in conjunction with the DFNS z-score convention: positive z-scores indicate sensory loss for threshold parameters and sensitization for MPS and WUR.

In interpreting the positions in Figure3.2, positive PC1 scores indicate relatively elevated thresholds (PPT, VDT, MPT) and negative PC1 scores indicate thermal asymmetry and mechanical sensitization (CDT, WDT, MDT, MPS, WUR); see Section 3.2.2 for the z-score convention.

Relative positioning reflected the loading structure described above. SCI-005 occupied the most extreme position along the positive PC1 axis, indicating relatively elevated thresholds for PPT, VDT, and MPT on the affected side, consistent with a profile dominated by sensory loss rather than sensitization. This participant was the only non-responder in the cohort and was visually separated from all other participants. SCI-004 was positioned at the negative extreme of PC1, indicating a profile dominated by thermal detection asymmetry and mechanical sensitization. SCI-012 demonstrated the highest PC2 score within the cohort, indicating a profile with relatively greater thermal sensory loss contributions. SCI-007, included in the baseline PCA but without six-month follow-up data, occupied a peripheral position at the negative extreme of PC2, indicating a profile with relatively greater mechanical sensitization contributions along that dimension. Other participants occupied intermediate positions around the cohort centroid, reflecting more balanced somatosensory configurations. Complete side-to-side z-scores per participant at baseline and six-month follow-up are provided in Appendix F.

3.3.2. Longitudinal changes in multivariate somatosensory structure

Individual trajectories within the PC1-PC2 space are shown in Figure 3.3. SCI-007 and SCI-012 did not have T3 QST data available and were therefore not projected ($n = 10$). Individual PCA scores and Euclidean distances are provided in Appendix G.

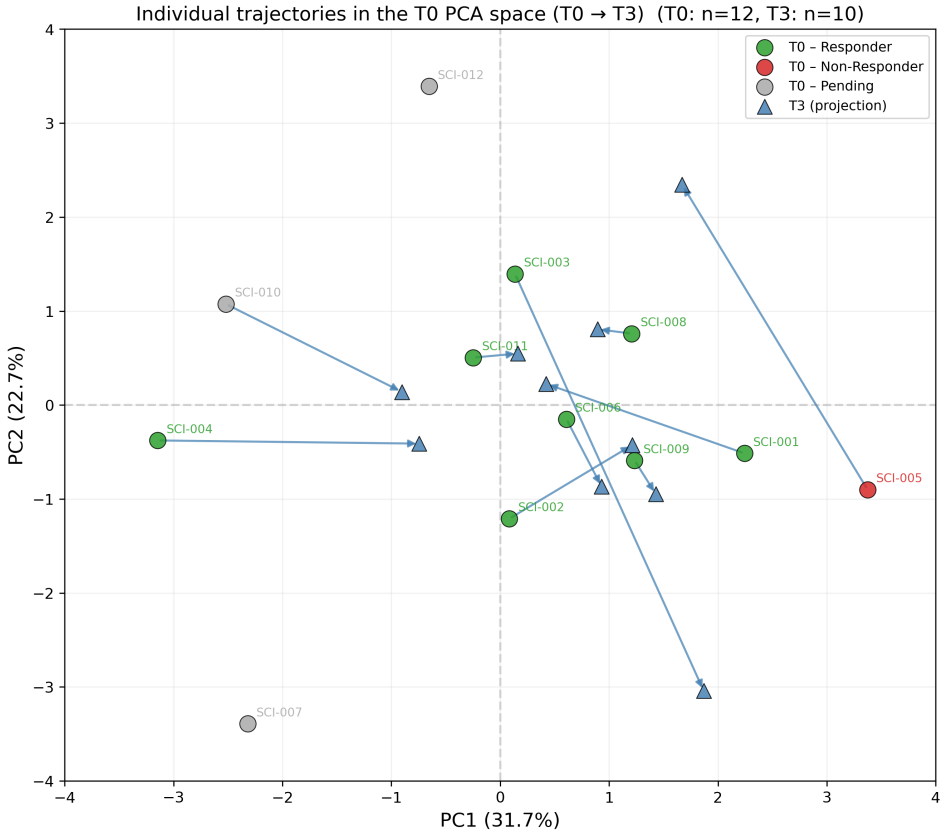

Figure 3.3: Individual trajectories in the PCA space between baseline (T0, circles) and six-month follow-up (T3, triangles). Lines connect paired observations per participant. T3 data were projected onto the component structure derived from baseline data ($n = 10$; SCI-007 and SCI-012 excluded due to absence of T3 QST data).

Group-level pattern

Across the cohort, the direction and magnitude of T0→T3 shifts were heterogeneous, with no uniform directional change at the group level. The Euclidean displacement between T0 and T3 positions ranged from 0.32 (SCI-008) to 4.76 (SCI-003), indicating substantial inter-individual variability in the degree of somatosensory reorganization following SCS.

Despite this heterogeneity, five of ten participants showed a decrease in Euclidean distance from the origin between T0 and T3, ranging from -0.22 (SCI-008) to -2.32 (SCI-004). Given that the origin represents the absence of side-to-side asymmetry, this pattern is broadly consistent with a reduction in somatosensory asymmetry following SCS in a subset of the cohort. Three participants showed a meaningful increase in distance from the origin: SCI-003 (Δ distance $= +2.17$), SCI-006 (Δ distance $= +0.65$) and SCI-009 (Δ distance $= +0.35$). Two participants showed negligible change in distance from the origin: SCI-002 (Δ distance $= +0.07$) and SCI-011 (Δ distance $= +0.01$).

Notable individual trajectories

SCI-003 demonstrated the largest Euclidean displacement (4.76), shifting from a positive PC2 position at baseline toward a strongly negative PC2 at follow-up, while also moving toward positive PC1. Given the loading structure, this trajectory corresponds to a shift from a profile with relatively greater thermal sensory loss contributions toward a profile with greater mechanical sensitization relative to thermal parameters. The distance from the origin increased by $+2.17$, indicating greater overall somatosensory asymmetry at follow-up despite a 50% reduction in NRS. This dissociation indicates that movement toward somatosensory symmetry is not a necessary condition for clinical response.

SCI-005 demonstrated the second largest displacement (3.67). At baseline, this participant occupied the most extreme positive PC1 position in the cohort, reflecting a profile characterized by elevated detection and pain thresholds with limited sensitization. At follow-up, the position shifted toward the positive

PC2 pole, reflecting greater thermal sensory loss contributions relative to mechanical parameters. The distance from the origin decreased by only -0.61, indicating that despite a pronounced redistribution of the multivariate sensory profile, the overall degree of somatosensory asymmetry remained largely unchanged. SCI-005 was the only non-responder in the cohort.

SCI-004, **SCI-001** and **SCI-010** showed the largest reductions in Euclidean distance from the origin (-2.32, -1.82 and -1.83 respectively), all shifting toward more symmetric somatosensory profiles. SCI-004 and SCI-001 were both complete responders with 100% NRS reduction. The six-month NRS assessment for SCI-010 is currently pending re-evaluation following a subsequent surgical intervention, and a definitive clinical classification is therefore not yet available.

3.3.3. Univariate analysis of QST change

No statistically significant change was observed for any of the 11 QST parameters following SCS after Holm correction for multiple comparisons. Individual ΔZ trajectories and group medians are shown in Figure 3.4. Complete results including median ΔZ, IQR, and p-values are provided in Appendix H.

Across parameters, individual trajectories were heterogeneous, with substantial within-parameter variability reflected by wide IQR. The largest absolute median shifts were observed for MPT (median $\Delta Z = -1.31$, IQR -4.17 to 0.91; $p = 0.432$) and PPT (median $\Delta Z = 0.96$, IQR -0.78 to 2.32; $p = 0.695$), indicating a tendency toward increased mechanical pain sensitivity and increased pressure pain threshold respectively on the affected side relative to the contralateral side, though neither reached statistical significance. WDT showed the largest median shift among thermal detection parameters (median $\Delta Z = -0.38$, IQR -1.33 to 0.28; $p = 0.193$). Parameters reflecting dynamic pain modulation (WUR, median $\Delta Z = 0.04$) and thermal pain thresholds (TSL, median $\Delta Z = -0.02$; HPT, median $\Delta Z = 0.12$) showed median values close to zero with wide IQR, indicating no consistent directional change at the group level.

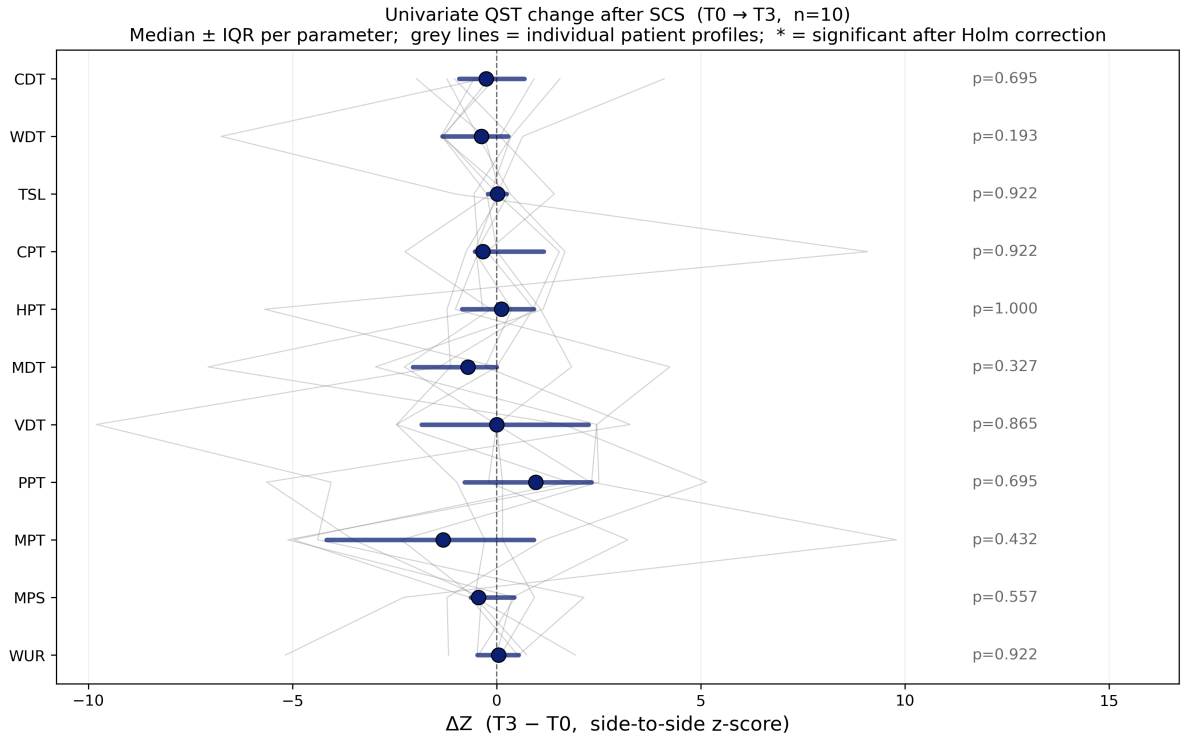

Figure 3.4: Univariate QST change following SCS (T0 $\rightarrow$ T3, $n = 10$). Each row represents one QST parameter. Grey lines indicate individual patient ΔZ trajectories. Colored markers represent the group median ΔZ per parameter with horizontal bars indicating the interquartile range. Parameters are color-coded by somatosensory domain. A vertical dashed line at zero indicates no change. Uncorrected p-values are shown on the right; no parameter reached statistical significance after Holm correction.

3.3.4. ΔZ-score PCA

PCA applied to the matrix of standardized ΔZ scores ($n = 10$) demonstrated that PC1 explained 33.2% of total variance and PC2 explained 27.5%, together accounting for 60.7% of the variance in somatosensory change patterns across participants. Loading patterns are shown in Appendix D (FigureD.2).

PC1: thermal parameters and sensitization versus mechanical and cold detection thresholds

PC1 was characterized by opposing contributions of two parameter groups. Positive loadings were observed for TSL, HPT, MPS, WUR and WDT, whereas VDT, MPT, PPT, CPT and MDT loaded negatively. Given the DFNS convention, a positive ΔZ for thermal detection parameters (WDT, TSL) indicates increasing asymmetry in the direction of thermal loss following SCS, positive ΔZ for HPT indicates increasing heat pain threshold asymmetry, and positive ΔZ for MPS and WUR indicates increasing mechanical sensitization. Negative ΔZ for CPT, MDT, VDT, PPT, and MPT indicates decreasing thresholds on the affected side relative to baseline. PC1 therefore represents a dominant axis along which participants differed in their pattern of somatosensory change following SCS, with thermal asymmetry and sensitization parameters on one side and decreasing mechanical and cold detection thresholds on the other.

PC2: mechanical sensitization versus thermal and mechanical threshold changes

PC2 was primarily driven by positive loadings for CPT, MPS and WUR, with negative loadings for most remaining parameters, particularly WDT, HPT, CDT and MPT. Given the DFNS convention, positive ΔZ for CPT indicates increasing cold pain threshold asymmetry, while positive ΔZ for MPS and WUR reflects increasing mechanical sensitization and wind-up. Negative loadings for CDT, WDT, HPT, and MPT indicate that participants at the negative extreme of PC2 showed broad changes across thermal detection and mechanical pain thresholds. PC2 therefore captures a dimension differentiating participants whose change pattern was dominated by increasing mechanical sensitization and wind-up from those showing broad changes across thermal and mechanical parameters. Given the parameter-dependent directionality of the DFNS z-score convention, this axis does not represent a clinically uniform contrast; interpretation requires explicit reference to the clinical meaning of each contributing parameter individually (see Section 3.4.7).

Distribution of participants in the ΔZ PC1-PC2 space

The distribution of participants within the ΔZ PC1–PC2 space is shown in Figure 3.5. The majority of participants clustered around the origin, indicating broadly comparable and modest patterns of somatosensory change. Three participants occupied peripheral positions. Given the parameter-dependent directionality of the DFNS z-score convention, individual positions in the PC1-PC2 space were interpreted in conjunction with the raw ΔZ scores per participant (Appendix F).

SCI-003 was positioned at the negative extreme of PC1 with high positive PC2. Inspection of raw ΔZ scores revealed that this position was primarily driven by a large increase in cold pain threshold asymmetry (CPT $\Delta Z = 9.09$) and marked decreases in warm detection threshold asymmetry (WDT $\Delta Z = -6.75$) and heat pain threshold asymmetry (HPT $\Delta Z = -5.69$), reflecting a change pattern dominated by thermal parameters. The large ΔZ for CPT reflects a reversal of asymmetry direction, from a negative z-score at baseline ($z = -4.48$) to a positive z-score at follow-up ($z = 4.61$), rather than a unidirectional increase. Mechanical sensitization parameters showed minimal change (MPS $\Delta Z = 0.93$, WUR $\Delta Z = 0.10$).

SCI-010 occupied the negative extreme of both PC1 and PC2, driven primarily by a large increase in mechanical pain threshold asymmetry (MPT $\Delta Z = 9.79$) and mechanical detection threshold asymmetry (MDT $\Delta Z = 4.24$), alongside decreases in wind-up ratio (WUR $\Delta Z = -5.17$) and mechanical pain sensitivity (MPS $\Delta Z = -2.28$), reflecting a change pattern of decreasing mechanical sensitization alongside increasing mechanical detection thresholds. The large increase in MPT asymmetry reflects a new asymmetry that was absent at baseline ($z = -0.73$), with the affected side showing markedly elevated mechanical pain thresholds at follow-up ($z = 9.06$).

SCI-005 occupied the most extreme positive PC1 position. At baseline, this participant showed a markedly elevated VDT asymmetry ($z = 9.80$), indicating substantially higher vibration detection thresholds on the affected side. At follow-up, this asymmetry decreased substantially (VDT $\Delta Z = -9.80$),

reflecting near-complete normalization toward the contralateral side rather than a new deficit. The position of SCI-005 on PC1 was further driven by decreases in mechanical pain threshold asymmetry (MPT $\Delta Z = -4.38$) and pressure pain threshold asymmetry (PPT $\Delta Z = -4.05$), with a modest increase in mechanical pain sensitivity (MPS $\Delta Z = 2.14$) and thermal asymmetry (TSL $\Delta Z = 1.41$).

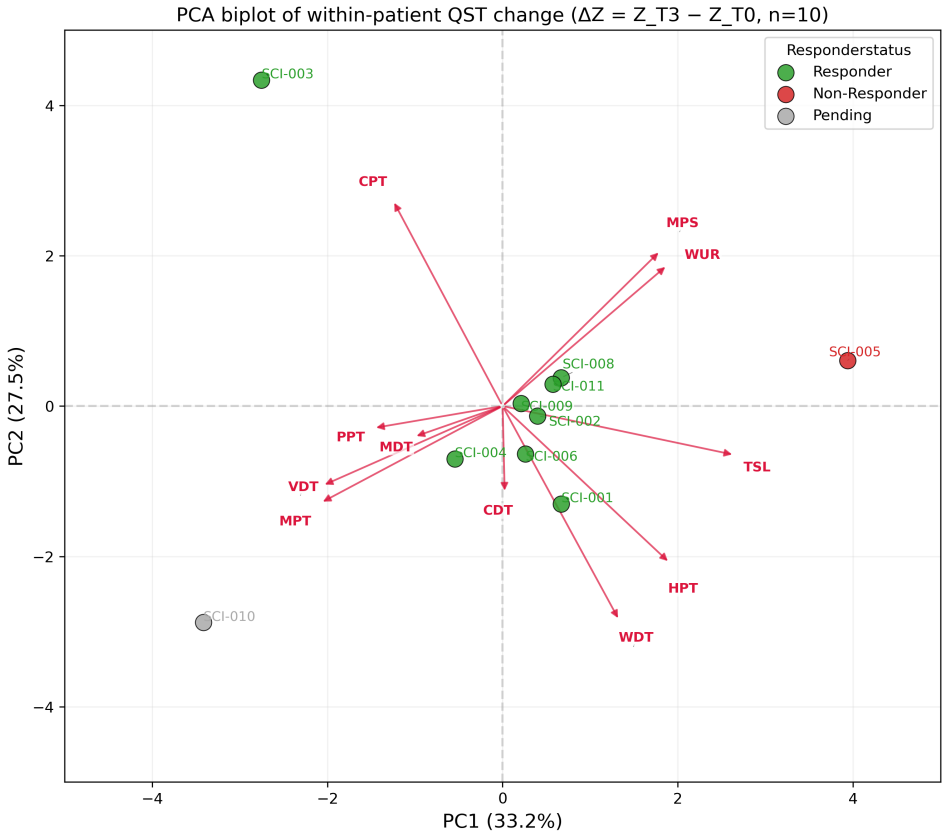

Figure 3.5: PCA biplot of within-patient QST change ($\Delta Z = Z_{T3} - Z_{T0}$, $n = 10$). Each point represents an individual participant positioned according to PC1 and PC2 scores, color-coded by responder status. Arrows indicate variable loadings. PC1 explained 33.2% and PC2 explained 27.5% of total variance. Loading directions should be interpreted in conjunction with the DFNS z-score convention as described in Section 3.2.2.

3.3.5. Endogenous pain modulation

Baseline CPM

At baseline ($n = 12$), CPM responses were heterogeneous across individuals and modalities (Figure 3.6a). For EPT, four participants showed inhibitory modulation (CI entirely above zero), whereas the remaining participants were classified as uncertain due to confidence intervals crossing zero. Within the uncertain group, several participants demonstrated point estimates on the positive side with lower bounds close to zero, indicating a trend toward inhibition that did not exceed within-session variability.

A comparable distribution was observed for EPTT, with inhibitory CPM present in four participants and uncertain responses in the remainder. Importantly, inhibitory classification did not consistently overlap between EPT and EPTT, indicating limited intra-individual consistency across electrical modalities.

For PPT, all participants were classified as uncertain at baseline, with confidence intervals crossing zero throughout, and no clear inhibitory or facilitatory pattern at the group level.

Longitudinal change in CPM

Follow-up data at T3 are shown in Figure 3.6b. Electrical modalities (EPT and EPTT) showed variable within-subject trajectories without a uniform directional shift across individuals.

In contrast, PPT at follow-up visually suggested a shift toward more positive ΔT values in most participants compared to baseline. Several individuals showed confidence intervals entirely above zero,

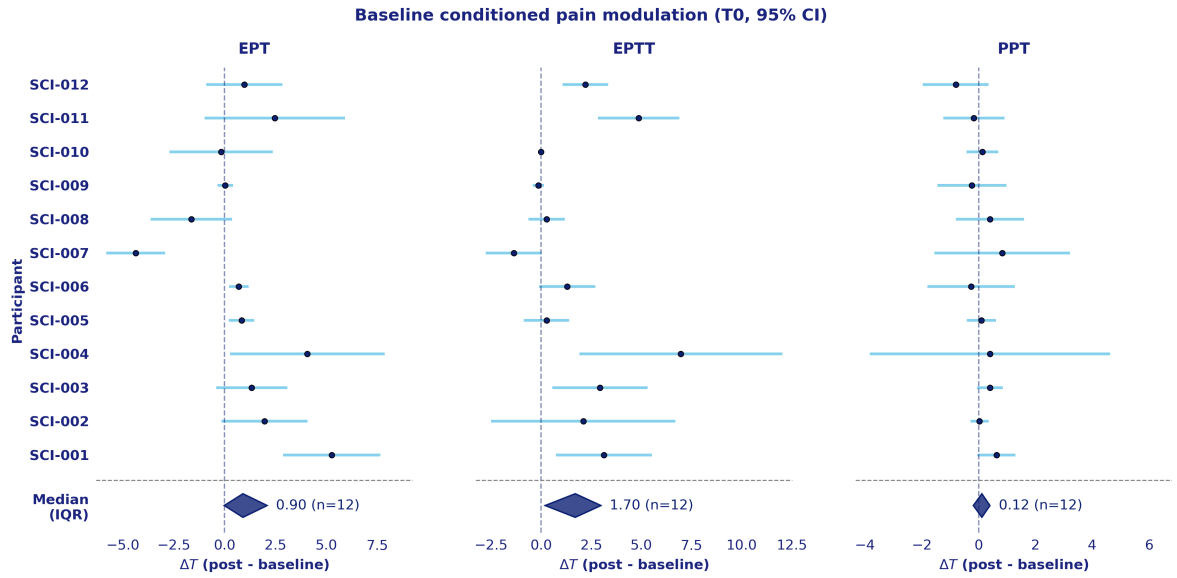

(a) Baseline CPM (T0, $n = 12$, 95% CI).

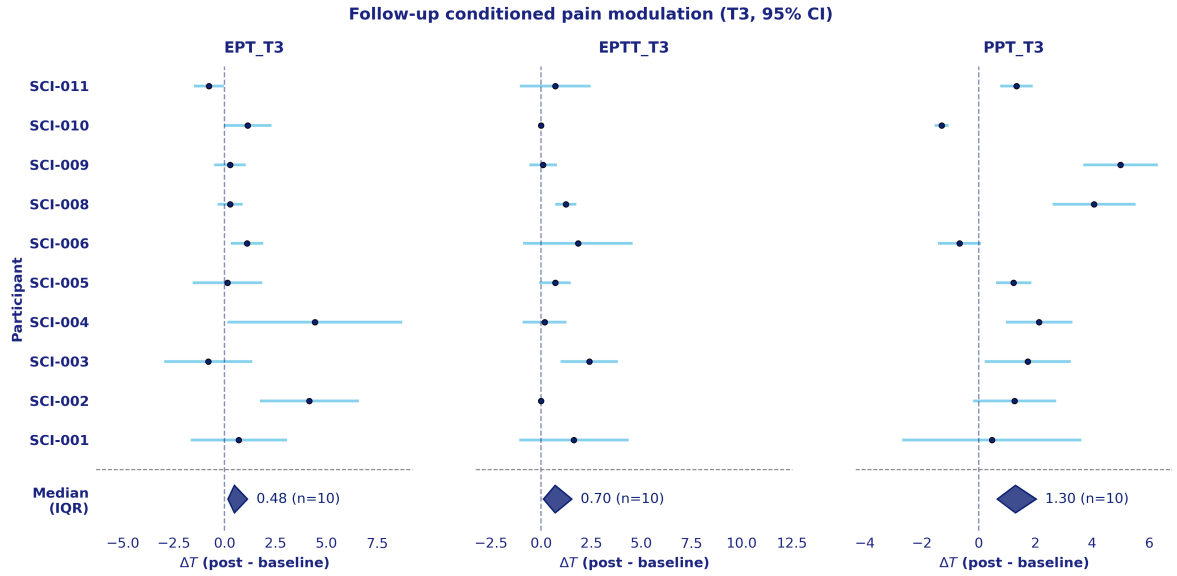

(b) Six-month follow-up CPM (T3, $n = 10$, 95% CI).

Figure 3.6: Individual 95% confidence intervals for CPM effects at baseline (A) and six-month follow-up (B). Each horizontal line represents the confidence interval of ΔT (post-conditioning minus pre-conditioning threshold) per participant; the vertical line at zero indicates no change. Intervals entirely above zero indicate inhibitory modulation; intervals crossing zero indicate uncertain responses. The diamond below the dashed line represents the median (centre) and interquartile range (width) of individual ΔT point estimates and serves as a visual reference for comparison between timepoints only; it does not represent a confidence interval around the median.

consistent with inhibitory modulation, whereas SCI-001 did not show this shift and remained close to the no-change line. A paired Wilcoxon signed-rank test indicated a non-significant trend toward greater inhibitory PPT-based CPM at six months (median ΔT 0.12 at T0 vs. 1.30 at T3, $p = 0.065$, Holm-corrected $p = 0.195$). Electrical modalities did not show a consistent directional shift (EPT: median ΔT 1.08 vs. 0.48, $p = 0.846$; EPTT: 1.70 vs. 0.70, $p = 0.250$; both Holm-corrected $p = 0.846$). Given the small sample size and absence of significance after correction, the PPT trend should be interpreted cautiously and is consistent with but does not confirm the hypothesis that SCS engages descending inhibitory pathways.

Individual CPM data per participant are provided in Appendix I.

3.3.6. Integration with treatment response

Somatosensory profile and treatment response

At baseline, responders as a group showed more central positioning in the PC1-PC2 space relative to the non-responder, clustering relatively closely around the cohort centroid. The responders have a median Euclidean distance from the origin of 1.40 (IQR 0.56-3.17), compared to 3.49 for SCI-005. The single non-responder (SCI-005) occupied the most extreme positive PC1 position, reflecting a profile characterized by elevated detection and pain thresholds with limited sensitization, and was visually separated from the central cluster of responders. The two complete responders with 100% NRS reduction (SCI-001 and SCI-004) illustrate the heterogeneity within the responder group: SCI-001 was positioned near the cohort centroid whereas SCI-004 occupied the negative extreme of PC1. Yet both achieved complete pain relief, indicating that no single somatosensory profile was consistently associated with favorable outcome.

Longitudinal somatosensory change and treatment response

Responders showed heterogeneous trajectories in Euclidean distance from the origin following SCS. Four of eight responders with T3 data demonstrated a clear reduction in Euclidean distance, two showed negligible change (SCI-002, Δ distance $= +0.07$; SCI-011, Δ distance $= +0.01$), and two showed a meaningful increase (SCI-003, Δ distance $= +2.17$; SCI-006, Δ distance $= +0.65$). The two complete responders (SCI-001 and SCI-004) both showed a shift toward the origin, with SCI-004 and SCI-001 demonstrating the largest reductions in Euclidean distance in the cohort (Δ distance $= -2.318$ and -1.823 respectively), consistent with marked reduction in somatosensory asymmetry following SCS. Both occupied central positions in the Δ PCA, indicating modest and broadly distributed change patterns. In contrast, SCI-005 showed only a small reduction in Euclidean distance from the origin (Δ distance $= -0.612$) and occupied the most extreme positive PC1 position in the Δ PCA, indicating a change pattern in which thermal asymmetry and sensitization parameters changed more than mechanical threshold parameters.

CPM and treatment response

No consistent pattern was observed linking baseline CPM classification to treatment response. At baseline, inhibitory CPM for electrical modalities was present in several responders, including both complete responders, but also in other participants across the cohort. The non-responder SCI-005 showed inhibitory modulation for EPT only at baseline, shifting to PPT only at follow-up. Longitudinal CPM changes were heterogeneous across individuals and no consistent directional shift was observed at the group level.

Overall pattern

Across all three sensory analyses, SCI-005 showed a consistent pattern of deviation from the responder group: an extreme sensory loss profile on PC1 at baseline, virtual absence of somatosensory normalization following SCS, and a change pattern dominated by decreasing mechanical threshold asymmetry rather than broad somatosensory normalization. No consistent pattern was observed linking baseline CPM classification to treatment response. Somatosensory organization and endogenous inhibitory modulation appeared to vary partly independently across individuals in this cohort. Given the small sample size and single non-responder available for comparison, these observations remain descriptive and hypothesis-generating.

3.4. Discussion

3.4.1. Principal findings

This chapter reported exploratory analyses of somatosensory organization and endogenous pain modulation in a prospective cohort of patients with refractory peripheral mononeuropathic pain treated with SCS. Three principal findings emerge from these analyses.

First, baseline somatosensory organization was heterogeneous across participants, with no evidence of discrete clustering. PC1 and PC2 distinguished profiles characterized by elevated detection thresholds with limited sensitization from profiles dominated by thermal asymmetry and mechanical sensitization. This is consistent with the expected heterogeneity of selective afferent fiber involvement in focal nerve injury.

Second, the single non-responder showed a consistent pattern of deviation from the responder group across three independent analyses, characterized by elevated detection thresholds, limited sensitization, and absence of somatosensory normalization following SCS. This pattern is consistent with the hypothesis that intact large-fiber afferent input may represent a relevant substrate for SCS efficacy, although this interpretation is based on a single non-responder and remains speculative.

Third, baseline CPM was variable and largely uncertain across modalities, with no consistent association with treatment response. Preliminary observations suggest a possible shift toward inhibitory PPT-based CPM following SCS, whereas electrical modalities showed no consistent directional change.

Taken together, these findings provide preliminary evidence that somatosensory heterogeneity in mononeuropathic pain may be structured along clinically interpretable dimensions and that certain somatosensory configurations may be associated with differential SCS response. Given the small sample size and the exploratory nature of all analyses, these observations are hypothesis-generating and require confirmation in larger prospective studies.

3.4.2. Somatosensory heterogeneity in mononeuropathy

The observed somatosensory heterogeneity in this cohort is consistent with the expected pathophysiology of peripheral mononeuropathy. Focal nerve injury can selectively affect different afferent fiber populations, producing profiles that range from predominant large-fiber loss to predominant small-fiber loss or mixed involvement [52, 53]. The dimensional rather than categorical organization of sensory variability observed in the PCA is consistent with this view and aligns with findings from large neuropathic pain cohorts demonstrating that sensory phenotypes in peripheral neuropathic pain vary along continuous rather than categorically distinct dimensions [13, 60].

The dominant axes identified by PCA reflected clinically interpretable dimensions. PC1 opposed profiles characterized by elevated detection and pain thresholds against profiles dominated by thermal asymmetry and mechanical sensitization. Because positive z-scores for detection threshold parameters reflect elevated thresholds on the affected side, indicating sensory loss, and positive z-scores for MPS and WUR reflect greater pain sensitivity, indicating sensitization, the opposing loading pattern of PC1 captures a clinically meaningful contrast between these two forms of somatosensory deviation. This suggests that the primary source of inter-individual variability in this cohort concerned the relative balance between sensory loss and sensitization [47, 52]. PC2 further distinguished profiles dominated by thermal sensory loss from those characterized by mechanical sensitization.

3.4.3. Somatosensory profile and treatment response

Hypothesis for the non-responder

The single non-responder (SCI-005) occupied a consistently peripheral position across three independent analyses, distinguished from the responder group by a somatosensory profile characterized by elevated side-to-side z-scores for detection and pain thresholds at baseline, virtual absence of somatosensory normalization following SCS, and a change pattern dominated by decreasing mechanical threshold asymmetry rather than broad somatosensory normalization. The consistency across analyses is notable given the small sample size and suggests that the multivariate somatosensory profile of this participant reflects a genuinely distinct configuration rather than random variation.

A mechanistically motivated interpretation of this pattern concerns the proposed role of large myeli-

nated Aβ-fiber projections in the dorsal column as the primary pathway for SCS-induced analgesia across multiple stimulation paradigms [7, 46]. VDT specifically reflects the function of large myelinated Aβ-fibers of the Pacinian corpuscle type [61, 62], which are particularly vulnerable to demyelination [63], and therefore provides a direct indicator of the integrity of the fiber population proposed to mediate SCS efficacy. SCI-005 showed a markedly elevated side-to-side z-score for VDT at baseline ($z = 9.80$; see Appendix F), indicating that the vibration detection threshold on the affected side was substantially higher than on the contralateral side. MDT, which also reflects large-fiber function but via mechanoreceptors sensitive to light touch rather than vibration [62], was less extreme within this cohort ($z = 2.54$, compared to a cohort median of 4.24; see Appendix F), suggesting that the large-fiber deficit in SCI-005 may be more pronounced for vibration than for light touch detection. This pattern is potentially consistent with selective demyelination rather than diffuse axonal loss, as the latter would be expected to affect both VDT and MDT comparably [63]. If Aβ-afferent input via the dorsal column pathway is functionally compromised, SCS-induced activation of that pathway may be limited, potentially reducing analgesic efficacy. This interpretation is anatomically supported by evidence that during SCS only a small fraction of dorsal column fibers are depolarized [64]. If the pool of available Aβ-fibers is already reduced by demyelination or axonal loss, as suggested by the markedly elevated VDT in this participant, the fraction of fibers that can be recruited by SCS may be insufficient to generate adequate inhibitory input. This would result in at most a partial analgesic effect.

However, this interpretation must be approached with considerable caution. Elevated detection thresholds may arise through multiple mechanisms, including axonal loss, demyelination, or central reorganization of somatosensory representation, and cannot be attributed to large-fiber dysfunction based on VDT alone. SCI-005 had a history of oncological treatment in the affected limb, which may have introduced additional contributions to somatosensory dysfunction beyond the focal mononeuropathy, as radiotherapy can cause peripheral nerve injury through axonal damage, demyelination, and radiation-induced fibrosis [65]. Furthermore, this interpretation rests on a single non-responder, and no direct measure of dorsal column integrity, such as somatosensory evoked potentials, was available in this cohort to corroborate this hypothesis.

Furthermore, all participants in this cohort showed abnormalities on electromyography, confirming the presence of peripheral nerve injury across the group. The distinct somatosensory profile of SCI-005 should therefore not be interpreted as evidence of unique or more severe nerve damage per se, but rather as a profile in which large-fiber sensory loss predominated over sensitization, in contrast to the more mixed profiles observed in the responder group. This qualitative difference in afferent involvement may be mechanistically relevant to SCS response, as discussed above.

Heterogeneity within the responder group

In the responder group, the two complete responders (SCI-001 and SCI-004) occupied markedly different positions in the PCA space, yet both achieved complete pain relief. This indicates that markedly different somatosensory profiles can be compatible with complete SCS response and that no single somatosensory profile can be identified as a necessary condition for favorable outcome. Evidence from pharmacological neuropathic pain trials similarly demonstrates that sensory phenotypes are associated with different treatment responses [13, 60], but the direction of this association varies across treatments and populations. This underscores the difficulty of predicting response from baseline sensory profiles alone.

3.4.4. Longitudinal changes in somatosensory organization

Somatosensory organization changed following SCS in the majority of participants, with five of ten showing a clear reduction in Euclidean distance from the origin of the baseline PCA space, while two participants showed negligible change. This pattern is broadly consistent with evidence from other neuromodulation populations suggesting that pain-related QST parameters can normalize following successful treatment [50, 54, 55].

An important mechanistic consideration is that SCS does not alter the underlying peripheral nerve lesion; the cause of the mononeuropathy remains intact. Changes in somatosensory organization following SCS are therefore expected to reflect modulation of central nociceptive processing rather than peripheral recovery. This limits the range of QST parameters expected to change in the univariate analysis. This interpretation is consistent with the broader literature characterizing SCS-induced

QST changes as modest and inconsistent [51]. The absence of significant univariate changes should therefore not be interpreted as evidence of absence of somatosensory reorganization; the multivariate longitudinal analysis demonstrates meaningful within-patient shifts in the PCA space that are not captured by individual parameter tests. The hypothesis that SCS would preferentially affect parameters reflecting dynamic pain processing and central sensitization, such as WUR and mechanical pain thresholds, was not supported: median shifts for WUR and MPT were modest and neither reached statistical significance after Holm correction.

Individual patterns of change

The two participants with the largest multivariate displacements illustrate the complexity of this relationship. SCI-003 achieved a 50% reduction in NRS despite an increase in Euclidean distance from the origin, indicating that movement toward somatosensory symmetry is not a necessary condition for clinical response. SCI-005, the only non-responder, showed only a marginal reduction in Euclidean distance from the origin. Taken together, these observations suggest that somatosensory normalization may not be required for clinical response, but its near-complete absence, as in SCI-005, may nonetheless be associated with lack of response. These patterns are hypothesis-generating and cannot be interpreted causally given the small sample size.

The ΔZ PCA further demonstrated that patients differed substantially in their pattern of somatosensory change. SCI-005 showed a change pattern dominated by decreasing mechanical threshold asymmetry rather than broad somatosensory normalization, in contrast to the modest and broadly distributed change patterns observed in most responders, who clustered around the origin of the ΔZ PC1-PC2 space. The hypothesis that responders would show preferential reduction in somatosensory asymmetry was only partially supported: although several responders showed a decrease in Euclidean distance from the origin, SCI-003 demonstrated the opposite pattern despite achieving 50% pain reduction, indicating that somatosensory normalization is not a necessary condition for clinical response. These differences suggest that SCS does not exert a uniform effect on somatosensory processing, and raise the hypothesis that the dimensions of somatosensory change may depend on the individual's baseline configuration.

3.4.5. Endogenous pain modulation

Baseline CPM

Baseline CPM was heterogeneous and largely classified as uncertain across modalities, with inhibitory modulation present in only a subset of participants for electrical modalities and absent for PPT. This pattern is consistent with evidence that chronic neuropathic pain is frequently associated with variable or impaired endogenous pain inhibition [14]. The heterogeneity observed here may reflect both genuine inter-individual differences in descending inhibitory capacity and methodological variability inherent to CPM assessment [66].

Because both test and conditioning stimuli were applied to non-symptomatic body segments, the CPM measurements are unlikely to reflect local peripheral nerve dysfunction at the site of the mononeuropathy. Rather, they capture central inhibitory modulation operating systemically via supraspinal descending pathways, providing a measure of endogenous inhibitory capacity that is independent of the local peripheral pathology.

A methodological consideration concerns the sequential ordering of test stimuli within the CPM protocol. PPT was assessed after EPT and EPTT, introducing a delay of several minutes between the end of the conditioning stimulus and the PPT measurement. Evidence suggests that CPM hypoalgesia diminishes over time following the offset of the conditioning stimulus [67], which may have attenuated the PPT-based CPM effect at baseline. This represents a methodological limitation that should be addressed in future studies by applying a parallel rather than sequential paradigm for PPT, or by reducing the interval between conditioning offset and PPT measurement.

Longitudinal change in CPM

A preliminary shift toward inhibitory PPT-based CPM was observed following SCS, whereas electrical modalities showed no consistent directional change. Although the sequential ordering of test stimuli may have attenuated the PPT-based CPM effect at baseline, this limitation applies equally to the six-month assessment, where the same testing order was maintained. The observation of inhibitory PPT-

based CPM at follow-up in the absence of such a pattern at baseline therefore cannot be attributed to procedural differences between timepoints, and is more likely to reflect a genuine longitudinal change in endogenous inhibitory capacity.

This pattern is consistent with the hypothesis that SCS activates descending inhibitory pathways, thereby improving endogenous inhibitory capacity [45]. The preferential effect on PPT over electrical modalities may be explained by differences in the degree to which each test stimulus depends on synaptic integration in the dorsal horn. A possible explanation is that mechanically evoked nociceptive input, as assessed by PPT, may be more sensitive to SCS-induced modulation of dorsal horn circuitry than directly electrically evoked pain thresholds, which activate peripheral nerve fibers more directly. However, direct empirical support for this differential sensitivity is lacking and this interpretation remains speculative.

A complementary explanation is provided by Reinders et al., who demonstrated that tonic SCS reduces cortical evoked responses to painful stimuli before CPM, suggesting that SCS may already partially engage the descending pain pathway and thereby limit the additional inhibitory capacity available to CPM for electrically evoked stimuli [68]. Under this framework, the absence of a clear CPM effect for electrical modalities after SCS does not necessarily reflect impaired descending inhibition, but may instead reflect that SCS itself already occupies part of that inhibitory capacity.

Given the preliminary nature of these observations and the small sample size, these findings remain hypothesis-generating and should be interpreted with caution.

3.4.6. Relationship between somatosensory organization and endogenous pain modulation

Visual inspection of baseline PCA positioning and CPM classification did not reveal a consistent association between multivariate somatosensory organization and endogenous inhibitory capacity. Participants with profiles dominated by detection loss, such as SCI-005, did not show a uniform CPM pattern, and participants with pronounced mechanical sensitization, such as SCI-004, did not consistently differ in inhibitory capacity from other participants.

This absence of a clear association suggests that somatosensory organization and endogenous pain modulation represent partly independent dimensions of nociceptive processing in this cohort. This is consistent with evidence from De Schoenmacker et al., who demonstrated that sensory phenotypes identified by cluster analysis were not straightforwardly linked to CPM profiles across chronic pain cohorts [69]. The two dimensions may reflect distinct aspects of the nociceptive system, peripheral and spinal somatosensory function on the one hand, and supraspinal descending modulatory capacity on the other, that can vary independently depending on the underlying pathophysiology.

From a clinical perspective, this independence has implications for patient characterization prior to SCS. If somatosensory profile and CPM efficiency provide complementary rather than redundant information, a comprehensive pre-implantation assessment combining both dimensions may offer greater predictive value than either measure alone. This hypothesis warrants investigation in larger prospective cohorts with sufficient statistical power to examine their joint contribution to treatment response.

3.4.7. Methodological limitations

Several methodological limitations must be acknowledged when interpreting the findings of this chapter.

Sample size and PCA stability

The most fundamental limitation concerns sample size. Although twelve participants were enrolled, only ten completed six-month follow-up and were included in the longitudinal analyses. The baseline PCA was performed on all twelve participants, but the PCA component structure remains sensitive to individual observations at this sample size, and the addition or removal of a single participant could meaningfully alter the axes of variance. The exploratory analyses were therefore not designed to yield stable or generalizable sensory phenotypes, and all observations should be interpreted as hypothesis-generating rather than confirmatory.

The DFNS z-score convention assigns direction-dependent clinical meaning to z-score deviations: positive values indicate sensory loss for threshold parameters but sensitization for pain sensitivity parame-

ters (MPS, WUR). This heterogeneity in directional meaning across parameters means that PCA component scores and loading directions cannot be interpreted uniformly without explicit reference to the clinical meaning of each contributing parameter. A directional recoding approach, multiplying threshold parameters by -1 prior to PCA so that positive z-scores uniformly indicate greater somatosensory deviation in the direction of pathology, was considered but not applied, because the covariance structure of this small cohort produced a negative correlation between MDT and VDT ($r = -0.31$). This would cause these two large-fiber parameters to load on opposite sides of the same component regardless of recoding, producing an internally inconsistent component structure. This is likely a sampling artifact given the small sample size rather than a biological phenomenon, but it renders a fixed directional recoding analytically unstable in this dataset. Component interpretation therefore requires explicit reference to the loading direction and the clinical meaning of each parameter, as described in the results. This interpretational constraint applies equally to the ΔZ PCA, where positive and negative loadings on PC1 and PC2 reflect a mixture of sensory loss and sensitization parameters on the same side of each component, precluding a straightforward clinical label for either axis.

Z-score pipeline

The WUR offset correction introduces a degree of arbitrariness into the z-score pipeline. Although an offset of $c = 1$ was selected empirically on the basis of minimizing z-score distortion across two independent datasets, no standardized correction method exists for this problem in the DFNS literature. The choice of offset may have influenced the relative contribution of WUR to the PCA component structure, and the sensitivity of results to alternative offset values was not formally evaluated.

The side-to-side standardization approach assumes that the contralateral limb provides a valid internal control, reflecting symmetric somatosensory function in the absence of pathology. In patients with bilateral or systemic conditions, such as SCI-005, who had a history of oncological treatment, the contralateral side may not be fully unaffected, potentially confounding the z-score estimates. Inspection of the raw VDT data for SCI-005 suggests that the reduction in VDT asymmetry at follow-up cannot be unambiguously attributed to SCS-induced neuromodulation, as deterioration of the contralateral side cannot be excluded in a patient with a history of oncological treatment. The underlying cause of this change therefore remains uncertain. This complicates the interpretation of somatosensory change in this participant and underscores the limitation of the side-to-side approach in patients with potential bilateral pathology. Furthermore, contralateral sensory abnormalities have been demonstrated in patients with unilateral peripheral nerve injury, including both sensory loss and pinprick hyperalgesia on the clinically unaffected side, independently of pain intensity or disease duration [70, 71]. This suggests that the contralateral limb may not represent a fully unaffected internal control in all patients, potentially confounding side-to-side z-score estimates. This assumption cannot be verified without contralateral nerve conduction studies or QST reference data from the same individual prior to injury.

Variable scaling prior to PCA standardizes each parameter to equal variance, which ensures that no single parameter dominates the component structure due to distributional differences in the clinical cohort. However, this procedure abstracts from the clinical magnitude of absolute z-score deviations. A parameter with consistently large z-scores in this cohort, such as VDT in SCI-005 ($z = 9.80$), receives the same statistical weight as a parameter with small z-scores, meaning that extreme individual deviations may be underrepresented in the component structure relative to their clinical magnitude.

CPM methodology

Regarding CPM, the sequential ordering of test stimuli means that PPT was assessed several minutes after the offset of the conditioning stimulus, potentially attenuating the CPM effect for this modality as discussed above. Furthermore, the CPM longitudinal dataset was incomplete at the time of analysis, and the preliminary follow-up observations should be interpreted accordingly.

Finally, the exploratory nature of all analyses in this chapter increases the risk of overinterpretation. The integration of PCA, longitudinal projection, univariate analysis, and CPM across a small cohort generates numerous descriptive observations, not all of which will replicate. The observations reported here are intended to inform hypothesis generation for future adequately powered studies, not to support clinical recommendations.

Interpretation of longitudinal changes
A further limitation concerns the interpretation of longitudinal QST and CPM changes. Because assessments at six-month follow-up were performed during active SCS, it is not possible to determine whether the observed somatosensory changes reflect a direct neuromodulatory effect of SCS on central nociceptive processing, or an indirect consequence of pain relief per se. Pain reduction from any cause can normalize somatosensory parameters through reduced peripheral and central sensitization, meaning that the observed changes cannot be uniquely attributed to the mechanism of SCS. A wash-out assessment, performed after temporary cessation of stimulation, would be required to disentangle these contributions, but was not feasible in this cohort given the clinical and ethical constraints of withdrawing an effective treatment.

Mechanistic interpretation
Another limitation concerns the absence of direct mechanistic measures. The hypotheses generated in this chapter regarding large-fiber afferent integrity and descending inhibitory pathways are based entirely on indirect behavioural measures, namely QST thresholds and CPM responses, without corroboration from neurophysiological assessments such as somatosensory evoked potentials. The mechanistic interpretations proposed here therefore remain speculative and require validation through studies that combine quantitative sensory assessment with direct measures of neural integrity.

3.4.8. Implications for future research
The findings of this chapter generate several hypotheses that warrant investigation in larger prospective studies.

Somatosensory profiling prior to SCS
The most immediately testable hypothesis concerns the relationship between baseline somatosensory profile and SCS response. The observation that the single non-responder showed a consistent pattern of large-fiber loss, most prominently for VDT, across three independent analyses suggests that pre-implantation QST profiling may identify patients who are less likely to benefit from SCS. Future studies should prospectively collect full DFNS QST batteries prior to SCS implantation in sufficiently large cohorts to examine whether baseline somatosensory configuration, particularly parameters reflecting large-fiber function such as VDT and MDT, is associated with treatment response. Given the heterogeneity of somatosensory profiles observed here, multivariate approaches such as PCA or cluster analysis are preferable to univariate analyses of individual parameters.

CPM assessment prior to SCS
The relationship between baseline CPM efficiency and SCS response also warrants prospective investigation. Although no consistent association was observed in this cohort, the sample size was insufficient to evaluate this relationship adequately. Future studies should incorporate standardized CPM assessment prior to SCS implantation, ideally using a parallel paradigm to avoid the timing limitations associated with sequential testing of PPT. The finding of a preliminary PPT-based CPM improvement following SCS supports the hypothesis that SCS engages descending inhibitory pathways, and future studies should examine whether this improvement correlates with clinical pain reduction.

Multimodal assessment and future study design
The potential independence of somatosensory organization and CPM efficiency suggests that these dimensions may provide complementary rather than redundant information about nociceptive processing prior to SCS, which warrants investigation of their combined predictive value in larger prospective studies. Prospective studies with sufficient statistical power should examine the joint and independent contributions of baseline somatosensory profile and CPM to treatment outcome, ideally in diagnostically homogeneous populations such as mononeuropathy to limit confounding by condition-specific pathophysiology.

Finally, the comparison between mononeuropathic pain and other chronic pain conditions such as complex regional pain syndrome with respect to somatosensory organization and CPM profile remains an open question. Studies combining standardized DFNS QST and CPM assessment across diagnostic groups, with sufficient sample sizes for between-group comparisons, would allow the hypothesis that mononeuropathy is characterized by a distinct somatosensory profile relative to complex regional pain syndrome to be formally tested.

3.5. Conclusion

This chapter demonstrates that somatosensory organization in refractory peripheral mononeuropathic pain is heterogeneous, with patients varying along a spectrum from predominant sensory loss to predominant mechanical sensitization rather than falling into distinct subgroups. Across three independent analyses, the single non-responder showed a consistent pattern of marked vibration detection loss, absent somatosensory normalization following SCS, and a qualitatively different change pattern compared to responders, suggesting that the integrity of large-fiber afferent input may be a mechanistically relevant determinant of SCS efficacy. Endogenous pain modulation assessed via CPM was variable at baseline and no consistent association with treatment response was observed, though the sample size was insufficient to evaluate this relationship adequately. A preliminary shift toward inhibitory PPT-based CPM following SCS suggests that SCS may engage descending inhibitory pathways. These observations are hypothesis-generating and require confirmation in larger prospective studies. Pre-implantation multivariate somatosensory profiling, particularly parameters reflecting large-fiber function, should be examined as a potential predictor of SCS response. Additionally, whether the preferential effect of SCS on PPT-based CPM reflects genuine engagement of descending inhibitory pathways and whether this correlates with clinical pain reduction remains to be established.

4

General Discussion

4.1. Principal findings

This thesis presents a prospective exploratory pilot study evaluating the clinical effects of SCS in patients with refractory peripheral mononeuropathic pain, complemented by exploratory analyses of somatosensory organization and endogenous pain modulation in the same cohort. Three principal findings emerge from the combined evidence.

First, SCS is associated with clinically meaningful and sustained reductions in pain intensity and improvements in QoL across the majority of patients, with a high trial success rate and without serious adverse events. These findings support the feasibility of SCS as a treatment option for refractory mononeuropathic pain and provide the first prospective data to inform effect size estimation for future controlled trials in this population.

Second, somatosensory organization was heterogeneous within this diagnostically homogeneous cohort, and the single non-responder showed a consistent pattern of deviation from the responder group across baseline profiling, longitudinal trajectory, and change pattern analyses. This observation generates the hypothesis that large-fiber afferent function may represent a relevant determinant of SCS response in mononeuropathic pain.

Third, baseline CPM was variable and did not predict treatment response, whereas a preliminary shift toward improved PPT-based CPM was observed following SCS, suggesting that SCS may engage descending inhibitory pathways in this population. A paired Wilcoxon signed-rank test indicated a non-significant trend toward greater inhibitory PPT-based CPM at six months ($p = 0.065$, Holm-corrected $p = 0.195$), which should be interpreted cautiously given the sample size. Somatosensory organization and CPM appeared to vary partly independently, suggesting they represent complementary dimensions of nociceptive processing.

Considered jointly, these findings illustrate the value of combining standardized clinical outcome assessment with quantitative sensory profiling in a single prospective cohort. The clinical findings of Chapter 2 establish that SCS produces meaningful pain relief on average in this population, but average group effects cannot identify which patients benefit through what mechanisms. The exploratory analysis of Chapter 3 addresses precisely this question within the same cohort. The convergence between clinical and somatosensory findings is notable: the single patient who did not respond clinically was also the only patient who showed no somatosensory normalization following SCS and who occupied a consistently peripheral position across all three independent somatosensory analyses. Although somatosensory normalization was not a necessary condition for clinical response, the absence of both clinical response and somatosensory normalization in the same patient, combined with a consistently deviant baseline profile, suggests a coherent rather than coincidental pattern. This convergence provides a preliminary empirical basis for the hypothesis that pre-implantation somatosensory profiling may carry predictive value beyond current selection criteria, a hypothesis that is elaborated in Section 4.3.

4.2. Clinical findings in context

The clinical findings in this thesis extend the prospective evidence base for SCS to a population that has received limited attention. Whereas SCS has demonstrated sustained efficacy in painful diabetic polyneuropathy and complex regional pain syndrome [4, 5], refractory mononeuropathic pain was previously supported only by case series and small retrospective analyses in mixed or anatomically distinct populations [9, 28, 29]. The present findings suggest that the analgesic potential of SCS is not restricted to polyneuropathic or sympathetically maintained pain conditions but extends to focal peripheral nerve injury with pain reductions and QoL improvements broadly comparable in magnitude to those reported in established indications. The high trial success rate likely reflects the stringent selection criteria applied and the comparatively lower trial success threshold of $\geq$30% pain reduction used in this study, relative to the $\geq$50% criterion commonly applied in the literature. Whether this profile generalizes to the broader clinical population remains to be established. The absence of a universally superior stimulation paradigm and the individual variation in paradigm preference support a personalized rather than fixed-paradigm approach to paradigm selection.

4.3. Somatosensory profiling as a potential tool for patient characterization

A central observation emerging from the combined findings of this thesis is that diagnostic homogeneity does not imply mechanistic homogeneity. Despite fulfilling the same inclusion criteria of EMG-confirmed peripheral mononeuropathy refractory to at least six months of conventional management, patients varied substantially in their baseline somatosensory profiles along dimensions of sensory loss and sensitization. This heterogeneity has a direct implication for interpreting the group-level clinical results reported in Chapter 2: the median NRS reduction of 3.3 points reflects an average across patients with fundamentally different somatosensory configurations, and the responder rate of 80% for $\geq$30% pain reduction conceals meaningful individual variation in both the magnitude and the mechanism of response. Reducing this variability through pre-implantation stratification is therefore not merely a methodological refinement but a necessity for understanding which patients benefit from SCS and why.

This hypothesis is consistent with the broader movement toward mechanism-based patient stratification in neuropathic pain research, where QST-derived sensory phenotypes have been associated with differential response to pharmacological treatments [13, 60]. Translating this stratification approach to SCS represents a logical next step and the present data provide a preliminary empirical basis for designing adequately powered prospective studies to test this hypothesis.

4.4. CPM as a complementary assessment dimension

The preliminary findings regarding CPM suggest that it reflects a dimension of nociceptive processing that is partly independent of somatosensory organization, as elaborated in Chapter 3. Whether baseline CPM efficiency and somatosensory profile contribute independently to SCS response is a question the present data were insufficient to address, but one that has direct implications for pre-implantation patient characterization. If both dimensions provide complementary predictive information, a multimodal assessment combining QST profiling and CPM may offer greater value than either alone for identifying patients likely to benefit from SCS.

4.5. Strengths and limitations

The principal strength of this thesis is its prospective single-cohort design combining standardized clinical outcome assessment with quantitative sensory profiling in a diagnostically homogeneous population. The use of a counterbalanced paradigm comparison phase minimizes period effects in the comparison of stimulation paradigms and the application of the full DFNS QST battery allows comparison with a large normative reference dataset.

The methodological limitations in Chapter 2 and 3 are discussed in detail in Sections 2.4.4 and 3.4.7 respectively. Of particular relevance to the interpretation of this thesis as a whole are the small sample size, which precludes definitive conclusions from the secondary and exploratory analyses, and the

absence of a control condition, which means that spontaneous improvement and regression to the mean cannot be excluded as contributors to the observed changes. The single-center design and predominantly post-traumatic etiology limit generalizability to other mononeuropathy subtypes and clinical settings.

A further limitation concerns the reliance on subjective outcome measures across both chapters. Clinical outcomes in Chapter 2 are based entirely on patient-reported measures, including NRS pain scores and standardized questionnaires, which are sensitive to daily fluctuations in mood, expectations, and contextual factors unrelated to treatment. QST and CPM assessments in Chapter 3, although based on standardized stimuli, depend on patient-reported thresholds and are therefore susceptible to variation in attention, distraction, and day-to-day fluctuations in pain sensitivity. These sources of measurement variability cannot be fully controlled and may have contributed to the inter- and intra-individual variability observed across both chapters.

Finally, follow-up was limited to six months. Although NRS scores and questionnaire outcomes were stable across the intermediate timepoints within this period, the durability of both clinical and somatosensory changes beyond six months remains unknown. Whether the observed somatosensory reorganization following SCS is sustained over longer follow-up periods, and whether it correlates with long-term clinical outcome, cannot be determined from the present data.

4.6. Implications for future research

The findings of this thesis support the design of a randomized controlled trial of SCS in refractory peripheral mononeuropathic pain. The prospective data provided here enable effect size estimation and variability assessment for power calculations, addressing a key barrier to conducting such a trial identified in the literature [10]. A future trial should incorporate a sham or best medical management control arm and allow for personalized paradigm selection rather than a fixed stimulation paradigm, given the individual variation in paradigm preference observed in this cohort. Notably, all 12 patients who underwent trial stimulation proceeded to permanent implantation, yet not all achieved sustained clinical response at six months. This raises the question of whether the trial phase is a sufficient selection instrument for predicting long-term SCS response in this population, and whether more stringent or extended trial criteria might improve the identification of patients who maintain meaningful benefit over time.

Pre-implantation QST profiling should be prioritized as a stratification variable in future trials. The consistent pattern of somatosensory deviation observed in the single non-responder across three independent analyses provides a more coherent empirical basis for prospective investigation than the CPM findings, which did not yield a consistent predictive signal in this cohort. Pre-implantation CPM assessment remains a theoretically motivated candidate for future research, but its predictive value for treatment response remains to be established in adequately powered studies with standardized methodology.

Finally, the extent to which the somatosensory profile of refractory mononeuropathic pain is distinct from that of other focal peripheral nerve injury conditions, particularly causalgia, warrants systematic investigation. The ACCURATE trial demonstrated moderate SCS efficacy in causalgia [30], a condition that shares focal nerve injury with mononeuropathy but is distinguished by autonomic and vasomotor features and classified separately under established neuropathic pain criteria [72]. Whether these clinical differences are accompanied by distinct somatosensory profiles, and whether such differences are mechanistically relevant to SCS response, remains unknown. Comparative DFNS QST assessment across diagnostically homogeneous cohorts would allow this question to be addressed and could strengthen the rationale for condition-specific rather than injury-based patient selection for SCS.

5

Conclusion

This thesis provides the first prospective evidence evaluating the clinical effects of SCS in patients with refractory peripheral mononeuropathic pain, a population for which evidence-based interventional treatment options were previously lacking. In this pilot study, SCS is associated with clinically meaningful and sustained reductions in pain intensity and improvements in quality of life across the majority of patients, with no serious adverse events. A median within-patient NRS reduction of 3.3 points was observed at six months, with 80% of patients achieving at least 30% pain reduction of whom five patients achieved at least 50% pain reduction. No single stimulation paradigm emerged as universally superior and individual variation in paradigm preference supports a personalized rather than fixed-paradigm approach to paradigm selection. These findings support the feasibility of SCS as a treatment option in this population and provide the empirical foundation for a future sham-controlled randomized controlled trial.

The integration of quantitative sensory assessment with clinical outcome evaluation in the same prospective cohort allowed the clinical findings to be examined alongside somatosensory and endogenous pain modulatory profiles within the same patients. Somatosensory profiles were heterogeneous across patients despite diagnostic homogeneity and the single non-responder showed a consistent pattern of large-fiber afferent loss across three independent analyses. This pattern was absent in responding patients. This observation generates the hypothesis that pre-implantation quantitative sensory testing, particularly parameters reflecting large-fiber function, may carry predictive value for SCS response beyond current selection criteria. Baseline conditioned pain modulation did not predict treatment response, though a preliminary shift toward inhibitory PPT-based conditioned pain modulation following SCS suggests that SCS may engage descending inhibitory pathways. These observations are hypothesis-generating and require confirmation in adequately powered prospective studies incorporating pre-implantation multivariate somatosensory profiling as a stratification variable.

AI Statement

During the preparation of this thesis, AI-based language tools, specifically Claude (Anthropic) and Grammarly, were used to assist with reformulating and editing text, and to support the formatting of figures and the LaTeX layout. All AI-generated suggestions were reviewed and revised by me before inclusion. These tools were not used for data collection, statistical analysis, interpretation of results, or the formulation of scientific conclusions. All scientific content, analyses, interpretations, and conclusions are my own. I take full responsibility for the integrity of the work as presented.

References

[1] Troels S. Jensen et al. “A new definition of neuropathic pain”. en-US. In: PAIN 152.10 (Oct. 2011), p. 2204. ISSN: 0304-3959. DOI: 10.1016/j.pain.2011.06.017.

[2] Nanna Brix Finnerup, Søren Hein Sindrup, and Troels Staehelin Jensen. “The evidence for pharmacological treatment of neuropathic pain”. eng. In: Pain 150.3 (Sept. 2010), pp. 573–581. ISSN: 1872-6623. DOI: 10.1016/j.pain.2010.06.019.

[3] Luana Colloca et al. “Neuropathic pain”. In: Nature reviews. Disease primers 3 (Feb. 2017), p. 17002. ISSN: 2056-676X. DOI: 10.1038/nrdp.2017.2.

[4] Cecile C. de Vos et al. “Spinal cord stimulation in patients with painful diabetic neuropathy: a multicentre randomized clinical trial”. eng. In: Pain 155.11 (Nov. 2014), pp. 2426–2431. ISSN: 1872-6623. DOI: 10.1016/j.pain.2014.08.031.

[5] M. A. Kemler et al. “Pain relief in complex regional pain syndrome due to spinal cord stimulation does not depend on vasodilation”. eng. In: Anesthesiology 92.6 (June 2000), pp. 1653–1660. ISSN: 0003-3022. DOI: 10.1097/00000542-200006000-00024.

[6] Jacob Caylor et al. “Spinal cord stimulation in chronic pain: evidence and theory for mechanisms of action”. eng. In: Bioelectronic Medicine 5 (June 2019), p. 12. ISSN: 2332-8886. DOI: 10.1186/s42234-019-0023-1.

[7] Anne Veenhuizen. Mechanisms of Action of Spinal Cord Stimulation Paradigms in Neuropathic Pain: A Scoping Review. Feb. 2026.

[8] Linda Kollenburg et al. “A forgotten frontier: spinal cord stimulation for iatrogenic and traumatic peripheral neuropathic pain”. English. In: Frontiers in Pain Research 6 (Nov. 2025). ISSN: 2673-561X. DOI: 10.3389/fpain.2025.1661520.

[9] Kevin Buffenoir et al. “Spinal cord stimulation of the conus medullaris for refractory pudendal neuralgia: a prospective study of 27 consecutive cases”. eng. In: Neurourology and Urodynamics 34.2 (Feb. 2015), pp. 177–182. ISSN: 1520-6777. DOI: 10.1002/nau.22525.

[10] Yilong Zheng et al. “Neurostimulation for Chronic Pain: A Systematic Review of High-Quality Randomized Controlled Trials With Long-Term Follow-Up”. eng. In: Neuromodulation: Journal of the International Neuromodulation Society 26.7 (Oct. 2023), pp. 1276–1294. ISSN: 1525-1403. DOI: 10.1016/j.neurom.2023.05.003.

[11] Miroslav Misha Backonja et al. “Value of quantitative sensory testing in neurological and pain disorders: NeuPSIG consensus”. eng. In: Pain 154.9 (Sept. 2013), pp. 1807–1819. ISSN: 1872-6623. DOI: 10.1016/j.pain.2013.05.047.

[12] Carina Fernandes et al. “Conditioned pain modulation as a biomarker of chronic pain: a systematic review of its concurrent validity”. eng. In: Pain 160.12 (Dec. 2019), pp. 2679–2690. ISSN: 1872-6623. DOI: 10.1097/j.pain.0000000000001664.

[13] Ralf Baron et al. “Peripheral neuropathic pain: a mechanism-related organizing principle based on sensory profiles”. en. In: Pain 158.2 (Nov. 2016), p. 261. DOI: 10.1097/j.pain.0000000000000753.

[14] David Yarnitsky. “Role of endogenous pain modulation in chronic pain mechanisms and treatment”. eng. In: Pain 156 Suppl 1 (Apr. 2015), S24–S31. ISSN: 1872-6623. DOI: 10.1097/01.j.pain.0000460343.46847.58.

[15] Nanna B. Finnerup et al. “Neuropathic pain: an updated grading system for research and clinical practice”. eng. In: Pain 157.8 (Aug. 2016), pp. 1599–1606. ISSN: 1872-6623. DOI: 10.1097/j.pain.0000000000000492.

[16] R Latinovic, M C Gulliford, and R A C Hughes. “Incidence of common compressive neuropathies in primary care”. In: Journal of Neurology, Neurosurgery, and Psychiatry 77.2 (Feb. 2006), pp. 263–265. ISSN: 0022-3050. DOI: 10.1136/jnnp.2005.066696.

[17] I. Atroshi et al. “Prevalence of carpal tunnel syndrome in a general population”. eng. In: JAMA 282.2 (July 1999), pp. 153–158. ISSN: 0098-7484. DOI: 10.1001/jama.282.2.153.

[18] Mauro Mondelli et al. “Incidence of ulnar neuropathy at the elbow in the province of Siena (Italy)”. eng. In: Journal of the Neurological Sciences 234.1-2 (July 2005), pp. 5–10. ISSN: 0022-510X. DOI: 10.1016/j.jns.2005.02.010.

[19] Alan D. Kaye et al. “Evolving Treatment Strategies for Neuropathic Pain: A Narrative Review”. In: Medicina 61.6 (June 2025), p. 1063. ISSN: 1010-660X. DOI: 10.3390/medicina61061063.

[20] Andreas Liampas et al. “Non-Pharmacological Management of Painful Peripheral Neuropathies: A Systematic Review”. eng. In: Advances in Therapy 37.10 (Oct. 2020), pp. 4096–4106. ISSN: 1865-8652. DOI: 10.1007/s12325-020-01462-3.

[21] Evan R. Zeldin et al. “An overview of the non-procedural treatment options for peripheral neuropathic pain”. eng. In: Muscle & Nerve 71.5 (May 2025), pp. 791–801. ISSN: 1097-4598. DOI: 10.1002/mus.28286.

[22] Rezvan Ahmadi et al. “The Diagnosis and Treatment of Neuropathic Pain”. eng. In: Deutsches Arzteblatt International 121.25 (Dec. 2024), pp. 825–832. ISSN: 1866-0452. DOI: 10.3238/arztebl.m2024.0215.

[23] Luca Padua et al. “Carpal tunnel syndrome: clinical features, diagnosis, and management”. eng. In: The Lancet. Neurology 15.12 (Nov. 2016), pp. 1273–1284. ISSN: 1474-4465. DOI: 10.1016/S1474-4422(16)30231-9.

[24] Jonathan Robert Staples and Ryan Calfee. “Cubital Tunnel Syndrome: Current Concepts”. eng. In: The Journal of the American Academy of Orthopaedic Surgeons 25.10 (Oct. 2017), e215–e224. ISSN: 1940-5480. DOI: 10.5435/JAAOS-D-15-00261.

[25] Maarten van Beek et al. “Severity of Neuropathy Is Associated With Long-term Spinal Cord Stimulation Outcome in Painful Diabetic Peripheral Neuropathy: Five-Year Follow-up of a Prospective Two-Center Clinical Trial”. In: Diabetes Care 41.1 (Nov. 2017), pp. 32–38. ISSN: 0149-5992. DOI: 10.2337/dc17-0983.

[26] Marius A. Kemler et al. “Effect of spinal cord stimulation for chronic complex regional pain syndrome Type I: five-year final follow-up of patients in a randomized controlled trial”. eng. In: Journal of Neurosurgery 108.2 (Feb. 2008), pp. 292–298. ISSN: 0022-3085. DOI: 10.3171/JNS/2008/108/2/0292.

[27] Xander Zuidema et al. “Long-Term Evaluation of Spinal Cord Stimulation in Patients With Painful Diabetic Polyneuropathy: An Eight-to-Ten–Year Prospective Cohort Study”. In: Neuromodulation: Technology at the Neural Interface 26.5 (July 2023), pp. 1074–1080. ISSN: 1094-7159. DOI: 10.1016/j.neurom.2022.12.003.

[28] K. Kumar, C. Toth, and R. K. Nath. “Spinal cord stimulation for chronic pain in peripheral neuropathy”. eng. In: Surgical Neurology 46.4 (Oct. 1996), pp. 363–369. ISSN: 0090-3019. DOI: 10.1016/s0090-3019(96)00191-7.

[29] Akira Nemoto and Hisashi Date. “Spinal Cord Stimulation Alleviates Chronic Peripheral Neuropathic Pain Due to Peripheral Nerve Injury: A Case Report”. In: Cureus 16.9 (), e69383. ISSN: 2168-8184. DOI: 10.7759/cureus.69383.

[30] Timothy R. Deer et al. “Dorsal root ganglion stimulation yielded higher treatment success rate for complex regional pain syndrome and causalgia at 3 and 12 months: a randomized comparative trial”. eng. In: Pain 158.4 (Apr. 2017), pp. 669–681. ISSN: 1872-6623. DOI: 10.1097/j.pain.0000000000000814.

[31] Michael Kretzschmar, Marco Reining, and Marcus A. Schwarz. “Three-Year Outcomes After Dorsal Root Ganglion Stimulation in the Treatment of Neuropathic Pain After Peripheral Nerve Injury of Upper and Lower Extremities”. eng. In: Neuromodulation: Journal of the International Neuromodulation Society 24.4 (June 2021), pp. 700–707. ISSN: 1525-1403. DOI: 10.1111/ner.13222.

[32] Treede Rd et al. “Neuropathic pain: redefinition and a grading system for clinical and research purposes”. en. In: Neurology 70.18 (Apr. 2008). ISSN: 1526-632X. DOI: 10.1212/01.wnl.0000282763.29778.59.

[33] EuroQol Group. “EuroQol–a new facility for the measurement of health-related quality of life”. eng. In: Health Policy 16.3 (Dec. 1990), pp. 199–208. ISSN: 0168-8510. DOI: 10.1016/0168-8510(90)90421-9.

[34] A. S. Zigmond and R. P. Snaith. “The Hospital Anxiety and Depression Scale”. en. In: Acta Psychiatrica Scandinavica 67.6 (1983). _eprint: https://onlinelibrary.wiley.com/doi/pdf/10.1111/j.1600-0447.1983.tb09716.x, pp. 361–370. ISSN: 1600-0447. DOI: 10.1111/j.1600-0447.1983.tb09716.x.

[35] C. S. Cleeland and K. M. Ryan. “Pain assessment: global use of the Brief Pain Inventory”. eng. In: Annals of the Academy of Medicine, Singapore 23.2 (Mar. 1994), pp. 129–138. ISSN: 0304-4602.

[36] John T. Farrar et al. “Clinical importance of changes in chronic pain intensity measured on an 11-point numerical pain rating scale”. eng. In: Pain 94.2 (Nov. 2001), pp. 149–158. ISSN: 0304-3959. DOI: 10.1016/S0304-3959(01)00349-9.

[37] Stephen J. Walters and John E. Brazier. “Comparison of the minimally important difference for two health state utility measures: EQ-5D and SF-6D”. eng. In: Quality of Life Research 14.6 (Aug. 2005), pp. 1523–1532. ISSN: 0962-9343. DOI: 10.1007/s11136-004-7713-0.

[38] Jacob S. Gandløse, Jonathan Vela, and Thorvaldur S. Palsson. “Estimation of the minimal important change for Brief Pain Inventory in patients with persistent spinal pain”. In: Musculoskeletal Science and Practice 80 (Nov. 2025), p. 103407. ISSN: 2468-7812. DOI: 10.1016/j.msksp.2025.103407.

[39] Rode Grönkvist et al. “Measurement Error, Minimal Detectable Change, and Minimal Clinically Important Difference of the Short Form-36 Health Survey, Hospital Anxiety and Depression Scale, and Pain Numeric Rating Scale in Patients With Chronic Pain”. eng. In: The Journal of Pain 25.9 (Sept. 2024), p. 104559. ISSN: 1528-8447. DOI: 10.1016/j.jpain.2024.104559.

[40] Steven A. Julious. “Sample size of 12 per group rule of thumb for a pilot study”. en. In: Pharmaceutical Statistics 4.4 (2005). _eprint: https://onlinelibrary.wiley.com/doi/pdf/10.1002/pst.185, pp. 287–291. ISSN: 1539-1612. DOI: 10.1002/pst.185.

[41] Rachel Slangen et al. “Spinal cord stimulation and pain relief in painful diabetic peripheral neuropathy: a prospective two-center randomized controlled trial”. eng. In: Diabetes Care 37.11 (Nov. 2014), pp. 3016–3024. ISSN: 1935-5548. DOI: 10.2337/dc14-0684.

[42] Krishna Kumar and J. R. Wilson. “Factors affecting spinal cord stimulation outcome in chronic benign pain with suggestions to improve success rate”. en. In: Operative Neuromodulation: Volume 1: Functional Neuroprosthetic Surgery. An Introduction. Ed. by Damianos E. Sakas, Brian A. Simpson, and Elliot S. Krames. Vienna: Springer, 2007, pp. 91–99. ISBN: 978-3-211-33079-1. DOI: 10.1007/978-3-211-33079-1_12.

[43] Rui V. Duarte and Simon Thomson. “Trial Versus No Trial of Spinal Cord Stimulation for Chronic Neuropathic Pain: Cost Analysis in United Kingdom National Health Service”. In: Neuromodulation: Technology at the Neural Interface 22.2 (Feb. 2019), pp. 208–214. ISSN: 1094-7159. DOI: 10.1111/ner.12898.

[44] Wesley Day et al. “Spinal cord stimulator utilization trends and predictors of unsuccessful trial-to-implant conversion”. eng. In: North American Spine Society Journal 22 (June 2025), p. 100616. ISSN: 2666-5484. DOI: 10.1016/j.xnsj.2025.100616.

[45] Sigrid Schuh-Hofer et al. “Spinal cord stimulation modulates descending pain inhibition and temporal summation of pricking pain in patients with neuropathic pain”. eng. In: Acta Neurochirurgica 160.12 (Dec. 2018), pp. 2509–2519. ISSN: 0942-0940. DOI: 10.1007/s00701-018-3669-7.

[46] John E. Gilbert et al. “Surround Inhibition Mediates Pain Relief by Low Amplitude Spinal Cord Stimulation: Modeling and Measurement”. eng. In: eNeuro 9.5 (2022), ENEURO.0058–22.2022. ISSN: 2373-2822. DOI: 10.1523/ENEURO.0058-22.2022.

[47] R. Rolke et al. “Quantitative sensory testing in the German Research Network on Neuropathic Pain (DFNS): standardized protocol and reference values”. eng. In: Pain 123.3 (Aug. 2006), pp. 231–243. ISSN: 1872-6623. DOI: 10.1016/j.pain.2006.01.041.

[48] Detlef Groth et al. “Principal Components Analysis”. en. In: Computational Toxicology: Volume II. Ed. by Brad Reisfeld and Arthur N. Mayeno. Totowa, NJ: Humana Press, 2013, pp. 527–547. ISBN: 978-1-62703-059-5. DOI: 10.1007/978-1-62703-059-5_22.

[49] David Yarnitsky et al. “Recommendations on terminology and practice of psychophysical DNIC testing”. eng. In: European Journal of Pain 14.4 (Apr. 2010), p. 339. ISSN: 1532-2149. DOI: 10.1016/j.ejpain.2010.02.004.

[50] Yannick J. G. M. Plantaz et al. “Changes in quantitative sensory testing and patient perspectives following spinal cord stimulation for persistent spinal pain syndrome: An observational study with long-term follow-up”. eng. In: European Journal of Pain 26.7 (Aug. 2022), pp. 1581–1593. ISSN: 1532-2149. DOI: 10.1002/ejp.1984.

[51] Turo Nurmikko et al. “Quantitative Sensory Testing in Spinal Cord Stimulation: A Narrative Review”. eng. In: Neuromodulation: Journal of the International Neuromodulation Society 27.6 (Aug. 2024), pp. 1026–1034. ISSN: 1525-1403. DOI: 10.1016/j.neurom.2024.03.005.

[52] C. Maier et al. “Quantitative sensory testing in the German Research Network on Neuropathic Pain (DFNS): somatosensory abnormalities in 1236 patients with different neuropathic pain syndromes”. eng. In: Pain 150.3 (Sept. 2010), pp. 439–450. ISSN: 1872-6623. DOI: 10.1016/j.pain.2010.05.002.

[53] Janne Gierthmühlen et al. “Sensory signs in complex regional pain syndrome and peripheral nerve injury”. en-US. In: PAIN 153.4 (Apr. 2012), p. 765. ISSN: 0304-3959. DOI: 10.1016/j.pain.2011.11.009.

[54] Nadia Kriek et al. “Allodynia, Hyperalgesia, (Quantitative) Sensory Testing and Conditioned Pain Modulation in Patients With Complex Regional Pain Syndrome Before and After Spinal Cord Stimulation Therapy”. eng. In: Neuromodulation: Journal of the International Neuromodulation Society 26.1 (Jan. 2023), pp. 78–86. ISSN: 1525-1403. DOI: 10.1016/j.neurom.2022.06.009.

[55] Thomas Kinfe et al. “Quantitative sensory phenotyping in chronic neuropathic pain patients treated with unilateral L4-dorsal root ganglion stimulation”. eng. In: Journal of Translational Medicine 18.1 (Oct. 2020), p. 403. ISSN: 1479-5876. DOI: 10.1186/s12967-020-02566-8.

[56] Claudia M. Campbell et al. “Dynamic pain phenotypes are associated with spinal cord stimulation-induced reduction in pain: A repeated measures observational pilot study”. In: Pain medicine (Malden, Mass.) 16.7 (July 2015), pp. 1349–1360. ISSN: 1526-2375. DOI: 10.1111/pme.12732.

[57] M. Mücke et al. “Quantitative sensory testing (QST). English version”. en. In: Der Schmerz 35.3 (Nov. 2021), pp. 153–160. ISSN: 1432-2129. DOI: 10.1007/s00482-015-0093-2.

[58] William Zwick and Wayne Velicer. “Comparison of Five Rules for Determining the Number of Components to Retain”. In: Psychological Bulletin 99 (May 1986), pp. 432–442. DOI: 10.1037/0033-2909.99.3.432.

[59] Sture Holm. “A Simple Sequentially Rejective Multiple Test Procedure”. In: Scandinavian Journal of Statistics 6.2 (1979), pp. 65–70. ISSN: 0303-6898.

[60] Jan Vollert et al. “Stratifying patients with peripheral neuropathic pain based on sensory profiles: algorithm and sample size recommendations”. eng. In: Pain 158.8 (Aug. 2017), pp. 1446–1455. ISSN: 1872-6623. DOI: 10.1097/j.pain.0000000000000935.

[61] Hamza Bajwa and Yasir Al Khalili. “Physiology, Vibratory Sense”. eng. In: StatPearls. Treasure Island (FL): StatPearls Publishing, 2026.

[62] Michael S. Fleming and Wenqin Luo. “The anatomy, function, and development of mammalian Aβ low-threshold mechanoreceptors”. In: Frontiers in biology 8.4 (Aug. 2013), 10.1007/s11515–013–1271–1. ISSN: 1674-7984. DOI: 10.1007/s11515-013-1271-1.

[63] Alon Abraham et al. “Elevated Vibration Perception Thresholds in CIDP Patients Indicate More Severe Neuropathy and Lower Treatment Response Rates”. en. In: PLOS ONE 10.11 (Nov. 2015), e0139689. ISSN: 1932-6203. DOI: 10.1371/journal.pone.0139689.

[64] Helwin Smits et al. “Experimental Spinal Cord Stimulation and Neuropathic Pain: Mechanism of Action, Technical Aspects, and Effectiveness”. en. In: Pain Practice 13.2 (2013). _eprint: https://onlinelibrary.wiley.com/doi/pdf/10.1111/j.1533-2500.2012.00579.x, pp. 154–168. ISSN: 1533-2500. DOI: 10.1111/j.1533-2500.2012.00579.x.

[65] “Late radiation injury to peripheral nerves”. en-US. In: Handbook of Clinical Neurology. Vol. 115. Elsevier, Jan. 2013, pp. 743–758. DOI: 10.1016/B978-0-444-52902-2.00043-6.

[66] Lewis S. Crawford et al. “Conditioned Pain Modulation, Placebo and Offset Analgesia: Rates of Behavioural Expression of Inhibitory, Nonresponse and Facilitatory Pain Modulatory Effects”. In: European Journal of Pain (London, England) 29.7 (Aug. 2025), e70088. ISSN: 1090-3801. DOI: 10.1002/ejp.70088.

[67] Alexia Coulombe-Lévêque et al. “The effect of conditioning stimulus intensity on conditioned pain modulation (CPM) hypoalgesia”. eng. In: Canadian Journal of Pain = Revue Canadienne De La Douleur 5.1 (Feb. 2021), pp. 22–29. ISSN: 2474-0527. DOI: 10.1080/24740527.2020.1855972.

[68] Laurien J. Reinders, Frank J. P. M. Huygen, and Cecile C. de Vos. “The Effects of Tonic and Burst Spinal Cord Stimulation on Cortical Pain Processing and Their Interaction With Conditioned Pain Modulation”. eng. In: Neuromodulation: Journal of the International Neuromodulation Society (Jan. 2026), S1094–7159(25)01204–8. ISSN: 1525-1403. DOI: 10.1016/j.neurom.2025.12.007.

[69] Iara De Schoenmacker et al. “Sensory phenotypes in complex regional pain syndrome and chronic low back pain-indication of common underlying pathomechanisms”. eng. In: Pain Reports 8.6 (Dec. 2023), e1110. ISSN: 2471-2531. DOI: 10.1097/PR9.0000000000001110.

[70] Elena Enax-Krumova et al. “Contralateral Sensory and Pain Perception Changes in Patients With Unilateral Neuropathy”. eng. In: Neurology 97.4 (July 2021), e389–e402. ISSN: 1526-632X. DOI: 10.1212/WNL.0000000000012229.

[71] Karl-Heinz Konopka et al. “Bilateral sensory abnormalities in patients with unilateral neuropathic pain; a quantitative sensory testing (QST) study”. eng. In: PloS One 7.5 (2012), e37524. ISSN: 1932-6203. DOI: 10.1371/journal.pone.0037524.

[72] Rolf-Detlef Treede et al. “Chronic pain as a symptom or a disease: the IASP Classification of Chronic Pain for the International Classification of Diseases (ICD-11)”. eng. In: Pain 160.1 (Jan. 2019), pp. 19–27. ISSN: 1872-6623. DOI: 10.1097/j.pain.0000000000001384.

A

Stimulation parameters per paradigm

Table A.1: Stimulation parameters per paradigm as applied during the comparison phase. Frequency was fixed per paradigm; pulse width varied across patients within the indicated range. Amplitude was titrated to suprathreshold perception for tonic stimulation and set at 30% of perception threshold for FAST stimulation. Amplitude parameters for burst and contour stimulation were device-controlled and not individually recorded. Contour stimulation was programmed at fixed parameters for all patients. FAST = Fast-Acting Sub-perception Therapy.

Paradigm	**Frequency (Hz)**	**Pulse width (μs)**	**Amplitude**
Tonic	40-80	200-310	Suprathreshold
FAST	90	210	30% of perception threshold
Burst (microburst)	450 (intra-burst)	200-260	Algorithm-controlled
Contour	200	200	Algorithm-controlled

B

Extended patient characteristics

Table B.1: Individual patient characteristics and clinical outcomes at baseline (T0) and six-month follow-up (T3). ΔNRS = percentage change in Numeric Rating Scale from baseline to six months. BPI = Brief Pain Inventory interference score. HADS-A = Hospital Anxiety and Depression Scale anxiety subscale; HADS-D = depression subscale. SCI-007 withdrew during follow-up; follow-up data are unavailable.

ID	Sex	Age	Pain dur. (months)	Nerve	Cause	NRS T0	NRS T3	ΔNRS	EQ-5D T0	EQ-5D T3	BPI T0	BPI T3	HADS-A T0	HADS-A T3	HADS-D T0	HADS-D T3	Preferred paradigm
SCI-001	F	55	48	Peroneal	Trauma	5.0	0.0	-100%	0.651	0.893	8.0	0.0	5	0	13	2	FAST
SCI-002	F	53	48	Sural	Surgical	7.0	2.0	-71%	0.441	0.874	7.0	1.0	8	3	6	1	Tonic
SCI-003	F	72	42	Ulnar	Trauma	7.0	3.5	-50%	0.467	0.707	7.0	4.0	7	3	10	3	FAST
SCI-004	M	59	19	Ulnar	Surgical	5.5	0.0	-100%	0.620	0.876	2.0	1.0	0	3	0	3	Burst
SCI-005	M	71	120	Peroneal	Surgical	6.5	7.0	$+8\%$	0.591	0.467	6.0	4.0	2	3	10	9	FAST
SCI-006	F	67	23	Peroneal	Trauma	6.0	3.5	-42%	0.514	0.651	7.0	4.0	11	10	9	8	FAST
SCI-007	F	27	72	Ulnar	Surgical	7.0	—	—	0.554	—	4.0	—	6	—	5	—	—
SCI-008	M	36	48	Saphenous	Trauma	8.0	5.0	-38%	0.334	0.608	8.0	5.0	6	5	8	7	Tonic
SCI-009	F	34	48	Peroneal	Trauma	7.0	5.0	-29%	0.565	0.651	10.0	8.0	8	15	6	10	FAST
SCI-010	F	48	60	Sural	Trauma	7.5	8.0	$+7\%$	0.432	0.363	5.0	6.0	6	7	5	2	Contour
SCI-011	M	53	72	Saphenous	Trauma	8.0	4.0	-50%	0.514	0.805	8.0	3.0	3	3	3	1	FAST
SCI-012	M	33	72	Ulnar	Surgical	8.0	—	—	0.552	—	4.0	—	5	—	6	—	—

C

Individual NRS-trajectories

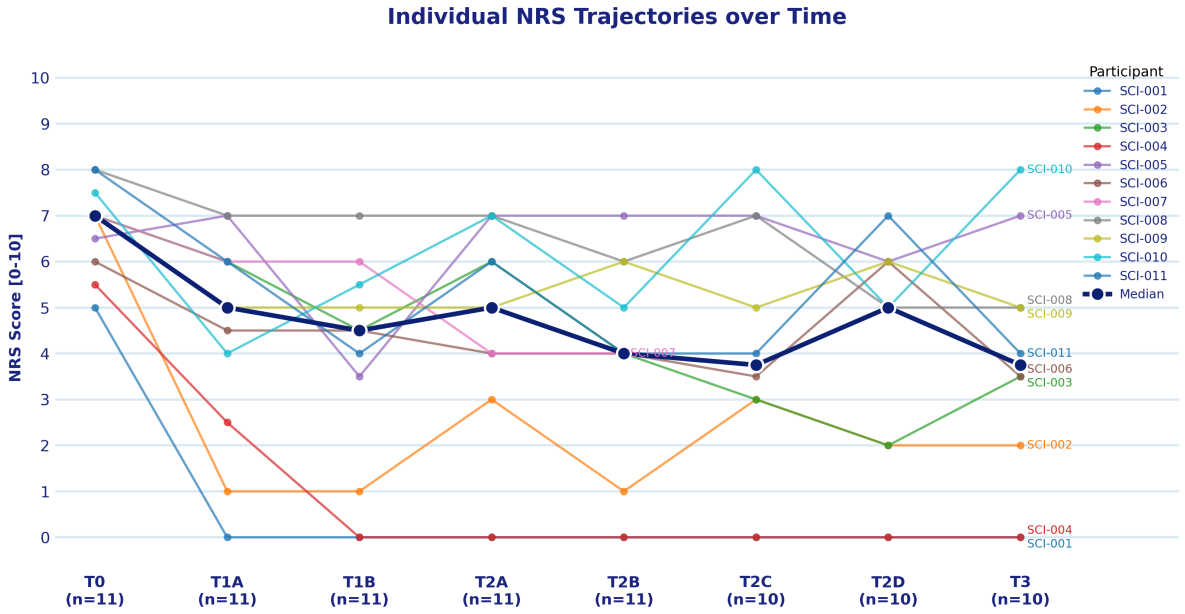

Figure C.1: Individual NRS trajectories over time from baseline (T0) through six-month follow-up (T3). Each colored line represents one participant. The dark blue line with filled markers represents the group median. SCI-007 withdrew during follow-up and is included up to the last available time point. T1A and T1B represent the two weeks of the trial phase (tonic and FAST in alternating order); T2A–T2D represent the four blocks of the comparison phase; T3 represents the six-month preference phase endpoint.

D

Loadings PCA

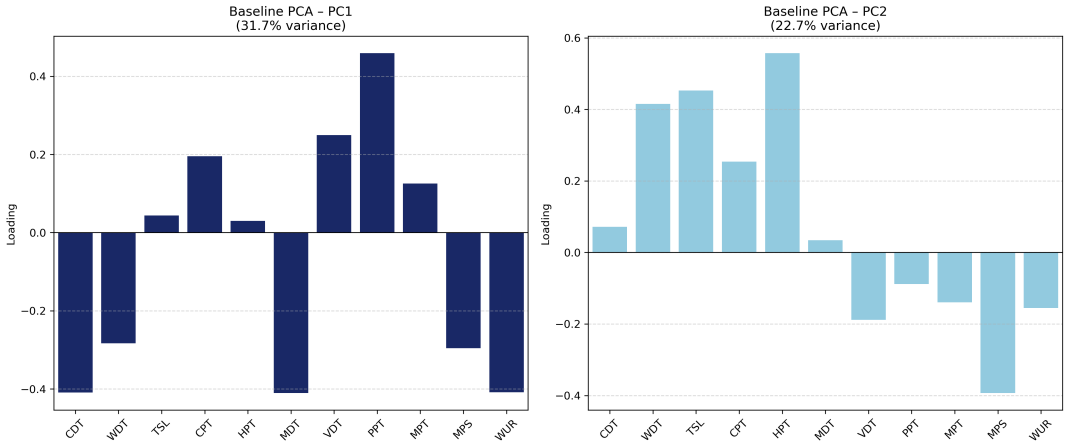

Figure D.1: Loadings of PC1 and PC2 from the baseline QST PCA ($n = 12$). Each bar represents the loading of one QST parameter on the respective component, indicating the direction and magnitude of its contribution. PC1 explained 31.7% and PC2 explained 22.7% of total variance. Positive z-scores indicate sensory loss for threshold parameters and sensitization for MPS and WUR.

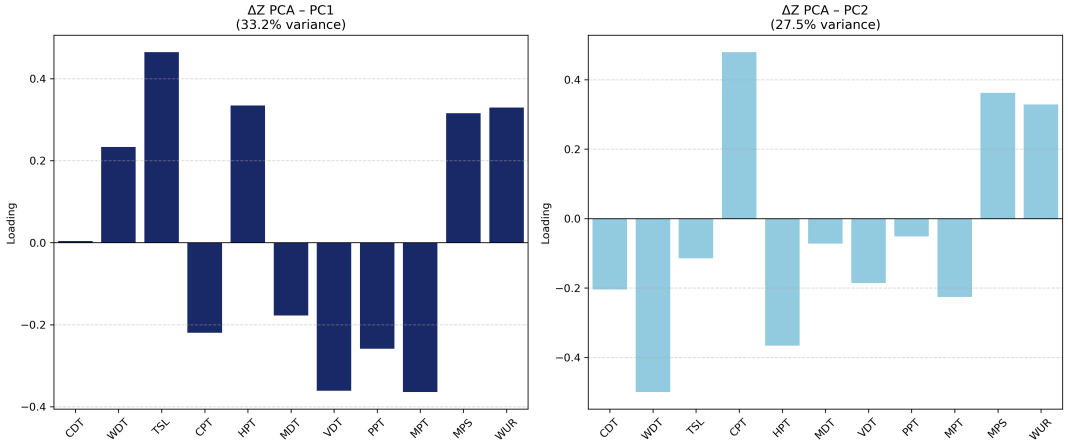

Figure D.2: Loadings of PC1 and PC2 from the ΔZ-score PCA ($n = 10$). Each bar represents the loading of one QST parameter on the respective component, reflecting the direction and magnitude of its contribution to patterns of somatosensory change following SCS. PC1 explained 33.2% and PC2 explained 27.5% of total variance. Positive ΔZ values indicate increasing asymmetry toward sensory loss for threshold parameters and increasing sensitization for MPS and WUR.

E

Scree Plot Baseline PCA

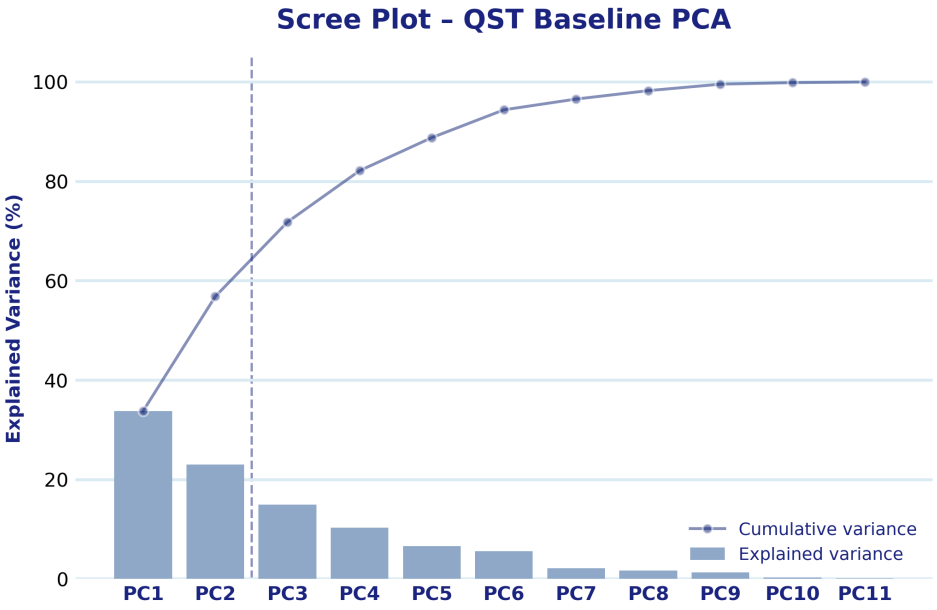

Figure E.1: Scree plot of the baseline QST PCA ($n = 12$). Bars represent the percentage of variance explained by each principal component. The cumulative variance curve is shown as a connected line. The dashed vertical line indicates the retention cutoff after PC2.

F

Side-to-side z-scores per participant

Table F.1: Side-to-side z-scores per participant at baseline (T0) and six-month follow-up (T3). Z-scores reflect the standardized deviation of the affected side from the contralateral side, expressed in units of the DFNS reference standard deviation for right-left differences. Positive z-scores indicate elevated thresholds on the affected side (sensory loss) for detection threshold parameters; for MPS and WUR, positive z-scores indicate greater pain sensitivity (sensitization). SCI-007 and SCI-012 had no T3 QST data available.

ID	T	CDT	WDT	TSL	CPT	HPT	MDT	VDT	PPT	MPT	MPS	WUR
SCI-001	T0	−0.32	0.01	−0.06	5.45	0.87	1.98	−2.45	2.55	2.19	1.24	1.53
	T3	3.79	0.64	−0.05	4.90	1.25	1.70	0.82	−3.08	−1.32	0.87	1.05
SCI-002	T0	2.09	−0.29	−0.16	−1.38	−1.01	4.24	−5.72	−3.05	1.17	0.50	1.11
	T3	0.86	−0.74	0.17	0.30	0.12	1.27	−3.27	−0.54	−1.17	−0.03	1.84
SCI-003	T0	1.00	3.62	0.49	−4.48	2.68	0.00	0.00	−4.13	−0.15	0.99	0.59
	T3	0.67	−3.13	−0.52	4.61	−3.01	0.00	0.00	−3.99	0.00	1.92	0.69
SCI-004	T0	3.16	3.07	−0.04	−0.79	1.84	13.85	0.82	−9.29	3.80	4.39	3.84
	T3	2.60	1.71	0.26	−1.29	1.50	6.78	2.45	−4.16	4.97	3.18	2.66
SCI-005	T0	−0.82	0.49	0.05	0.00	0.26	2.54	9.80	0.64	3.80	−0.73	−1.07
	T3	0.09	0.57	1.46	−0.23	1.18	1.13	0.00	−3.41	−0.58	1.41	−0.53
SCI-006	T0	3.47	0.38	0.14	−0.77	−0.05	4.38	0.00	−1.08	−0.44	0.07	−0.16
	T3	2.43	0.73	−0.01	−3.01	−0.19	2.12	0.00	−1.28	2.78	0.45	−0.17
SCI-007	T0	3.35	1.53	0.01	−5.40	−6.34	6.78	0.82	−5.00	−0.29	8.05	2.23
	T3	*No T3 data available*										
SCI-008	T0	2.36	2.64	0.26	−0.18	1.39	0.00	2.45	−1.14	0.00	1.53	−1.21
	T3	2.17	1.33	0.28	1.35	2.27	0.00	0.00	−2.12	−0.29	0.99	0.71
SCI-009	T0	2.00	1.03	0.02	−0.73	−0.53	−1.27	0.00	−3.67	4.38	−0.25	0.08
	T3	1.95	−0.31	−0.22	−0.72	0.55	0.57	0.00	−1.37	−0.73	0.20	−0.36
SCI-010	T0	3.85	2.86	−0.14	0.44	3.04	10.32	−4.90	−7.63	−0.73	−0.12	3.12
	T3	5.40	3.22	−0.69	0.00	2.02	14.56	−2.45	−5.30	9.06	−2.39	−2.05
SCI-011	T0	4.13	2.87	0.16	0.75	1.26	10.18	−2.45	0.06	6.58	2.16	−0.52
	T3	2.17	2.57	0.25	0.00	0.05	9.05	−4.90	1.84	1.61	1.50	0.00
SCI-012	T0	2.86	3.88	0.71	2.37	3.08	7.35	−4.08	−5.49	−0.99	−0.84	0.00
	T3	*No T3 data available*										

G

Euclidean distances in PCA space

Table G.1: Individual PCA scores and Euclidean distances at baseline (T0) and six-month follow-up (T3), sorted by Euclidean displacement. PC1 and PC2 scores reflect position in the baseline PCA space; T3 scores represent projections onto the baseline component structure. Distance from origin reflects overall somatosensory asymmetry relative to the contralateral side. A negative Δ distance indicates movement toward somatosensory symmetry following SCS. Euclidean displacement represents the magnitude of the within-patient shift in PCA space between T0 and T3, irrespective of direction. SCI-007 and SCI-012 are excluded due to absence of T3 QST data.

ID	$PC1_{T0}$	$PC2_{T0}$	$PC1_{T3}$	$PC2_{T3}$	$Dist_{T0}$	$Dist_{T3}$	Δ dist	Displacement
SCI-003	0.14	1.40	1.87	−3.04	1.40	3.57	+2.17	4.76
SCI-005	3.37	−0.90	1.67	2.35	3.49	2.88	−0.61	3.67
SCI-004	−3.15	−0.38	−0.74	−0.41	3.17	0.85	−2.32	2.40
SCI-001	2.24	−0.51	0.42	0.23	2.30	0.48	−1.82	1.97
SCI-010	−2.52	1.07	−0.90	0.14	2.74	0.91	−1.82	1.87
SCI-002	0.08	−1.21	1.21	−0.42	1.21	1.28	+0.07	1.38
SCI-006	0.61	−0.15	0.93	−0.87	0.63	1.27	+0.65	0.79
SCI-011	−0.25	0.51	0.16	0.55	0.56	0.57	+0.01	0.41
SCI-009	1.23	−0.59	1.43	−0.95	1.37	1.71	+0.35	0.41
SCI-008	1.21	0.76	0.90	0.81	1.43	1.21	−0.22	0.32

H

Univariate analyses QST change

Table H.1: Univariate analysis of QST change following SCS (T0 $\rightarrow$ T3, $n = 10$). Median within-patient delta z-scores ($\Delta Z = Z_{T3} - Z_{T0}$) with interquartile range (Q1-Q3), uncorrected Wilcoxon signed-rank p-values, and Holm-corrected p-values. No parameter reached statistical significance after Holm correction.

Parameter	Median ΔZ	Q1	Q3	p (uncorrected)	p (Holm)
CDT	-0.26	-0.92	0.68	0.695	1.000
WDT	-0.38	-1.33	0.28	0.193	1.000
TSL	0.02	-0.21	0.24	0.922	1.000
CPT	-0.34	-0.54	1.16	0.922	1.000
HPT	0.12	-0.84	0.91	1.000	1.000
MDT	-0.71	-2.05	0.00	0.327	1.000
VDT	0.00	-1.84	2.25	0.865	1.000
PPT	0.96	-0.78	2.32	0.695	1.000
MPT	-1.31	-4.17	0.91	0.432	1.000
MPS	-0.45	-0.63	0.43	0.557	1.000
WUR	0.04	-0.47	0.53	0.922	1.000

I

Conditioned Pain Modulation data per participant

Table I.1: Conditioned pain modulation (CPM) effects per participant at baseline (T0, $n = 12$). ΔT represents the mean post-conditioning minus pre-conditioning threshold per modality. The 95% confidence interval (CI) was calculated using a Welch-adjusted standard error. Intervals entirely above zero indicate inhibitory modulation; intervals crossing zero indicate uncertain responses; intervals entirely below zero indicate facilitatory modulation. EPT = electrical pain threshold; EPTT = electrical pain tolerance threshold; PPT = pressure pain threshold.

ID	Modality	Mean ΔT	95% CI lower	95% CI upper
SCI-001	EPT	5.27	2.88	7.65
	EPTT	3.13	0.74	5.53
	PPT	0.63	−0.04	1.30
SCI-002	EPT	1.97	−0.15	4.08
	EPTT	2.10	−2.50	6.70
	PPT	0.03	−0.29	0.35
SCI-003	EPT	1.33	−0.41	3.08
	EPTT	2.93	0.56	5.31
	PPT	0.40	−0.05	0.85
SCI-004	EPT	4.07	0.26	7.87
	EPTT	6.97	1.91	12.02
	PPT	0.40	−3.83	4.63
SCI-005	EPT	0.83	0.21	1.46
	EPTT	0.27	−0.86	1.40
	PPT	0.10	−0.41	0.61
SCI-006	EPT	0.70	0.23	1.17
	EPTT	1.30	−0.10	2.70
	PPT	−0.27	−1.80	1.27
SCI-007	EPT	−4.37	−5.82	−2.92
	EPTT	−1.36	−2.76	0.03
	PPT	0.83	−1.56	3.22
SCI-008	EPT	−1.63	−3.63	0.37
	EPTT	0.27	−0.64	1.17
	PPT	0.40	−0.80	1.60
SCI-009	EPT	0.03	−0.35	0.42
	EPTT	−0.13	−0.41	0.15
	PPT	−0.23	−1.46	0.99
SCI-010	EPT	−0.17	−2.71	2.37
	EPTT	0.00	0.00	0.00
	PPT	0.13	−0.43	0.69
SCI-011	EPT	2.47	−0.99	5.92
	EPTT	4.87	2.83	6.90
	PPT	−0.17	−1.24	0.91
SCI-012	EPT	0.97	−0.90	2.84
	EPTT	2.20	1.06	3.34
	PPT	−0.80	−1.96	0.36

Table I.2: Conditioned pain modulation (CPM) effects per participant at six-month follow-up (T3, $n = 10$). See Table I.1 for explanation of columns and classification criteria.

ID	Modality	Mean ΔT	95% CI lower	95% CI upper
SCI-001	EPT	0.70	−1.67	3.07
	EPTT	1.63	−1.10	4.37
	PPT	0.47	−2.69	3.62
SCI-002	EPT	4.17	1.74	6.59
	EPTT	0.00	0.00	0.00
	PPT	1.27	−0.20	2.73
SCI-003	EPT	−0.80	−2.97	1.37
	EPTT	2.40	0.97	3.83
	PPT	1.73	0.22	3.25
SCI-004	EPT	4.43	0.14	8.73
	EPTT	0.17	−0.93	1.26
	PPT	2.13	0.96	3.31
SCI-005	EPT	0.13	−1.58	1.84
	EPTT	0.70	−0.09	1.49
	PPT	1.23	0.61	1.86
SCI-006	EPT	1.10	0.31	1.89
	EPTT	1.84	−0.90	4.57
	PPT	−0.67	−1.43	0.09
SCI-008	EPT	0.27	−0.35	0.89
	EPTT	1.23	0.70	1.76
	PPT	4.07	2.60	5.53
SCI-009	EPT	0.27	−0.51	1.04
	EPTT	0.10	−0.58	0.78
	PPT	5.00	3.69	6.31
SCI-010	EPT	1.14	−0.03	2.30
	EPTT	0.00	0.00	0.00
	PPT	−1.30	−1.55	−1.05
SCI-011	EPT	−0.77	−1.50	−0.04
	EPTT	0.70	−1.07	2.47
	PPT	1.33	0.76	1.91

J

Literature Review

Mechanisms of Action of Spinal Cord Stimulation Paradigms in Neuropathic Pain: A Scoping Review

Anne W. Veenhuizen

Student MSc Technical Medicine
Delft University of Technology; Erasmus Medical Centre Rotterdam; Leiden University Medical Centre, the Netherlands

Supervisors

Dr. Ir. Cecile C. de Vos, *Medical Physicist*
Department of Anaesthesiology, Erasmus Medical Centre Rotterdam, the Netherlands

Prof. Dr. Frank J.P.M. Huygen, *Professor/Pain Specialist*
Department of Anaesthesiology, Erasmus Medical Centre Rotterdam, the Netherlands

March 12, 2026

Abstract

Background: Spinal cord stimulation (SCS) is used to treat neuropathic pain and is delivered through multiple stimulation paradigms that differ in waveform, frequency, amplitude and pulse width. Paradigms such as tonic, burst and high-frequency stimulation are proposed to engage distinct neurobiological mechanisms. However, the exact mechanism of SCS-induced analgesia remains only partly understood, and mechanistic evidence is heterogeneous across preclinical and clinical studies.

Objective: With this scoping review, I aimed to systematically map and compare spinal, supraspinal and molecular mechanisms associated with different SCS paradigms and to identify paradigm-specific mechanistic patterns in the current literature.

Method: I conducted a scoping review of preclinical and clinical studies investigating mechanistic effects of SCS. Stimulation paradigms were included when multiple mechanistic studies were available. Findings were synthesized qualitatively across spinal, supraspinal and molecular domains.

Results: SCS modulates pain-related processing across all investigated levels in a paradigm-dependent manner. Tonic stimulation is most consistently associated with spinal inhibition. High-density SCS engages spinal circuits without dorsal column recruitment, whereas burst stimulation is characterized by modulating affective–attentional networks. High-frequency stimulation primarily functions through the attenuation of synaptic transmission, dampening nociceptive input. Lastly, 10-kHz and Differential Target Multiplexed SCS stand out for their extensive modulation of neuro-glial and molecular signalling pathways.

Conclusion: This review demonstrates that SCS engages multiple mechanistic pathways with paradigm-specific patterns. However, these fingerprints are often inferred from simplified computational models or indirect measures of neural activity. Methodological variability across studies and lack of direct paradigm comparisons limit direct comparison between paradigms, underscoring the need for standardized mechanistic research that systematically examines comparable parameters across different SCS paradigms and patient populations.

Keywords: Spinal Cord Stimulation, Neuropathy, Mononeuropathy, Mechanism of Action

1 Abbreviations

CRPS	Complex Regional Pain Syndrome
DC	Dorsal Column
DH	Dorsal Horn
DTM	Differential Target Multiplexed
ECAP	Evoked Compound Action Potential
ECM	Extracellular Matrix
HD	High Dose/Density
HF	High-Frequency
PDPN	Peripheral Diabetic Polyneuropathy
PSPS	Persistent Spinal Pain Syndrome
SCS	Spinal Cord Stimulation
SEP	Somatosensory Evoked Potential
WDR	Wide Dynamic Range

2 Introduction

Chronic neuropathic pain is a global health problem, affecting an estimated 9% of the population [1, 2]. It is not only highly distressing but also associated with substantial impairments in quality of life and significant socioeconomic burden [3, 4]. Despite a range of therapeutic options, including pharmacotherapy and nerve blocks, neuropathic pain remains notoriously difficult to treat. Conventional treatments often provide limited relief, with 40% of patients not achieving meaningful pain reduction [5]. This therapeutic gap has driven growing interest in neuromodulation techniques such as spinal cord stimulation (SCS).

2.1 Evolution of Spinal Cord Stimulation

SCS was first introduced in 1967, inspired by the "gate control theory of pain" proposed by Melzack and Wall [6]. According to this model, activation of large-diameter afferent fibers (Aβ-fibers) in the dorsal columns (DC) could "close the gate" to nociceptive transmission in the dorsal horn (DH) and thereby attenuate pain perception. Technically, this involves epidurally implanted electrodes that deliver controlled electrical pulses to the spinal cord, modulating ongoing neural activity. Initially, SCS was designed to produce paresthesia through low-frequency tonic stimulation, aiming to mask or block pain. However, it has since become increasingly recognized that the effects of SCS extend beyond classical gating, with proposed mechanisms operating at spinal, supraspinal, and molecular and cellular levels.

Over the past decades, several SCS paradigms have been developed, ranging from conventional tonic stimulation to burst, high-frequency (HF), high-density (HD), and more recently Differential Target Multiplexed (DTM) approaches. Whereas conventional tonic stimulation delivers continuous low-frequency pulses, burst SCS applies clusters of high-frequency pulses embedded within low-frequency cycles, and HF (1–10 kHz) SCS delivers continuous kilohertz stimulation without inducing paresthesia [7, 8]. HD SCS further modifies stimulation intensity and pulse characteristics to increase overall stimulation density, while DTM SCS applies multiple stimulation patterns across electrode contacts simultaneously [9, 10]. The development of these paradigms was driven by the hypothesis that variations in stimulation parameters could engage neural circuits beyond those targeted by classical tonic stimulation, resulting in analgesic effects not fully explained by spinal inhibition alone [11, 12].

2.2 Conceptual Framework and Terminology

To facilitate interpretation of the mechanistic literature reviewed in this study, Figure 1 provides anatomical and cellular context for the terminology used throughout this review.

- **Figure 1a** illustrates the organization of the spinal DH, including laminar structure, primary afferent fiber types, and key neuronal populations such as wide dynamic range (WDR) neurons and inhibitory interneurons.
- **Figure 1b** depicts cortical and subcortical brain regions commonly implicated in pain processing, serving as a reference framework for supraspinal modulation.
- **Figure 1c** provides a schematic overview of molecular and cellular mechanisms within the spinal cord, highlighting interactions between neurons, astrocytes, and microglia, as well as signaling mediators such as TNF-α and IL-1β.

Figure 1 is intended for conceptual orientation only and does not imply paradigm-specific or causal effects of SCS.

2.3 Problem Statement and Research Questions

While the clinical effectiveness of SCS is supported by increasing evidence, its precise mechanisms of action remain only partially understood [12]. Mechanistic research has predominantly focused on com-

plex conditions such as peripheral diabetic polyneuropathy (PDPN), persistent spinal pain syndrome (PSPS), and complex regional pain syndrome (CRPS), whereas mononeuropathies have received comparatively little attention. Yet, the localized pathophysiology of mononeuropathy may offer unique insights into the mechanisms of SCS.

The clinical necessity of clarifying these mechanisms is further underscored by the broader socioeconomic impact of chronic neuropathic pain. As previously noted, chronic neuropathic pain represents a significant public health challenge, imposing a substantial socioeconomic strain through high direct healthcare costs and indirect costs related to productivity loss [3–5]. As SCS remains a resource-intensive intervention, a precise mechanistic framework is required to optimize treatment cost-effectiveness. By mapping these biological drivers, this review aims to support a more targeted application of neuromodulation, potentially reducing the trial-and-error approach that currently characterizes clinical practice.

Against this background, this scoping review aims to provide an overview of the proposed mechanisms of action attributed to different SCS paradigms as reported in the animal model and human study literature. Specifically, it addresses the following questions:

1. What are the hypothesized mechanisms of action of the major SCS paradigms (tonic, burst, HF, 10 kHz, DTM, and HD)?
2. What evidence supports each of these mechanistic hypotheses across spinal processing, supraspinal modulation, and molecular and cellular levels?
3. How might these mechanistic profiles relate to different neuropathic pain phenotypes, including mononeuropathy, polyneuropathies, and CRPS?

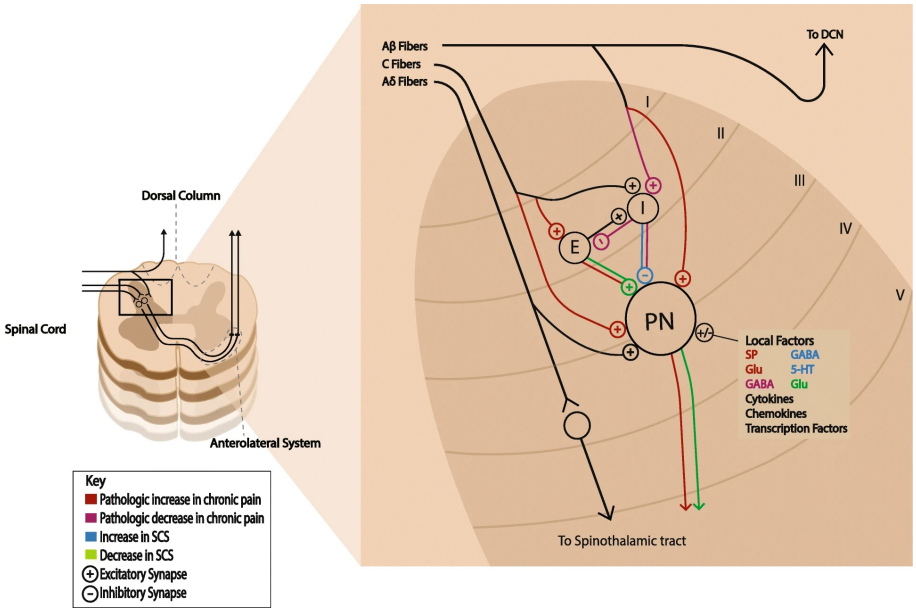

(a) Spinal level: Organization of the dorsal horn, illustrating the laminar structure (I-V), primary afferent fibers ($A\beta$, $A\delta$, C), and the neurochemical balance between Wide Dynamic Range projection neurons and interneurons. Reproduced from Caylor et al [13]

.

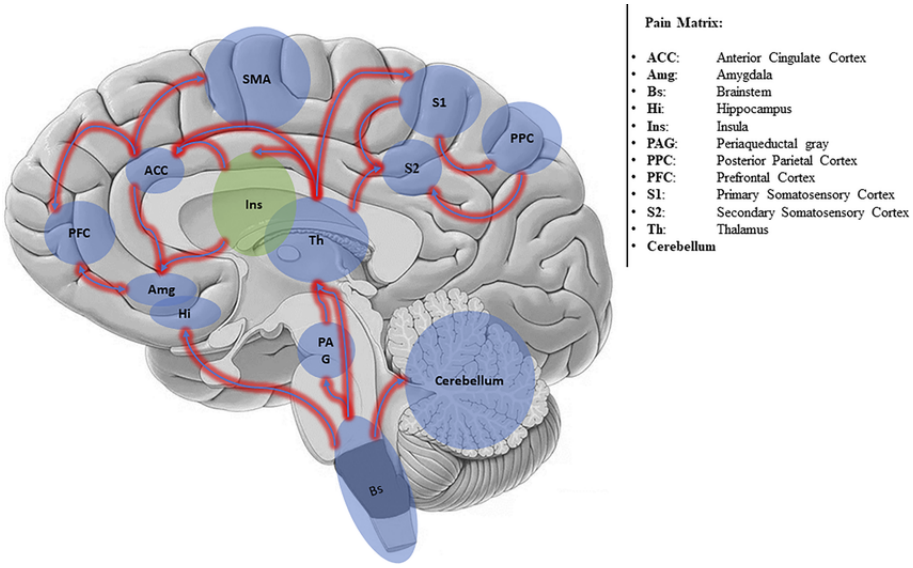

(b) Supraspinal level: cortical and subcortical regions commonly discussed in relation to pain processing and supraspinal modulation, including sensory, affective, and cognitive networks. Reproduced from Riganello et al [14].

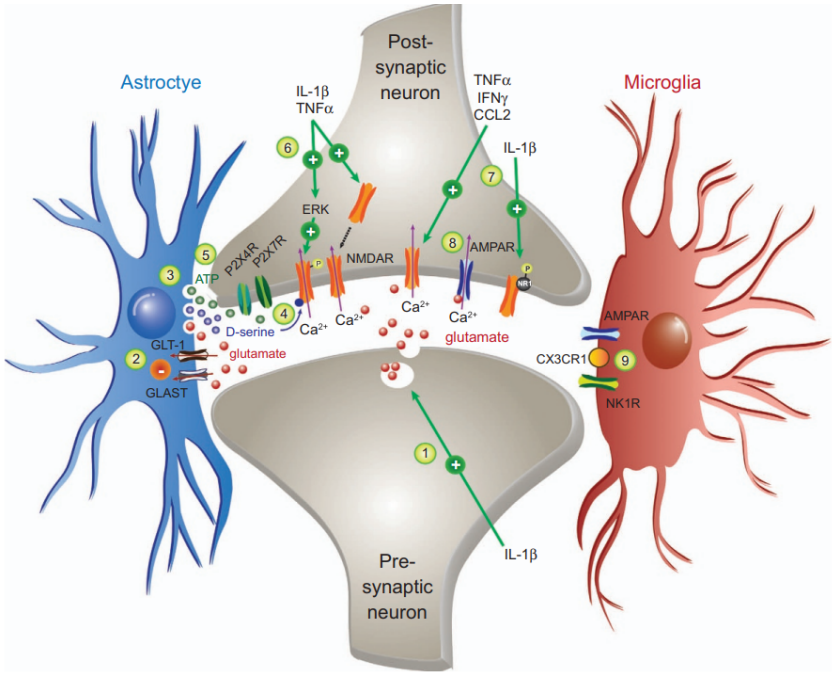

(c) Molecular and cellular level: schematic illustration of neuronal and glial components within the spinal dorsal horn, highlighting interactions between neurons, astrocytes, and microglia and representative mediators such as TNF-α and IL-1β. Reproduced from Ray et al [15].

Figure 1: Anatomical and cellular context for the mechanistic terminology used throughout this review. Panels a-c illustrate representative spinal, supraspinal, and molecular levels at which SCS has been proposed to influence pain processing. The figure is provided for conceptual orientation only; arrows and signaling pathways are intended to aid visualization and should not be interpreted as causal or paradigm-specific mechanistic effects.

3 Methods

This scoping review was conducted in accordance with the Preferred Reporting Items for Systematic Reviews and Meta-Analyses extension for Scoping Reviews (PRISMA-ScR) guidelines [16]. The objective was to map and synthesize the existing evidence on the mechanisms of action of SCS in neuropathic pain.

3.1 Selection Criteria

The inclusion and exclusion criteria were defined and refined iteratively during the screening process. Studies were eligible for inclusion if they met the following criteria:

- Investigated SCS as the main intervention.
- Reported or discussed mechanistic effects at any level (spinal, supraspinal, or molecular and cellular).
- Included any experimental or human model relevant to SCS mechanisms, including neuropathic, nociceptive, inflammatory, or healthy conditions.
- Used an animal model, human study, or computational model.
- Published in English after 2005; multiple SCS paradigms (e.g., burst and HF stimulation) emerged after this period, and earlier literature primarily focused on clinical efficacy rather than mechanisms.

Studies were excluded if they met any of the following criteria:

- Investigated SCS for non-pain indications such as movement disorders (e.g. spasticity), motor function, or autonomic dysfunction.
- Examined other neuromodulation techniques (e.g., peripheral nerve stimulation, dorsal root ganglion stimulation, deep brain stimulation, transcranial direct current stimulation, or transcranial magnetic stimulation) without SCS.
- Reported only clinical efficacy outcomes without mechanistic assessment or discussion.
- Were conference abstracts, editorials, or letters lacking original data.
- Were review papers that did not contain original

experimental, clinical, or computational data, but rather summarized previously published findings.

3.2 Search Strategy

A comprehensive literature search was conducted in Embase, Medline, Web of Science Core Collection, and Cochrane Central Register of Controlled Trials. The search strategy combined MeSH terms and free-text terms related to SCS, mechanisms, and neuropathic pain. The last search was performed on 17-09-2025. Full search strings are provided in Appendix A.

3.3 Study Selection

Records were imported into Covidence for deduplication and screening. Titles and abstracts were screened, followed by full-text eligibility assessment based on the predefined criteria. The number of records at each stage is depicted in the PRISMA-ScR flowchart (Figure 2). Studies performed in healthy models were included if they provided mechanistic insights relevant to the action of SCS.

3.4 Data Extraction

I developed a standardized data extraction form, which I used to extract data for this review. Extracted information comprised bibliographic details (author, year), study type (animal, human, or computational), pain model or condition, stimulation paradigm and parameters, level of mechanistic assessment (spinal, supraspinal, molecular), and the proposed mechanistic explanations and corresponding reported findings as described by the authors and interpreted by me.

Because terminology overlaps across studies, categorization was not based on frequency alone. While "high-dose" and "high-density" SCS refer to distinct technical aspects, they are frequently used interchangeably to describe tonic paradigms delivering elevated electrical charge per second at intensities below sensory threshold (no paresthesia). To maintain consistency, such protocols were collectively classified as HD-SCS. Stimulation paradigms explicitly described as high-frequency or kilohertz SCS, or operating above 1000 Hz, were categorized as HF-SCS. Only paradigms investigated across multiple studies were included in the mechanistic synthesis to allow for identification of convergent evidence.

3.5 Functional Framework for Synthesis

Mechanistic findings were grouped into three functional domains, corresponding to the levels illustrated in Figure 1. In this review, the term electrophysiological recordings is used as an umbrella term for measurements of neural electrical activity, including invasive spinal recordings in animal models and non-invasive techniques (e.g., EEG, MEG) in human studies. Findings were organized into:

1. **Spinal**, comprising fast neuronal and synaptic processes within the DC and DH, primarily derived from invasive recordings in animal models.
2. **Supraspinal**, encompassing alterations across distributed brain regions involved in pain processing, assessed using neuroimaging and non-invasive electrophysiological techniques as EEG, MEG, and evoked potentials.
3. **Molecular and cellular mechanisms**, describing changes in neurochemical, glial, and intracellular signaling pathways.

3.6 Data Analysis and Presentation

Extracted data were summarized descriptively according to stimulation paradigm and functional level. Paradigms are presented in an order reflecting increasing deviation from tonic frequency. Findings were tabulated and synthesized narratively to identify convergent and divergent mechanisms, highlight domain-specific trends, and delineate gaps in the current understanding of SCS mechanisms.

4 Results

In total, 89 studies were included in this scoping review after removal of duplicates and full-text eligibility assessment following screening of 1040 records identified through database searches (Figure 2). A comprehensive overview of all extracted study characteristics per paradigm is provided in Appendix B-G.

The included literature covers a broad methodological range, encompassing animal models ($n = 53$), human studies ($n = 27$), and computational models ($n = 9$). Among these, six main stimulation paradigms were identified: tonic, HD, burst, HF, 10-kHz, and DTM SCS. The included studies were published between 2007 and 2025, with a marked increase in mechanistic investigations after 2020.

To provide an overview of the evidence base, Table 1 summarizes the number of studies contributing to each mechanistic level per paradigm, alongside the distribution of human, animal, and computational models. Because some studies examined multiple paradigms or mechanistic domains, the counts represent contributions per domain rather than unique article totals.

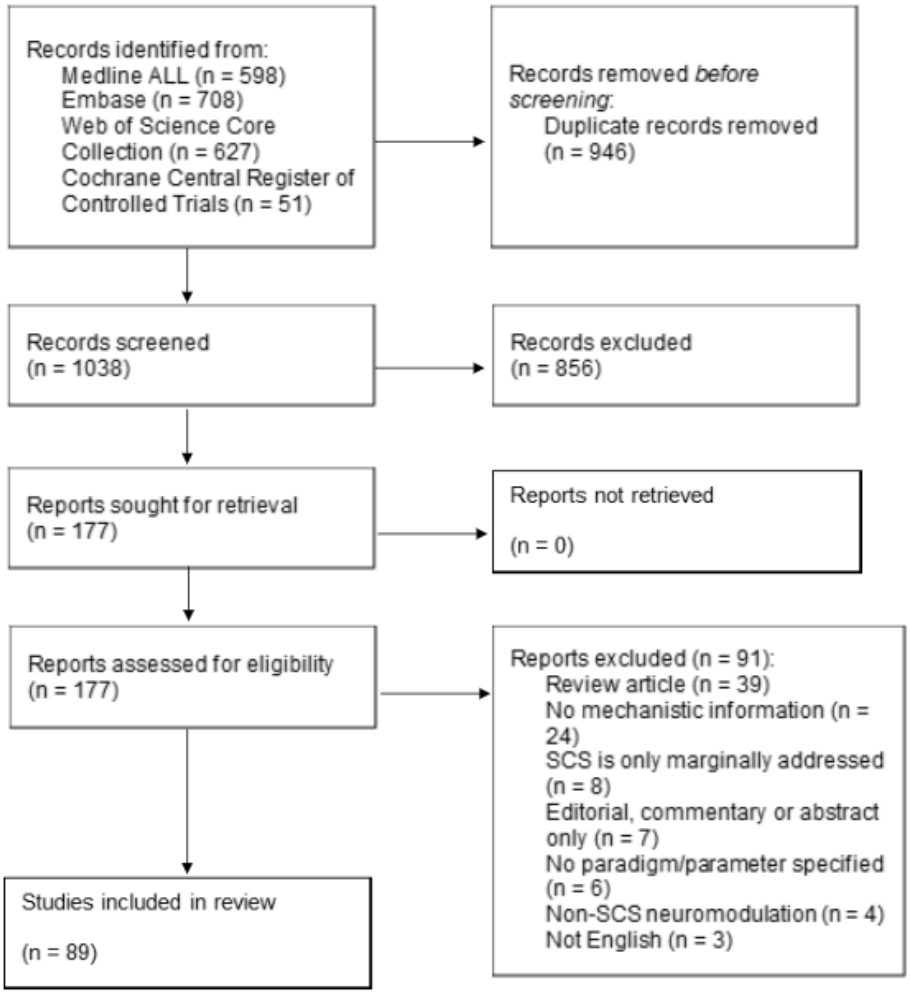

Figure 2: PRISMA-ScR flow diagram of study identification and selection. SCS = Spinal Cord Stimulation.

Overall, the included studies illustrate methodological diversity, with heterogeneous models, stimulation parameters, and outcome measures. Nevertheless, recurring mechanistic patterns can be distinguished within and across paradigms, indicating both shared and paradigm-specific mechanisms. The following sections provide a synthesis of mechanistic findings for each paradigm as reported in the literature.

4.1 Tonic SCS

Conventional or tonic SCS delivers continuous low-frequency stimulation, typically in the range of 40-60 Hz. The paradigm was originally developed to activate large-diameter afferent fibers (Aβ-fibers) within the DC, based on the Gate Control Theory of Pain [6], whereby afferent input inhibits nociceptive transmission in the DH via local inhibitory interneurons. Although initially framed as a purely spinal mechanism, subsequent work has suggested that tonic SCS may engage additional spinal processing and supraspinal processes. The included articles are listed in Appendix B.

4.1.1 Spinal neuronal mechanisms

Evidence from human studies, animal models, and computational models demonstrates that tonic SCS produces pronounced spinal-level modulation. In animal models, invasive spinal electrophysiological recordings demonstrate that 50-60 Hz stimulation evokes synchronized action potentials in DC axons of Aβ-fibers and inhibits wind-up in WDR neurons, consistent with spinal inhibition as described by the classical gate control theory [17–21].

Computational models indicate that tonic stimulation generates highly synchronized DC firing patterns that are consistent with mechanisms underlying paresthesia reported during low-frequency SCS, while also engaging DH inhibition [22]. Within the DH, tonic SCS evokes AMPA receptor-mediated excitatory potentials

Table 1: Overview of mechanistic evidence across SCS paradigms

SCS Paradigm	Total	Model Type			Mechanistic Level		
		Human	Animal	Computational	Spinal	Supraspinal	Molecular
Tonic	61	18	38	5	33	19	16
HD	12	7	3	2	6	6	1
Burst	23	13	7	2	10	12	3
HF	16	2	12	2	11	2	4
10-kHz	24	6	14	4	14	4	6
DTM	8	0	8	0	4	0	7

Note: Counts reflect the number of studies reporting on each type of evidence. Studies may contribute to multiple categories. SCS = Spinal Cord Stimulation, HF = High-Frequency, DTM = Differential Target Multiplexed, HD = High-Density.

that progressively diminish during sustained stimulation [23]. It increases firing rates of excitatory interneurons more than inhibitory ones, suggesting selective recruitment of local spinal circuits [24]. In animal models, 60 Hz stimulation also induces bilateral c-fos expression near the electrode site, confirming local neuronal activation [25], while recordings from DC nuclei show that 50 Hz SCS modulates neuronal activity at this first relay station, suggesting these nuclei help transmit DC input rostrally and may contribute to supraspinal modulation [26].

In human studies, Electrically Evoked Compound Action Potential (ECAP) recordings confirm recruitment of Aβ-fibers within the DC during tonic SCS. 50 Hz stimulation maintains synchronous activation by delivering pulses during the late subnormal phase of the axonal recovery cycle, producing stable ECAP morphology [27]. Increasing stimulation frequency reduces ECAP amplitude while enhancing paresthesia intensity, indicating that paresthesia intensity is not determined by the number of activated fibers, but rather by how synchronously the recruited fibers fire [28]. Computational models support this, showing preferential polarization of axons over neuronal somas, consistent with presynaptic modulation of DH interneurons [29, 30]. Additional modeling suggests that tonic stimulation does not invert recruitment thresholds across fiber diameters, indicating that enhanced paresthesia results from changes in activation dynamics within the recruited population rather than selective recruitment of larger fibers [31].

4.1.2 Supraspinal and network mechanisms

Neuroimaging and electrophysiological evidence consistently demonstrate supraspinal modulation by tonic SCS. Human studies using fMRI and PET show increased activation and metabolism in the thalamus, premotor, and frontal cortices, including the anterior cingulate and parietal association areas, during 50-60 Hz stimulation [32–34]. Simultaneously, bilateral deactivation occurs in limbic regions such as the parahippocampus and retrosplenial cortex [7, 32].

Non-invasive electrophysiological recordings, including EEG, MEG, and evoked potential measurements in human studies, corroborate these findings. Specifically, tonic SCS decreases cortical theta activity and suppresses nociceptive laser-evoked potentials and somatosensory evoked potentials (SEPs) [9, 21, 35]. The amplitude of the P40 LEP, an early cortical component associated with nociceptive processing, shows a dose-dependent reduction, consistent with robust DC activation [36]. EEG and MEG studies report decreases in delta, theta, and beta band power during stimulation, indicating reduced global cortical excitability. Compared with no stimulation or HD-SCS, tonic SCS yields the lowest mean power across these frequency bands, suggesting a stronger inhibitory effect on cortical oscillatory activity [37, 38]. In animal models, 40 Hz SCS increased firing in the gracile nucleus, accompanied by inhibition of spinal nociceptive responses [39].

4.1.3 Molecular and cellular mechanisms

In animal models, tonic SCS has been reported to partially reverse injury-induced neuroinflammation through the modulation of spinal mTOR signaling [40]. As a key regulator of cellular metabolism and inflammatory responses, mTOR modulation is accompanied by widespread molecular remodeling. Proteomic and lipidomic analyses reveal altered expression of over 150 proteins involved in ECM organization, metabolic processes, and neuroinflammatory regulation [41–43]. These changes likely reflect downstream effects of sustained neuromodulation rather than direct actions of stimulation alone. Transcriptomic profiling further demonstrates that SCS makes nerve cells in the spinal cord less sensitive to pain by breaking down the supporting structures of pain receptors and normalizing the chemical communication between cells [44, 45].

Across various animal models, tonic SCS induces broad molecular remodeling characterized by the par-

tial restoration of ECM organization and modulation of immune-related gene expression, consistent with a shift toward the re-establishment of spinal homeostasis [45–47]. Most studies report that tonic SCS reduces neuroinflammation by calming overactive microglia and decreasing the production of inflammatory signaling molecules (pro-inflammatory cytokines). However, these molecular responses are not always uniform. In some models, researchers observed a temporary shift of immune cells into an aggressive, pro-inflammatory state (transient M1-like activation) and an increase in specific inflammatory markers such as TNF-α [48–50]. These varied findings suggest that the molecular and cellular mechanisms of tonic SCS are context-dependent and may change depending on the timing or the specific pain condition. Furthermore, repetitive low-frequency SCS has been reported to engage the spinal endocannabinoid system, which acts as a natural brake to reduce the over-activity of pain-transmitting receptors (NMDA receptors). This process helps lower the overall sensitivity of the spinal cord, effectively counteracting the process of central sensitization [51].

In addition to its effects within the spinal cord, tonic SCS also influences the rest of the body, including the blood vessels and peripheral nerves. Vasodilation occurs because SCS reduces the "fight-or-flight" signals from the sympathetic nervous system and triggers specific sensory fibers to release a molecule that naturally increases local blood flow [52, 53]. In animal models of PDPN, tonic SCS has even been shown to increase the density of small nerve fibers in the skin, suggesting that the treatment helps repair damaged nerve structures [54]. In human studies, these central effects also lead to a decrease in circulating cytokines and growth factors while improving endothelial function, likely reflecting downstream consequences of central modulation [55].

4.1.4 Summary

Tonic SCS is primarily associated with the activation of Aβ-fibers within the DC, consistent with gate-control principles that promote spinal inhibition of nociceptive transmission in the DH. Across studies, tonic stimulation engages multiple inhibitory pathways, including serotonergic, GABAergic, and opioid systems, and is frequently associated with reduced WDR neuron activity and attenuation of neuroinflammatory markers. Beyond the spinal level, tonic SCS influences supraspinal modulation of pain networks, including thalamo-cortical and limbic circuits, leading to reduced cortical responsiveness to afferent input. While its mechanistic profile depends on stimulation parameters, converging evidence suggests a multi-level shift toward rebalancing excitatory and inhibitory processing and partial normalization of injury-related states.

4.2 High-Density SCS

High-density or high-dose (HD) SCS comprises tonic stimulation paradigms that increase total electrical charge delivery while maintaining subthreshold intensities. This is typically achieved through higher stimulation frequencies within the sub-kilohertz range and/or shortened pulse widths, without employing burst patterns or continuous kilohertz stimulation. In this review, HD-SCS includes tonic protocols described as high-density or high-dose in the primary literature, as well as paradigms operating up to approximately 1000 Hz. The included articles are listed in Appendix C.

4.2.1 Spinal processing

Across human studies, animal models, and computational models, HD-SCS operates in a subthreshold regime that preserves DC activation while altering spinal excitability. In human studies, stimulation at HD parameters did not evoke EMG responses or abolish SEPs, indicating recruitment of Aβ-fibers without motor activation, comparable to tonic stimulation [36, 56].

Computational models show that increasing tonic frequency alters Aβ-fiber firing dynamics, with reduced phase-locked firing above approximately 300–400 Hz due to sodium channel recovery kinetics, without inducing complete conduction block [57]. In frequency-comparison studies using animal models, stimulation at 100 Hz and 500 Hz reduced DH field potentials and WDR neuron firing relative to conventional low-frequency tonic stimulation, consistent with attenuation of nociceptive processing at sub-kilohertz frequencies [22, 28]. In contrast, stimulation at 1000 Hz did not further suppress spinal responses seen at 100–500 Hz but instead altered the pattern of spinal signal processing, suggesting a qualitatively different mode of modulation at the upper limit of the sub-kilohertz range.

Beyond modulation of WDR activity, sub-kilohertz HD-SCS suppresses activation of superficial lamina I NK1R-positive neurons in animal models, indicating reduced nociceptive output from the DH [58]. Recordings from the DC nuclei further demonstrate that higher sub-kilohertz stimulation alters activity at this first supraspinal relay, suggesting that frequency-dependent changes in afferent signaling are transmitted beyond the spinal cord [59].

4.2.2 Supraspinal modulation

Neuroimaging studies in humans report parameter-dependent supraspinal changes during HD-SCS, with altered activity in prefrontal, cingulate, insular, and somatosensory cortices observed across stimulation settings [32, 60]. Higher tonic frequencies described as HD-SCS

were associated with bilateral insular and frontal activation alongside deactivation of parietal and midline regions such as the precuneus and posterior cingulate cortex. However, available data do not establish whether these supraspinal changes reflect direct neuromodulatory effects of stimulation or indirect consequences of altered spinal processing and pain perception.

Supraspinal electrophysiological measures further support altered cortical processing during HD-SCS. Suppression of SEPs suggests reduced transmission of sensory input to cortical targets [9], while EEG and resting-state fMRI studies report changes in spectral power, functional coupling, and connectivity within default-mode and salience-related networks during HD stimulation [37, 60]. Together, these findings indicate supraspinal correlates of HD-SCS, although mechanistic specificity remains limited.

4.2.3 Molecular and cellular mechanisms

Evidence remains limited at this level, as no studies included in this review directly investigated molecular or cellular mechanisms specific to HD-SCS. Gene expression, glial activation, and inflammatory signaling have not been assessed in the context of HD stimulation, leaving its molecular effects unresolved.

4.2.4 Summary

HD-SCS represents tonic stimulation paradigms that operate in a subthreshold regime and preserve DC conduction. Experimental and computational studies show frequency-dependent modulation of afferent signaling and DH excitability at sub-kilohertz frequencies, with attenuation of nociceptive neuronal responses relative to conventional tonic stimulation. At the supraspinal level, HD-SCS is associated with modulation of cortical and subcortical networks involved in pain processing, although these effects overlap with those reported for other subthreshold and HF paradigms. Evidence at the molecular and cellular level is currently scarce. Taken together, HD-SCS is best understood as part of a frequency-dependent continuum between tonic and HF stimulation rather than a mechanistically distinct paradigm.

4.3 Burst SCS

Burst SCS delivers trains of high-frequency pulses, typically around 500 Hz within bursts, separated by low-frequency inter-burst intervals of approximately 40 Hz. The paradigm was developed to mimic natural burst firing patterns observed in thalamic relay neurons and to provide analgesia without continuous paresthesia. Proposed mechanisms suggest that burst stimulation modulates spinal processing while simultaneously influencing supraspinal modulation of networks involved in the affective and attentional dimensions of pain [7, 61]. The included articles are listed in Appendix D.

4.3.1 Spinal processing

Animal models and computational models consistently show that burst SCS produces strong spinal inhibition. In animal models, recordings from DH neurons demonstrate suppression of WDR firing, reduced wind-up, and decreased post-discharge activity, indicating effective gating of nociceptive transmission [61–63]. In ovine models, burst stimulation increases hemodynamic and metabolic activity in the superficial DH, reflecting recruitment of both excitatory and inhibitory neuronal populations [64]. Single-neuron recordings show activation of adapting and non-adapting interneurons, suggesting a broader modulation compared with HF-SCS [65].

Mechanistically, burst SCS combines elements of low- and high-frequency paradigms. The burst packet recruits Aβ-fiber input into the DC while avoiding continuous temporal summation, thereby reducing DH excitability at intensities below sensory threshold [61, 64]. Computational models indicate that burst waveforms promote asynchronous Aβ-fiber activation and limit sustained depolarization of DC axons, reducing adaptation and maintaining dynamic gating [29, 30]. Passive-recharge configurations produce the strongest inhibitory effects, whereas active-recharge patterns are less effective [63]. At the neurochemical level, burst SCS engages partial $GABA_B$- and adenosine-dependent mechanisms. Some studies report $GABA_B$-mediated suppression of DH hyperexcitability [35, 66], while another animal model describes limited GABAergic involvement [61].

4.3.2 Supraspinal modulation

Burst SCS induces pronounced reorganization of cortical and subcortical networks compared with tonic stimulation. In human studies, EEG and MEG show enhanced event-related desynchronization over somatosensory cortices and modulation of theta and beta oscillations, reflecting altered sensory processing [35, 67, 68]. The amplitude of nociceptive LEPs decreases, consistent with reduced cortical salience of painful input [36].

Functional imaging confirms supraspinal modulation, with activation of medial and lateral pain networks, such as the anterior cingulate, insula, and prefrontal cortex and concurrent deactivation of limbic and default-mode network regions [7, 33, 69]. This pattern suggests coordinated modulation of sensory-discriminative and affective-emotional circuits. Human electrophysiology further shows that burst SCS reduces cortical attention to somatosensory input, demonstrated by decreased

P300 amplitudes [70]. Animal models corroborate these findings, showing altered firing in gracile and thalamic relay neurons indicative of modified thalamo-cortical gating [39, 61].

4.3.3 Molecular and cellular mechanisms

Burst SCS is associated with changes in both local spinal and systemic immune markers. In human studies involving patients with PSPS or CRPS, burst SCS has been reported to increase the anti-inflammatory cytokine IL-10 and to normalize circulating inflammatory markers, potentially reflecting improved endothelial function [55, 71].

In the DH, animal models demonstrate reduced expression of sensitization-related markers such as c-fos and GluN2B following burst SCS [61, 63]. Burst stimulation has also been shown to increase spinal blood flow and to reduce microglial activation, suggesting partial restoration of local metabolic and immune balance within the spinal cord [64, 65].

4.3.4 Summary

Burst SCS combines high-frequency pulse trains delivered at a low burst rate to achieve subthreshold modulation of spinal processing without inducing paresthesia. Animal models demonstrate pronounced spinal inhibitory effects, including reduced nociceptive signaling associated with asynchronous Aβ-fiber recruitment and altered temporal integration of afferent input. Neurochemical evidence indicates engagement of inhibitory $GABA_B$- and adenosine-dependent mechanisms, although their relative contribution varies across models. At the supraspinal level, burst stimulation is associated with reorganization of thalamo-cortical and limbic networks, consistent with reduced salience and affective processing of painful stimuli. At the molecular and cellular level, studies report downregulation of excitatory markers, reduced microglial activation, and increased IL-10 expression, suggesting partial modulation of neuroimmune processes.

4.4 High-Frequency SCS

High-Frequency SCS (HF-SCS) refers to stimulation paradigms delivering pulses in the kilohertz range and was developed to provide analgesia without the paresthesia associated with tonic stimulation. In this review, HF-SCS includes paradigms explicitly described as high-frequency or kilohertz stimulation in the primary literature. Proposed mechanisms emphasize modulation of axonal and synaptic activity, including altered synchronization of DC signaling, rather than direct activation of Aβ-fibers. The included articles are listed in Appendix E.

Although 10 kHz stimulation falls within the kilohertz frequency range, it is discussed separately because it has been proposed to represent a distinct paradigm with a unique mechanistic profile.

4.4.1 Spinal processing

Experimental and computational models indicate that HF-SCS operates through subthreshold modulation of axonal and synaptic activity rather than classical spinal inhibition. Kilohertz-rate stimulation induces asynchronous and transient onset firing in DC axons, in contrast to the regular stimulus-synchronous firing observed during low-frequency tonic stimulation [17]. Sustained conduction block is therefore unlikely to account for analgesic effects, as such block typically occurs only at or above motor threshold.

Consistent with this non-gating mode of action, computational models suggest that HF-SCS primarily modulates afferent signal transmission rather than directly activating neurons. Kilohertz stimulation preferentially affects axonal compartments, with minimal somatic depolarization, supporting a predominantly presynaptic mechanism under subthreshold conditions [30, 72]. In this model, the high-frequency pulses are proposed to achieve an attenuation of synaptic transmission, effectively dampening nociceptive input before it reaches the DH neurons. The magnitude of these effects varies across fiber populations and depends on stimulation frequency and waveform characteristics.

At the level of spinal processing, electrophysiological recordings demonstrate limited and heterogeneous effects on neuronal firing across the lower kilohertz range at subthreshold amplitudes. At 1-1.2 kHz, stimulation did not significantly alter evoked or spontaneous WDR neuron firing or wind-up, indicating minimal direct inhibition of DH neurons at these frequencies [18, 63]. In contrast, recordings across a broader frequency spectrum show increasing neuronal activation with rising frequency, with the strongest responses observed at higher kilohertz frequencies (8-10 kHz), particularly in deeper DH laminae [73]. Similarly, stimulation between 1 and 5 kHz did not selectively recruit inhibitory interneurons, whereas higher frequencies elicited more widespread DH activation [74, 75].

4.4.2 Supraspinal modulation

Evidence for supraspinal modulation during HF-SCS remains limited. Human studies using fMRI demonstrate that subthreshold kilohertz stimulation modulates discrete cortical and subcortical regions in a frequency-dependent manner [32].

Complementary in vivo recordings in animals further in-

dicate that HF-SCS can influence supraspinal processing. In one study, 1 kHz stimulation altered cortical excitability and pain-related oscillatory activity despite limited direct effects at the DH level, suggesting that kilohertz stimulation can engage cortical networks indirectly, potentially via changes in afferent signal transmission rather than through direct spinal inhibition [20].

4.4.3 Molecular and cellular mechanisms

Several studies in animal models suggest that HF-SCS influences neuroimmune signaling rather than directly suppressing neuronal activity. In these models, kilohertz stimulation alleviated neuropathic pain and spasticity in association with reduced glial activation and modulation of inflammatory pathways [75]. Transcriptomic analyses show that 1.2 kHz stimulation partially reverses microglial gene expression changes associated with neuropathic pain, although these effects were reported to be less pronounced than those observed with DTM-SCS [46].

Additional work in animal models demonstrates that kilohertz stimulation reduces mechanical hypersensitivity and shifts the spinal inflammatory balance toward an anti-inflammatory profile, characterized by increased IL-10 expression [49]. Together, these findings indicate that HF-SCS is associated with modulation of molecular and cellular mechanisms linked to neuroimmune regulation.

4.4.4 Summary

HF-SCS comprises kilohertz-range stimulation paradigms that operate in a subthreshold regime and do not rely on classical DC gate-control mechanisms. Electrophysiological and computational studies indicate that HF-SCS alters axonal excitability and afferent signal transmission through frequency-dependent modulation of axonal compartments. This is consistent with an attenuation of synaptic transmission through predominantly presynaptic effects, rather than direct neuronal activation. Evidence for supraspinal modulation is limited but suggests changes in discrete cortical networks that are likely secondary to altered spinal processing. In animal models, HF-SCS engages glial and inflammatory pathways, supporting a contribution of neuroimmune modulation to its analgesic effects. Overall, current evidence characterizes HF-SCS as a paradigm defined by the subthreshold dampening of afferent signaling and neuroimmune processes rather than robust spinal inhibition mediated by the classical gate-control mechanism.

4.5 10-kHz SCS

10-kHz SCS delivers continuous stimulation at 10,000 Hz and was developed to achieve analgesia without paresthesia. In the literature, this paradigm is widely proposed to differ mechanistically from classical Aβ-fiber–mediated gate-control stimulation, operating at sub-perceptual amplitudes. Rather than relying on clear DC activation, its effects are attributed to frequency-dependent neuromodulatory processes. The included articles are listed in Appendix F.

4.5.1 Spinal processing

Animal models indicate that 10-kHz SCS modulates spinal processing through frequency-dependent effects on DH circuitry rather than through classical DC gating. Studies demonstrate robust DH activation at 10 kHz, particularly in deeper laminae, while low-intensity stimulation selectively engages inhibitory interneurons without recruiting DC fibers [65, 73, 74]. Computational models show that these effects occur at stimulation amplitudes below those required for DC recruitment or sustained conduction block [76].

Computational models further suggest that axonal activation thresholds during 10-kHz stimulation are higher than those associated with burst paradigms [29, 30]. At the behavioral level, one animal model study reported that 10-kHz SCS reduces mechanical hypersensitivity more rapidly than tonic 50 Hz stimulation, although the underlying mechanisms were not directly examined [18]. Together, these findings support a model in which 10-kHz SCS alters spinal nociceptive processing via local inhibitory and presynaptic mechanisms rather than through Aβ-fiber activation.

4.5.2 Supraspinal modulation

Evidence from neuroimaging and human studies indicates that 10-kHz SCS is associated with supraspinal functional and structural reorganization, reflecting engagement of plastic processes within pain-related brain networks. EEG studies show that 10-kHz stimulation shifts cortical activity toward increased alpha-band power in frontal and somatosensory regions, a pattern that correlates with clinical pain improvement [38].

Structural MRI demonstrates bilateral reductions in hippocampal gray-matter volume after three months of therapy, interpreted as a normalization of pain-associated structural alterations [77]. Resting-state fMRI further reveals strengthened functional connectivity between the anterior insula and dorsolateral prefrontal cortex within salience and executive control networks, correlating with improvements in sleep quality and emotional aspects of

pain processing [78]. In addition, suppression of SEPs suggests modulation of lemniscal sensory pathways, consistent with altered supraspinal processing of afferent input [9].

4.5.3 Molecular and cellular mechanisms

Evidence for molecular and cellular mechanisms of 10-kHz SCS is primarily derived from animal models and indicates modulation of neuroimmune and intracellular signaling. In the DH, 10-kHz stimulation attenuates intracellular signaling pathways associated with central sensitization and normalizes glutamatergic transmission, partly through enhanced glutamate transporter activity [79, 80]. In addition, 10-kHz SCS is proposed to restore cellular homeostatic processes, including lysosomal function and autophagic flux [81].

At the glial level, 10-kHz SCS reduces microglial activation and shifts the spinal inflammatory environment toward an anti-inflammatory profile [50]. Systemically, in human studies, increased IL-10 and reduced pro-inflammatory cytokines have been reported, consistent with broader immunomodulatory effects [82]. Pharmacological studies in animal models further indicate involvement of endogenous opioid systems, with coordinated engagement of opioid receptors (μ-, δ-, κ) contributing to analgesia [83].

4.5.4 Summary

10-kHz SCS provides paresthesia-free analgesia through modulation of spinal processing and supraspinal modulation rather than classical DC–mediated gate control. Experimental and computational studies indicate that 10-kHz stimulation alters DH excitability via presynaptic mechanisms and local inhibitory circuits, without direct activation or sustained block of Aβ-fiber. At the supraspinal level, it is associated with reorganization of cortical and subcortical networks involved in sensory and affective pain processing. At the molecular and cellular level, animal models demonstrate modulation of neuroimmune and intracellular signaling pathways, including normalization of glutamatergic transmission and engagement of endogenous opioid systems. Together, these findings suggest that 10-kHz SCS achieves analgesia through integrated modulation of spinal excitability and neuroimmune processes rather than through classical Aβ-fiber–mediated mechanisms.

4.6 Differential Target Multiplexed SCS

Differential Target Multiplexed (DTM) SCS was developed to modulate both neuronal and glial components of spinal processing through multiplexed stimulation patterns. The paradigm typically combines low-frequency stimulation (around 50 Hz) with kilohertz-range (around 1.2 kHz) frequency stimulation delivered across different electrode contacts. DTM-SCS is proposed to restore disrupted neuro–glial interactions and promote the re-establishment of spinal homeostasis following neuropathic injury, distinguishing it conceptually from paradigms primarily targeting neuronal excitability [10, 46, 84]. The included articles are listed in Appendix G.

4.6.1 Spinal processing

At the spinal level, animal models show that DTM-SCS does not alter DC fiber recruitment compared with tonic stimulation. A stable ECAP-to-Motor Threshold ratio during continuous stimulation indicates unchanged Aβ-fiber activation [85]. Despite this preserved electrophysiological profile, behavioral analgesia persists, suggesting that DTM-induced pain relief does not primarily arise from altered DC excitability but from downstream biochemical modulation [85].

Consistent with this interpretation, studies in animal models of PDPN report that DTM-SCS produces significant pain relief, although reductions in mechanical hypersensitivity were not reported to be greater than those observed with tonic SCS [49]. Together, these findings suggest that the spinal analgesic effects of DTM-SCS are not primarily driven by changes in DC fiber recruitment, but may instead involve molecular and cellular mechanisms.

4.6.2 Supraspinal modulation

No studies to date have reported on the supraspinal modulation or cortical effects of DTM stimulation.

4.6.3 Molecular and cellular mechanisms

DTM-SCS is associated with broad transcriptomic, proteomic, and lipidomic changes within the DH, consistent with partial molecular normalization after neuropathic injury. Weighted gene co-expression analyses in animal models show that approximately half of injury-affected gene modules shift toward naïve expression patterns across neuronal, oligodendrocytic, and glial populations [10, 84].

The most pronounced effects are observed within microglial gene networks, which shift toward neuroprotective and repopulating phenotypes alongside downregulation of pro-inflammatory receptor genes (*Tlr1*, *Tlr2*) [46]. In parallel, DTM-SCS alters the spinal immune milieu toward an anti-inflammatory profile [49].

Lipidomic analyses further indicate that DTM-SCS promotes a partial metabolic normalization of lipid species

associated with neuropathic pain [42]. At the protein level, DTM-SCS modulates the activation states of proteins linked to the mTOR pathway, which is a key regulator of inflammatory signaling. By resetting these molecular triggers, DTM-SCS reverses a substantial portion of the injury-induced changes in cellular activity [40].

In addition, DTM-SCS has been reported to restore the ECM more effectively than tonic stimulation. It normalizes the composition between cells and reduces the over-activity of supporting cells, such as astrocytes [47].

4.6.4 Summary

DTM-SCS is proposed to exert its analgesic effects primarily through molecular and cellular mechanisms rather than through direct changes in neuronal recruitment. Animal models demonstrate normalization of transcriptional, proteomic, and lipidomic signatures within the DH, consistent with restoration of neuro–glial communication and attenuation of inflammatory signaling involving mTOR- and ECM–related pathways. These molecular changes suggest a shift toward a more homeostatic spinal environment. However, behavioral outcomes in animal models do not consistently exceed those observed with conventional tonic SCS, and corresponding mechanistic evidence in human studies remains limited.

4.7 Summary of Mechanistic Findings

Across paradigms, the included studies indicate that SCS influences multiple mechanistic levels, with distinct and partially overlapping patterns of engagement. Tonic SCS is most consistently associated with reduced DH excitability, which is traditionally interpreted through Aβ-fiber–mediated spinal inhibition. HD-SCS is characterized by changes in spinal processing without the recruitment of DC fibers, while burst SCS is consistently reported to combine spinal inhibitory effects with the modulation of cortical networks involved in sensory–affective pain processing.

Based on the available literature, HF-SCS is characterized by the attenuation of synaptic transmission, showing limited influence on higher brain centers but engaging neuroimmune signaling in animal models. In contrast, 10-kHz SCS presents a more integrative profile, with studies documenting a spectrum of effects ranging from the resetting of spinal interneuronal circuits to supraspinal reorganization and the stabilization of intracellular glial pathways. DTM-SCS occupies a distinct niche. While it shows minimal electrophysiological impact at the spinal level, it stands out for its extensive data regarding the recalibration of the molecular and neuroglial environment in animal models.

Importantly, the strength and nature of mechanistic evidence vary substantially across paradigms and experimental contexts. The absence of reported effects at a given mechanistic level should not be interpreted as evidence that such mechanisms are not involved, but may reflect differences in study design or the specific hypotheses tested. The findings are incorporated in Table 2, which summarizes the primary mechanistic effects reported for each paradigm.

5 Discussion and Interpretation

In this scoping review, I mapped the evidence for various SCS paradigms across spinal, supraspinal, and molecular levels. While spinal inhibition is a common thread, the "hardness" of the conclusions varies significantly per paradigm, as the underlying evidence is often indirect or derived from simplified models (Table 2).

5.1 Evidence Quality

Theoretical Foundations vs. Biological Reality:

A part of the rationale for newer paradigms, such as 10-kHz and HF-SCS, is built on computational models [19, 86]. While these provide plausible biophysical frameworks for "subthreshold filtering" or "conduction blocks," they rely on simplified neural geometry. By excluding the complex interactions of inhibitory interneurons and glial cells, these models may overestimate direct axonal effects. Consequently, these findings should be interpreted as theoretical possibilities rather than definitive biological proof.

Furthermore, several spinal findings rely on small sample sizes or specific animal models that only partially reflect chronic human conditions. For example, the work on endocannabinoid signaling [51] and NK1R imaging [58] provides crucial insights but lacks large-scale validation. Species differences in DC architecture further complicate this translation, as seen in the varying results between ovine and rodent models regarding DH activation and laminar recruitment [65, 73].

Measures of supraspinal effects:

Supraspinal findings for Burst and 10-kHz SCS offer intriguing insights into the sensory-affective component of pain, yet they rely on indirect measures. Many human EEG studies, such as those by De Ridder et al. [7], used low-density electrode montages. This limits spatial resolution, making it difficult to pinpoint exact cor-

Table 2: Summary of proposed mechanistic effects across SCS paradigms

Paradigm	Spinal Processing	Supraspinal Modulation	Molecular & Cellular
Tonic SCS	• Activates Aβ-fiber–mediated spinal inhibition • Reduces DH neuronal excitability • Enhances inhibitory signaling (GABA, 5-HT, opioids) • Suppresses wind-up in WDR neurons	• Reduces cortical responsiveness to nociceptive input • Attenuates sensory and attentional processing • Alters thalamo-limbic network activity	• Partial normalization of inflammatory and ECM pathways • Reduced glial activation (variable) • Attenuation of central sensitization markers
HD-SCS	• Subthreshold reduction of DH excitability • Preserved DC conduction • Frequency-dependent suppression of sensory potentials	• Altered frontal-cingulate and somatosensory activity • Parameter-dependent changes in large-scale connectivity	*No evidence available*
Burst SCS	• Strong inhibition of DH neuronal activity • Broad interneuron engagement • Asynchronous, dynamic spinal gating	• Reduced salience of painful stimuli • Altered affective-attentional network activity • Reorganization of cingulate–insular–prefrontal circuits	• Reduced excitatory synaptic signaling • Decreased glial reactivity • Increased IL-10 expression
HF-SCS	• Attenuation of synaptic transmission (subthreshold) • Limited classical spinal inhibition • Increased activation at higher kHz frequencies	• Limited and heterogeneous evidence • Changes in frontal and insular regions	• Reduced glial activation • Partial shift toward anti-inflammatory signaling
10-kHz SCS	• Subthreshold reduction of DH hyperexcitability • Engagement of inhibitory interneurons • No recruitment or block of DC fibers	• Shift toward alpha cortical rhythms • Altered salience and hippocampal network connectivity	• Suppression of neuroinflammatory signaling • Normalization of intracellular pathways (autophagy) • Broad glial involvement
DTM-SCS	• Minimal change in DC recruitment • Analgesia not explained by electrophysiology alone	*No evidence available*	• Broad normalization of neuro-glial gene networks • Restoration of ECM and inflammatory pathways • Strong microglial recalibration

Note: SCS = Spinal Cord Stimulation; HF = High-Frequency; DTM = Differential Target Multiplexed; HD = High-Density; ECM = Extracellular Matrix; DH = Dorsal Horn; WDR = Wide Dynamic Range.

tical generators with confidence. Similarly, fMRI and PET findings [32] measure changes in blood oxygenation or metabolic markers rather than direct neuronal firing. These are indirect observations; frequency shifts or BOLD signal changes do not provide definitive evidence of specific cellular or synaptic mechanisms.

Paradigm-Specific Research Bias:

A notable distinction exists in the depth and focus of mechanistic investigation across paradigms. DTM-SCS stands out primarily because it was conceptually designed to modulate neuro-glial interactions, leading to extensive study through transcriptomic, proteomic, and lipidomic lenses [10, 41]. While these data demonstrate a "recalibration" of the neuro-glial environment toward a homeostatic state, the absence of comparable omics data for paradigms like burst or HD-SCS makes it impossible to determine if this molecular effect is truly unique to DTM.

Similarly, because burst stimulation was specifically developed to mimic endogenous thalamic firing patterns, research has naturally gravitated toward its effects on supraspinal and affective-attentional networks [7]. This targeted approach creates a measurement bias where the mechanistic landscape is heavily shaped by the initial hypotheses. Consequently, the reported mechanistic "fingerprints" may reflect a selective research focus—finding what one is specifically looking for—rather than definitive evidence that these mechanisms are absent in other forms of stimulation.

5.2 Mechanistic Validity and Weight of Evidence

When weighing the reported mechanisms against the methodological rigor of the underlying studies, a hierarchy of "mechanistic confidence" emerges across paradigms.

The evidence for tonic SCS remains the most robust, as its spinal inhibitory effects are consistently replicated across decades of animal and human electrophysiological research. In contrast, the mechanistic profiles of newer paradigms like 10-kHz and HF-SCS rely more heavily on computational models and acute animal studies, which, while plausible, lack the long-term biological validation required to be considered definitive.

Furthermore, the perceived uniqueness of certain paradigms, such as the molecular "recalibration" attributed to DTM-SCS, must be interpreted with caution. Because extensive "omics" investigations have not been performed to the same extent for other forms of SCS except tonic, it remains unclear whether these effects are truly paradigm-specific or simply a reflection of a selective research focus. Similarly, the supraspinal "fingerprints" of burst SCS often lack direct comparison with other active paradigms, making it difficult to exclude the possibility that these changes are a common signature of effective pain relief rather than a unique feature of the burst waveform.

Consequently, the current mechanistic landscape should be viewed as a collection of plausible theoretical frameworks that are supported by varying levels of experimental "hardness". Moving forward, the field must address the "absence of evidence" in older paradigms to determine if the biological distinctions reported today are genuine neurobiological divergences or artifacts of uneven scientific investigation.

5.3 Mechanistic Implications for Neuropathic Pain Phenotypes

In this section, I extend the mechanistic findings of this review toward distinct neuropathic-like pain phenotypes. The considerations below reflect an interpretation of the reported spinal, supraspinal, and molecular mechanisms and how these may conceptually relate to specific biological drivers of neuropathic-like pain. These proposed alignments are intended as a hypothesis-generating framework rather than definitive treatment recommendations.

Mononeuropathies are primarily driven by ectopic afferent discharges and pronounced segmental hyperexcitability within DH circuits [87]. Paradigms with strong spinal inhibitory mechanisms align most closely with this biology. Based on the synthesized evidence, tonic SCS and HD-SCS show the clearest association with suppression of WDR neuron firing, reduction of temporal summation, and restoration of inhibitory-excitatory balance within the DH[cite: 64]. If segmental hyperexcitability is the dominant driver, the mechanistic rationale for paradigms that primarily target glial networks (DTM-SCS) or reflect subthreshold attenuation of synaptic transmission (HF-SCS) is interpreted as being comparatively weaker.

CRPS presents a more heterogeneous profile involving neuroinflammation, autonomic dysregulation, and supraspinal modulation through maladaptive cortical reorganization [88, 89]. Within this condition, inflammatory-dominant ("warm") and sympathetically maintained ("cold") phenotypes are distinguished[cite: 69]. In my interpretation, inflammation-dominant CRPS may align better with paradigms that strongly modulate molecular signaling and supraspinal networks, such as 10-kHz, DTM, or burst SCS. In contrast, CRPS II presentations with a confirmed peripheral nerve lesion and a prominent afferent component, or "cold" CRPS with clear segmental hyperexcitability, may respond more favorably to spinal inhibition paradigms such as conven-

tional tonic or HD-SCS.

PDPN is a neuropathic-like condition with substantial metabolic or glial contribution [90, 91]. This phenotype has the strongest theoretical alignment with paradigms that modulate inflammatory, metabolic, and intracellular signaling pathways. DTM-SCS produces the most extensive reported normalization of injury-induced transcriptomic, proteomic, and lipidomic changes in animal models, whereas 10-kHz SCS has been associated with broad effects on microglial activation and intracellular signaling. These paradigms therefore offer a plausible mechanistic fit for PDPN and other glia- or metabolism-driven neuropathies. However, the apparent strength of molecular effects may partly reflect a paradigm-specific research focus facilitated by the use of advanced "omics" technologies—rather than true biological superiority over other paradigms.

Although these mechanistic alignments offer a plausible rationale for matching SCS paradigms to neuropathic-like phenotypes, they remain theoretical. To date, no controlled human studies have directly compared SCS paradigms across clearly defined neuropathic-like phenotypes [13]. Current evidence derives almost entirely from separate mechanistic studies and broad clinical cohorts rather than phenotype-stratified trials. Consequently, the proposed links between underlying biology and optimal stimulation parameters remain hypothetical. Prospective studies that stratify patients based on mechanistic profiles are needed to determine whether certain paradigms genuinely outperform others in specific subgroups. Establishing such evidence is essential to move beyond the current trial-and-error approach and allow for more targeted and reliable application of SCS.

5.4 Limitations

Several limitations of this review must be acknowledged, as they influence the robustness and generalizability of the synthesized mechanistic profiles.

First, as a single-reviewer, the processes of study selection and data extraction are inherently subject to potential bias. Although predefined eligibility criteria were applied, the absence of independent screening by a second reviewer increases the risk of selection bias or the inadvertent misclassification of complex mechanistic findings.

Second, the search strategy may have missed relevant mechanistic data, particularly if such findings were embedded in clinical trials where physiological or molecular outcomes were secondary to clinical efficacy. Furthermore, as reference lists of included studies were not systematically screened, the retrieval of supporting evidence may be incomplete.

Third, in accordance with scoping review methodology, no formal risk-of-bias assessment was conducted. The methodological quality of the included literature varies substantially, ranging from high-fidelity preclinical experiments to observational human studies with small sample sizes. Consequently, not all reported findings carry equal weight, and the "hardness" of the evidence for newer paradigms remains lower than that of conventional tonic SCS.

Fourth, substantial heterogeneity in experimental models, electrode configurations, and stimulation parameters complicates direct comparison across paradigms. The overlap in parameter ranges—particularly regarding "high-dose" or "high-density" settings—makes it difficult to attribute specific mechanistic effects solely to one distinct paradigm.

Finally, the interpretation of biological action is often constrained by the nature of the available markers. Many studies rely on surrogate measures of neural activity, such as c-fos expression, BOLD signal changes, or oscillatory power shifts, which reflect correlates rather than direct causal evidence of analgesic action. These measures, combined with the reliance on acute animal models, may not fully capture the complex, time-dependent neuroplastic changes occurring in chronic human neuropathic pain states.

5.5 Future Research

A fundamental limitation identified in this review is that current research typically examines a single paradigm against a no-stimulation control. This approach makes it impossible to determine whether a reported mechanism is truly unique to that paradigm or represents a common effect across multiple forms of SCS. Therefore, future research should prioritize direct comparisons of different paradigms within the same experimental setup. Such a consolidated approach is essential to progress beyond theoretical "fingerprints" and to establish whether specific biological profiles truly require distinct stimulation patterns. Furthermore, prospective clinical trials that stratify patients according to their mechanistic pain profile are necessary to determine if these theoretical alignments translate into superior clinical outcomes.

6 Conclusion

This scoping review demonstrates that the literature attributes distinct mechanistic profiles to various SCS paradigms. Tonic SCS remains most consistently associated with Aβ-fiber-mediated spinal inhibition, while HD-SCS is characterized by subthreshold spinal modulation. Burst stimulation adds pronounced modulation of affective-attentional networks, whereas HF-SCS is pri-

marily characterized by attenuation of synaptic transmission. Both 10-kHz and DTM-SCS are associated with broader neuro-glial effects, with DTM-SCS standing out for its extensive molecular "recalibration" of the spinal environment.

However, these distinctions must be interpreted with caution. The apparent mechanistic divergence is influenced by an uneven research focus and often relies on simplified computational models or indirect measures of neural activity. Therefore, described differences may reflect variations in study design and tested hypotheses as much as true biological divergence.

While these fingerprints suggest plausible alignments with neuropathic pain phenotypes, they remain largely theoretical. Future research should prioritize direct comparisons of paradigms and phenotype-stratified trials. Such evidence is essential to move beyond the current trial-and-error approach toward targeted, phenotype-based SCS selection for individual patients.

7 Generative AI disclosure

For this scoping review, generative AI was used to assist in rewriting sentences, refining phrasing and improving clarity and coherence of text. It was also helpful in identifying and correcting grammatical errors. Generative AI was not used to write original content, formulate conclusions or interpret mechanisms.

References

1. Baskozos G, Hébert HL, Pascal MM, Themistocleous AC, Macfarlane GJ, Wynick D, Bennett DL, and Smith BH. Epidemiology of Neuropathic Pain: An Analysis of Prevalence and Associated Factors in UK Biobank. Pain reports 2023 Mar; 8:e1066. DOI: 10.1097/PR9.0000000000001066
2. van Hecke O, Austin SK, Khan RA, Smith BH, and Torrance N. Neuropathic Pain in the General Population: A Systematic Review of Epidemiological Studies. Pain 2014 Apr; 155:654–62. DOI: 10.1016/j.pain.2013.11.013
3. O'Connor AB. Neuropathic Pain: Quality-of-Life Impact, Costs and Cost Effectiveness of Therapy. PharmacoEconomics 2009; 27:95–112. DOI: 10.2165/00019053-200927020-00002
4. Langley PC, Van Litsenburg C, Cappelleri JC, and Carroll D. The Burden Associated with Neuropathic Pain in Western Europe. Journal of medical economics 2013; 16:85–95. DOI: 10.3111/13696998.2012.729548
5. Breivik H, Collett B, Ventafridda V, Cohen R, and Gallacher D. Survey of Chronic Pain in Europe: Prevalence, Impact on Daily Life, and Treatment. European Journal of Pain 2006; 10:287–7. DOI: 10.1016/j.ejpain.2005.06.009. eprint: https://onlinelibrary.wiley.com/doi/pdf/10.1016/j.ejpain.2005.06.009
6. Melzack R and Wall PD. Pain Mechanisms: A New Theory. Science (New York, NY). 1965 Nov 19; 150:971–9. DOI: 10.1126/science.150.3699.971. PMID: 5320816
7. De Ridder D and Vanneste S. Burst and Tonic Spinal Cord Stimulation: Different and Common Brain Mechanisms. Neuromodulation: Technology at the Neural Interface. 2016 Jan; 19:47–59. DOI: 10.1111/ner.12368. Available from: https://linkinghub.elsevier.com/retrieve/pii/S1094715921048790
8. Russo M and Van Buyten JP. 10-kHz High-Frequency SCS Therapy: A Clinical Summary. Pain medicine (Malden, Mass). 2015 May; 16:934–42. DOI: 10.1111/pme.12617. PMID: 25377278
9. Buonocore M and Demartini L. Inhibition of Somatosensory Evoked Potentials During Different Modalities of Spinal Cord Stimulation: A Case Report. Neuromodulation: Technology at the Neural Interface. 2016 Dec; 19:882–4. DOI: 10.1111/ner.12380. Available from: https://linkinghub.elsevier.com/retrieve/pii/S1094715921054088
10. Vallejo R, Kelley CA, Gupta A, Smith WJ, Vallejo A, and Cedeño DL. Modulation of neuroglial interactions using differential target multiplexed spinal cord stimulation in an animal model of neuropathic pain. Molecular Pain. 2020 Jan; 16:1744806920918057. DOI: 10.1177/1744806920918057. Available from: https://journals.sagepub.com/doi/10.1177/1744806920918057
11. Sdrulla AD, Guan Y, and Raja SN. Spinal Cord Stimulation: Clinical Efficacy and Potential Mechanisms. Pain practice : the official journal of World Institute of Pain. 2018 Nov; 18:1048–67. DOI: 10.1111/papr.12692. PMID: 29526043
12. Vallejo R, Bradley K, and Kapural L. Spinal Cord Stimulation in Chronic Pain: Mode of Action. Spine. 2017; 42. Available from: https://journals.lww.com/spinejournal/fulltext/2017/07151/spinal_cord_stimulation_in_chronic_pain__mode_of.4.aspx

13. Caylor J, Reddy R, Yin S, Cui C, Huang M, Huang C, Rao R, Baker DG, Simmons A, Souza D, Narouze S, Vallejo R, and Lerman I. Spinal Cord Stimulation in Chronic Pain: Evidence and Theory for Mechanisms of Action. Bioelectronic Medicine 2019 Jun; 5:12. DOI: 10.1186/s42234-019-0023-1
14. Riganello F, Soddu A, and Tonin P. Addressing Pain for a Proper Rehabilitation Process in Patients with Severe Disorders of Consciousness. Frontiers in Pharmacology 2021 Feb; 12. DOI: 10.3389/fphar.2021.628980
15. Ray AL, Ullmann R, and Francis MC. Pain as a Perceptual Experience. *Comprehensive Treatment of Chronic Pain by Medical, Interventional, and Integrative Approaches: The AMERICAN ACADEMY of PAIN MEDICINE Textbook on Patient Management*. Ed. by Deer TR, Leong MS, Buvanendran A, Gordin V, Kim PS, Panchal SJ, and Ray AL. New York, NY: Springer New York, 2013 :745–57. DOI: 10.1007/978-1-4614-1560-2_70
16. Tricco AC, Lillie E, Zarin W, O'Brien KK, Colquhoun H, Levac D, Moher D, Peters MDJ, Horsley T, Weeks L, Hempel S, Akl EA, Chang C, McGowan J, Stewart L, Hartling L, Aldcroft A, Wilson MG, Garritty C, Lewin S, Godfrey CM, Macdonald MT, Langlois EV, Soares-Weiser K, Moriarty J, Clifford T, Tunçalp Ö, and Straus SE. PRISMA Extension for Scoping Reviews (PRISMA-ScR): Checklist and Explanation. Annals of internal medicine 2018 Oct; 169:467–73. DOI: 10.7326/M18-0850
17. Crosby ND, Janik JJ, and Grill WM. Modulation of activity and conduction in single dorsal column axons by kilohertz-frequency spinal cord stimulation. Journal of Neurophysiology. 2017 Jan 1; 117:136–47. DOI: 10.1152/jn.00701.2016. Available from: https://www.physiology.org/doi/10.1152/jn.00701.2016
18. Shechter R, Yang F, Xu Q, Cheong YK, He SQ, Sdrulla A, Carteret AF, Wacnik PW, Dong X, Meyer RA, Raja SN, and Guan Y. Conventional and Kilohertz-frequency Spinal Cord Stimulation Produces Intensity- and Frequency-dependent Inhibition of Mechanical Hypersensitivity in a Rat Model of Neuropathic Pain. Anesthesiology. 2013 Aug; 119:422–32. DOI: 10.1097/ALN.0b013e31829bd9e2. Available from: https://journals.lww.com/10.1097/ALN.0b013e31829bd9e2
19. Arle JE, Carlson KW, Mei L, Iftimia N, and Shils JL. Mechanism of Dorsal Column Stimulation to Treat Neuropathic but not Nociceptive Pain: Analysis With a Computational Model. Neuromodulation: Technology at the Neural Interface. 2014 Oct; 17:642–55. DOI: 10.1111/ner.12178. Available from: https://linkinghub.elsevier.com/retrieve/pii/S1094715914601410
20. Kuo SW, Zhang T, Esteller R, and Grill WM. In Vivo Measurements Reveal that Both Low- and High-frequency Spinal Cord Stimulation Heterogeneously Modulate Superficial Dorsal Horn Neurons. Neuroscience. 2023 Jun; 520:119–31. DOI: 10.1016/j.neuroscience.2023.04.010. Available from: https://linkinghub.elsevier.com/retrieve/pii/S0306452223001690
21. Shinoda M, Fujita S, Sugawara S, Asano S, Koyama R, Fujiwara S, Soma K, Tamagawa T, Matsui T, Ikutame D, Ando M, Osada A, Kimura Y, Kobayashi K, Yamamoto T, Kusama-Eguchi K, Kobayashi M, Hayashi Y, and Iwata K. Suppression of Superficial Microglial Activation by Spinal Cord Stimulation Attenuates Neuropathic Pain Following Sciatic Nerve Injury in Rats. International Journal of Molecular Sciences. 2020 Mar 30; 21:2390. DOI: 10.3390/ijms21072390. Available from: https://www.mdpi.com/1422-0067/21/7/2390
22. Rogers ER, Capogrosso M, and Lempka SF. Biophysics of Frequency-Dependent Variation in Paresthesia and Pain Relief during Spinal Cord Stimulation. The Journal of Neuroscience. 2024 Jun 26; 44:e2199232024. DOI: 10.1523/JNEUROSCI.2199-23.2024. Available from: https://www.jneurosci.org/lookup/doi/10.1523/JNEUROSCI.2199-23.2024
23. Sharma M, Bhaskar V, Yang L, FallahRad M, Gebodh N, Zhang T, Esteller R, Martin J, and Bikson M. Novel Evoked Synaptic Activity Potentials (ESAPs) Elicited by Spinal Cord Stimulation. eneuro. 2023 May; 10:ENEURO.0429–22.2023. DOI: 10.1523/ENEURO.0429-22.2023. Available from: https://www.eneuro.org/lookup/doi/10.1523/ENEURO.0429-22.2023
24. Lee KY, Lee D, Wang D, Kagan ZB, and Bradley K. Simultaneous 10 kHz and 40 Hz spinal cord stimulation increases dorsal horn inhibitory interneuron activity. Neuroscience Letters. 2022 Jun; 782:136705. DOI: 10.1016/j.neulet.2022.136705. Available from: https://linkinghub.elsevier.com/retrieve/pii/S0304394022002622
25. Maeda Y, Ikeuchi M, Wacnik P, and Sluka KA. Increased c-fos immunoreactivity in the spinal cord and brain following spinal cord stimulation is frequency-dependent. Brain Research. 2009 Mar; 1259:40–50. DOI: 10.1016/j.brainres.2008.12.060. Available from: https://linkinghub.elsevier.com/retrieve/pii/S0006899308031399

26. Qin C, Yang X, Wu M, Farber J, Linderoth B, and Foreman R. Modulation of neuronal activity in dorsal column nuclei by upper cervical spinal cord stimulation in rats. Neuroscience. 2009 Dec; 164:770–6. DOI: 10.1016/j.neuroscience.2009.08.001. Available from: https://linkinghub.elsevier.com/retrieve/pii/S0306452209012937
27. Gmel GE, Santos Escapa R, Parker JL, Mugan D, Al-Kaisy A, and Palmisani S. The Effect of Spinal Cord Stimulation Frequency on the Neural Response and Perceived Sensation in Patients With Chronic Pain. Frontiers in Neuroscience. 2021 Jan 21; 15:625835. DOI: 10.3389/fnins.2021.625835. Available from: https://www.frontiersin.org/articles/10.3389/fnins.2021.625835/full
28. Ladner K, Versantvoort EM, Mugan D, Vuong QC, Dietz BE, Hu A, Thijssen ME, Gorman RB, Petersen E, and Obara I. Preclinical Insights Into the Effects of Frequency and Pulse Width on Evoked Compound Action Potential Morphology During Spinal Cord Stimulation. Neuromodulation: Technology at the Neural Interface. 2025 Jun :S1094715925001849. DOI: 10.1016/j.neurom.2025.05.001. Available from: https://linkinghub.elsevier.com/retrieve/pii/S1094715925001849
29. Rogers ER, Zander HJ, and Lempka SF. Influence of Morphology and Waveform Parameters on the Neural Response to Spinal Cord Stimulation. *2021 10th International IEEE/EMBS Conference on Neural Engineering (NER)*. 2021 10th International IEEE/EMBS Conference on Neural Engineering (NER). Italy: IEEE, 2021 May 4:259–62. DOI: 10.1109/NER49283.2021.9441267. Available from: https://ieeexplore.ieee.org/document/9441267/
30. Rogers ER, Mirzakhalili E, and Lempka SF. Model-based analysis of subthreshold mechanisms of spinal cord stimulation for pain. Journal of Neural Engineering. 2023 Dec 1; 20:066003. DOI: 10.1088/1741-2552/ad0858. Available from: https://iopscience.iop.org/article/10.1088/1741-2552/ad0858
31. Arle JE, Mei L, and Carlson KW. Fiber Threshold Accommodation as a Mechanism of Burst and High-Frequency Spinal Cord Stimulation. Neuromodulation: Technology at the Neural Interface. 2020 Jul; 23:582–93. DOI: 10.1111/ner.13076. Available from: https://linkinghub.elsevier.com/retrieve/pii/S1094715921002841
32. De Groote S, De Jaeger M, Van Schuerbeek P, Sunaert S, Peeters R, Loeckx D, Goudman L, Forget P, De Smedt A, and Moens M. Functional magnetic resonance imaging: cerebral function alterations in subthreshold and suprathreshold spinal cord stimulation. Journal of Pain Research. 2018 Oct; Volume 11:2517–26. DOI: 10.2147/JPR.S160890. Available from: https://www.dovepress.com/functional-magnetic-resonance-imaging-cerebral-function-alterations-in-peer-reviewed-article-JPR
33. Meuwissen KP, Van Der Toorn A, Gu JW, Zhang TC, Dijkhuizen RM, and Joosten EA. Active Recharge Burst and Tonic Spinal Cord Stimulation Engage Different Supraspinal Mechanisms: A Functional Magnetic Resonance Imaging Study in Peripherally Injured Chronic Neuropathic Rats. Pain Practice. 2020 Jun; 20:510–21. DOI: 10.1111/papr.12879. Available from: https://onlinelibrary.wiley.com/doi/10.1111/papr.12879
34. Kishima H, Saitoh Y, Oshino S, Hosomi K, Ali M, Maruo T, Hirata M, Goto T, Yanagisawa T, Sumitani M, Osaki Y, Hatazawa J, and Yoshimine T. Modulation of neuronal activity after spinal cord stimulation for neuropathic pain; H215O PET study. NeuroImage. 2010 Feb; 49:2564–9. DOI: 10.1016/j.neuroimage.2009.10.054. Available from: https://linkinghub.elsevier.com/retrieve/pii/S1053811909011252
35. Bocci T, De Carolis G, Paroli M, Barloscio D, Parenti L, Tollapi L, Valeriani M, and Sartucci F. Neurophysiological Comparison Among Tonic, High Frequency, and Burst Spinal Cord Stimulation: Novel Insights Into Spinal and Brain Mechanisms of Action. Neuromodulation: Technology at the Neural Interface. 2018 Jul; 21:480–8. DOI: 10.1111/ner.12747. Available from: https://linkinghub.elsevier.com/retrieve/pii/S1094715921022595
36. Urasaki E, Miyagi Y, Muramatsu S, and Ezaki Y. Comparison of the Interference Effects on Somatosensory Evoked Potential from Tonic, Burst, and High-dose Spinal Cord Stimulations. Neurologia medico-chirurgica. 2022 Jul 15; 62:313–21. DOI: 10.2176/jns-nmc.2021-0298. Available from: https://www.jstage.jst.go.jp/article/nmc/62/7/62_2021-0298/_article
37. Goudman L, Linderoth B, Nagels G, Huysmans E, and Moens M. Cortical Mapping in Conventional and High Dose Spinal Cord Stimulation: An Exploratory Power Spectrum and Functional Connectivity Analysis With Electroencephalography. Neuromodulation: Technology at the Neural Interface. 2020 Jan; 23:74–81. DOI: 10.1111/ner.12969. Available from: https://linkinghub.elsevier.com/retrieve/pii/S1094715921020729
38. Telkes L, Hancu M, Paniccioli S, Grey R, Briotte M, McCarthy K, Raviv N, and Pilitsis JG. Differences in EEG patterns between tonic and high frequency spinal cord stimulation in chronic pain patients. Clinical

Neurophysiology. 2020 Aug; 131:1731–40. DOI: 10.1016/j.clinph.2020.03.040. Available from: https://linkinghub.elsevier.com/retrieve/pii/S1388245720301656

39. Tang R, Martinez M, Goodman-Keiser M, Farber JP, Qin C, and Foreman RD. Comparison of Burst and Tonic Spinal Cord Stimulation on Spinal Neural Processing in an Animal Model. Neuromodulation: Technology at the Neural Interface. 2014 Feb; 17:143–51. DOI: 10.1111/ner.12117. Available from: https://linkinghub.elsevier.com/retrieve/pii/S1094715914600519
40. Tilley DM, Vallejo R, Vetri F, Platt DC, and Cedeno DL. Activation of Neuroinflammation via mTOR Pathway is Disparately Regulated by Differential Target Multiplexed and Traditional Low-Rate Spinal Cord Stimulation in a Neuropathic Pain Model. Journal of Pain Research. 2022 Sep; Volume 15:2857–66. DOI: 10.2147/JPR.S378490. Available from: https://www.dovepress.com/activation-of-neuroinflammation-via-mtor-pathway-is-disparately-regula-peer-reviewed-fulltext-article-JPR
41. Tilley DM, Lietz CB, Cedeno DL, Kelley CA, Li L, and Vallejo R. Proteomic Modulation in the Dorsal Spinal Cord Following Spinal Cord Stimulation Therapy in an In Vivo Neuropathic Pain Model. Neuromodulation: Technology at the Neural Interface. 2021 Jan; 24:22–32. DOI: 10.1111/ner.13103. Available from: https://linkinghub.elsevier.com/retrieve/pii/S1094715921001318
42. De Geus TJ, Franken G, Flinders B, Cuypers E, and Joosten EA. The Effect of Spinal Cord Stimulation on Spinal Dorsal Horn Lipid Expression in Experimental Painful Diabetic Polyneuropathy: A Matrix-Assisted Laser Desorption/Ionization Time-of-Flight Mass Spectrometry Imaging Study. Neuromodulation: Technology at the Neural Interface. 2024 Dec; 27:1360–71. DOI: 10.1016/j.neurom.2024.09.005. Available from: https://linkinghub.elsevier.com/retrieve/pii/S1094715924007104
43. Fabregat-Cid G, Cedeño DL, Harutyunyan A, Rodríguez-López R, Monsalve-Dolz V, Mínguez-Martí A, Hernández-Cádiz MJ, Escrivá-Matoses N, Villanueva-Pérez V, Asensio Samper JM, De Andrés J, and Vallejo R. Effect of Conventional Spinal Cord Stimulation on Serum Protein Profile in Patients With Persistent Spinal Pain Syndrome: A Case-Control Study. Neuromodulation: Technology at the Neural Interface. 2023 Oct; 26:1441–9. DOI: 10.1016/j.neurom.2023.05.004. Available from: https://linkinghub.elsevier.com/retrieve/pii/S1094715923006797
44. Stephens KE, Chen Z, Sivanesan E, Raja SN, Linderoth B, Taverna SD, and Guan Y. RNA-seq of spinal cord from nerve-injured rats after spinal cord stimulation. Molecular Pain. 2018 Jan; 14:1744806918817429. DOI: 10.1177/1744806918817429. Available from: https://journals.sagepub.com/doi/10.1177/1744806918817429
45. Vallejo R, Gupta A, Kelley CA, Vallejo A, Rink J, Williams JM, Cass CL, Smith WJ, Benyamin R, and Cedeño DL. Effects of Phase Polarity and Charge Balance Spinal Cord Stimulation on Behavior and Gene Expression in a Rat Model of Neuropathic Pain. Neuromodulation: Technology at the Neural Interface. 2020 Jan; 23:26–35. DOI: 10.1111/ner.12964. Available from: https://linkinghub.elsevier.com/retrieve/pii/S1094715921020699
46. Smith WJ, Cedeño DL, Thomas SM, Kelley CA, Vetri F, and Vallejo R. Modulation of microglial activation states by spinal cord stimulation in an animal model of neuropathic pain: Comparing high rate, low rate, and differential target multiplexed programming. Molecular Pain. 2021 Jan; 17:1744806921999013. DOI: 10.1177/1744806921999013. Available from: https://journals.sagepub.com/doi/10.1177/1744806921999013
47. Tilley DM, Vallejo R, Vetri F, Platt DC, and Cedeño DL. Regulation of Expression of Extracellular Matrix Proteins by Differential Target Multiplexed Spinal Cord Stimulation (SCS) and Traditional Low-Rate SCS in a Rat Nerve Injury Model. Biology. 2023 Mar 31; 12:537. DOI: 10.3390/biology12040537. Available from: https://www.mdpi.com/2079-7737/12/4/537
48. Shu B, He SQ, and Guan Y. Spinal Cord Stimulation Enhances Microglial Activation in the Spinal Cord of Nerve-Injured Rats. Neuroscience Bulletin. 2020 Dec; 36:1441–53. DOI: 10.1007/s12264-020-00568-6. Available from: https://link.springer.com/10.1007/s12264-020-00568-6
49. De Geus TJ, Franken G, and Joosten EA. Conventional, high frequency and differential targeted multiplexed spinal cord stimulation in experimental painful diabetic peripheral neuropathy: Pain behavior and role of the central inflammatory balance. Molecular Pain. 2023 Jun; 19:17448069231193368. DOI: 10.1177/17448069231193368. Available from: https://journals.sagepub.com/doi/10.1177/17448069231193368
50. Yu J, Wong S, Lin Z, Shan Z, Fan C, Xia Z, Cheung M, Zhu X, Liu JA, and Cheung CW. High-Frequency Spinal Stimulation Suppresses Microglial Kaiso-P2X7 Receptor Axis-Induced Inflammation to Alleviate Neuropathic Pain in Rats. Annals of Neurology. 2024 May; 95:966–83. DOI: 10.1002/ana.26898. Available from: https://onlinelibrary.wiley.com/doi/10.1002/ana.26898

51. Sun L, Tai L, Qiu Q, Mitchell R, Fleetwood-Walker S, Joosten E, and Cheung C. Endocannabinoid activation of CB_1 receptors contributes to long-lasting reversal of neuropathic pain by repetitive spinal cord stimulation. European Journal of Pain. 2017 May; 21:804–14. DOI: 10.1002/ejp.983. Available from: https://onlinelibrary.wiley.com/doi/10.1002/ejp.983
52. Wu M, Komori N, Qin C, Farber JP, Linderoth B, and Foreman RD. Roles of peripheral terminals of transient receptor potential vanilloid-1 containing sensory fibers in spinal cord stimulation-induced peripheral vasodilation. Brain Research. 2007 Jul; 1156:80–92. DOI: 10.1016/j.brainres.2007.04.065. Available from: https://linkinghub.elsevier.com/retrieve/pii/S0006899307009742
53. Gao J, Wu M, Li L, Qin C, Farber JP, Linderoth B, and Foreman RD. Effects of spinal cord stimulation with "standard clinical" and higher frequencies on peripheral blood flow in rats. Brain Research. 2010 Feb; 1313:53–61. DOI: 10.1016/j.brainres.2009.11.072. Available from: https://linkinghub.elsevier.com/retrieve/pii/S0006899309025918
54. Geus TD, Franken G, Zuidema X, Van Zundert J, and Joosten EAJ. Structural changes in the nociceptive system induced by long-term conventional spinal cord stimulation in experimental painful diabetic polyneuropathy. Regional Anesthesia & Pain Medicine. 2024 Nov 14 :rapm–2024–105919. DOI: 10.1136/rapm-2024-105919. Available from: https://rapm.bmj.com/lookup/doi/10.1136/rapm-2024-105919
55. Kriek N, Schreurs MW, Groeneweg JG, Dik WA, Tjiang GC, Gültuna I, Stronks DL, and Huygen FJ. Spinal Cord Stimulation in Patients With Complex Regional Pain Syndrome: A Possible Target for Immunomodulation? Neuromodulation: Technology at the Neural Interface. 2018 Jan; 21:77–86. DOI: 10.1111/ner.12704. Available from: https://linkinghub.elsevier.com/retrieve/pii/S1094715921021693
56. Falowski SM. An Observational Case Series of Spinal Cord Stimulation Waveforms Visualized on Intraoperative Neuromonitoring. Neuromodulation: Technology at the Neural Interface. 2019 Feb; 22:219–28. DOI: 10.1111/ner.12781. Available from: https://linkinghub.elsevier.com/retrieve/pii/S1094715921018766
57. Solanes C, Dura JL, De Andres J, and Saiz J. What Is the Role of Frequency on Neural Activation in Tonic Stimulation in SCS Therapy? A Computational Study on Sensory A Nerve Fibers. IEEE Access. 2021; 9:107446–61. DOI: 10.1109/ACCESS.2021.3099986. Available from: https://ieeexplore.ieee.org/document/9495784/
58. Xu Q, Zheng Q, Cui X, Cleland A, Hincapie J, Raja SN, Dong X, and Guan Y. Visualizing the modulation of neurokinin 1 receptor–positive neurons in the superficial dorsal horn by spinal cord stimulation in vivo. Pain. 2025 Feb; 166:428–37. DOI: 10.1097/j.pain.0000000000003361. Available from: https://journals.lww.com/10.1097/j.pain.0000000000003361
59. Tang S, Cuellar CA, Song P, Islam R, Huang C, Wen H, Knudsen BE, Gong P, Lok UW, Chen S, and Lavrov IA. Changes in spinal cord hemodynamic reflect modulation of spinal network with different parameters of epidural stimulation. 2019 Nov 6. DOI: 10.1101/833202. Available from: http://biorxiv.org/lookup/doi/10.1101/833202
60. De Groote S, Goudman L, Peeters R, Linderoth B, Van Schuerbeek P, Sunaert S, De Jaeger M, De Smedt A, De Andrés J, and Moens M. The influence of High Dose Spinal Cord Stimulation on the descending pain modulatory system in patients with failed back surgery syndrome. NeuroImage: Clinical. 2019; 24:102087. DOI: 10.1016/j.nicl.2019.102087. Available from: https://linkinghub.elsevier.com/retrieve/pii/S2213158219304346
61. Crosby ND, Weisshaar CL, Smith JR, Zeeman ME, Goodman-Keiser MD, and Winkelstein BA. Burst and Tonic Spinal Cord Stimulation Differentially Activate GABAergic Mechanisms to Attenuate Pain in a Rat Model of Cervical Radiculopathy. IEEE Transactions on Biomedical Engineering. 2015 Jun; 62:1604–13. DOI: 10.1109/TBME.2015.2399374. Available from: http://ieeexplore.ieee.org/document/7031405/
62. Meuwissen KP, Gu JW, Zhang TC, and Joosten EA. Conventional-SCS vs. Burst-SCS and the Behavioral Effect on Mechanical Hypersensitivity in a Rat Model of Chronic Neuropathic Pain: Effect of Amplitude. Neuromodulation: Technology at the Neural Interface. 2018 Jan; 21:19–30. DOI: 10.1111/ner.12731. Available from: https://linkinghub.elsevier.com/retrieve/pii/S1094715921021747
63. Kent AR, Weisshaar CL, Venkatesan L, and Winkelstein BA. Burst & High-Frequency Spinal Cord Stimulation Differentially Effect Spinal Neuronal Activity After Radiculopathy. Annals of Biomedical Engineering. 2020 Jan; 48:112–20. DOI: 10.1007/s10439-019-02336-8. Available from: http://link.springer.com/10.1007/s10439-019-02336-8
64. Lim K, Slee S, Kibler A, Falowski S, and Amirdelfan K. Functional Ultrasound Imaging Reveals Activation Properties of Clinical Spinal Cord Stimulation Therapy Programming. Journal of Pain Research. 2025 Feb; Volume 18:849–67. DOI: 10.2147/JPR.S502432. Available from: https://www.dovepress.com/

functional-ultrasound-imaging-reveals-activation-properties-of-clinica-peer-reviewed-fulltext-article-JPR

65. Lee KY, Lee D, Kagan ZB, Wang D, and Bradley K. Differential Modulation of Dorsal Horn Neurons by Various Spinal Cord Stimulation Strategies. Biomedicines. 2021 May 18; 9:568. DOI: 10.3390/biomedicines9050568. Available from: https://www.mdpi.com/2227-9059/9/5/568
66. Meuwissen KP, De Vries LE, Gu JW, Zhang TC, and Joosten EA. Burst and Tonic Spinal Cord Stimulation Both Activate Spinal GABAergic Mechanisms to Attenuate Pain in a Rat Model of Chronic Neuropathic Pain. Pain Practice. 2020 Jan; 20:75–87. DOI: 10.1111/papr.12831. Available from: https://onlinelibrary.wiley.com/doi/10.1111/papr.12831
67. Hewitt D, Byrne A, Henderson J, Wilford K, Chawla R, Sharma ML, Frank B, Fallon N, Brown C, and Stancak A. Pulse Intensity Effects of Burst and Tonic Spinal Cord Stimulation on Neural Responses to Brushing in Patients With Neuropathic Pain. Neuromodulation: Technology at the Neural Interface. 2023 Jul; 26:975–87. DOI: 10.1016/j.neurom.2022.11.001. Available from: https://linkinghub.elsevier.com/retrieve/pii/S1094715922013496
68. Reinders LJ and De Vos CC. Cortical evoked responses to evaluate the effect of spinal cord stimulation on the pain pathways. Clinical Neurophysiology Practice. 2025; 10:167–71. DOI: 10.1016/j.cnp.2025.04.003. Available from: https://linkinghub.elsevier.com/retrieve/pii/S2467981X25000204
69. Vanneste S and De Ridder D. BurstDR spinal cord stimulation rebalances pain input and pain suppression in the brain in chronic neuropathic pain. Brain Stimulation. 2023 Jul; 16:1186–95. DOI: 10.1016/j.brs.2023.07.058. Available from: https://linkinghub.elsevier.com/retrieve/pii/S1935861X23018727
70. Niso G, Tjepkema-Cloostermans MC, Lenders MWPM, and de Vos CC. Modulation of the Somatosensory Evoked Potential by Attention and Spinal Cord Stimulation. Frontiers in neurology. 2021; 12:694310. DOI: 10.3389/fneur.2021.694310. PMID: 34413825
71. Kinfe TM, Muhammad S, Link C, Roeske S, Chaudhry SR, and Yearwood TL. Burst Spinal Cord Stimulation Increases Peripheral Antineuroinflammatory Interleukin 10 Levels in Failed Back Surgery Syndrome Patients With Predominant Back Pain. Neuromodulation: Technology at the Neural Interface. 2017 Jun; 20:322–30. DOI: 10.1111/ner.12586. Available from: https://linkinghub.elsevier.com/retrieve/pii/S1094715921038666
72. Arle JE, Mei L, Carlson KW, and Shils JL. High-Frequency Stimulation of Dorsal Column Axons: Potential Underlying Mechanism of Paresthesia-Free Neuropathic Pain Relief. Neuromodulation: Technology at the Neural Interface. 2016 Jun; 19:385–97. DOI: 10.1111/ner.12436. Available from: https://linkinghub.elsevier.com/retrieve/pii/S1094715921053812
73. Wang D, Lee KY, Kagan ZB, Bradley K, and Lee D. Frequency-Dependent Neural Modulation of Dorsal Horn Neurons by Kilohertz Spinal Cord Stimulation in Rats. Biomedicines. 2024 Jun 18; 12:1346. DOI: 10.3390/biomedicines12061346. Available from: https://www.mdpi.com/2227-9059/12/6/1346
74. Lee KY, Bae C, Lee D, Kagan Z, Bradley K, Chung JM, and La JH. Low-intensity, Kilohertz Frequency Spinal Cord Stimulation Differently Affects Excitatory and Inhibitory Neurons in the Rodent Superficial Dorsal Horn. Neuroscience. 2020 Jan; 428:132–9. DOI: 10.1016/j.neuroscience.2019.12.031. Available from: https://linkinghub.elsevier.com/retrieve/pii/S0306452219308863
75. Lee J, Kang W, Choi W, Park EH, Kwon J, Kwon M, Ok H, Kim J, Park SM, and Kim J. The Analgesic and Antispastic Effects of Epidural Spinal Stimulation Depending on the Frequency and Intensity After Spinal Cord Injury. Neuromodulation: Technology at the Neural Interface. 2025 Oct; 28:1157–67. DOI: 10.1016/j.neurom.2025.06.016. Available from: https://linkinghub.elsevier.com/retrieve/pii/S1094715925002624
76. Lempka SF, McIntyre CC, Kilgore KL, and Machado AG. Computational Analysis of Kilohertz Frequency Spinal Cord Stimulation for Chronic Pain Management. Anesthesiology. 2015 Jun; 122:1362–76. DOI: 10.1097/ALN.0000000000000649. Available from: https://journals.lww.com/10.1097/ALN.0000000000000649
77. De Groote S, Goudman L, Linderoth B, Buyck F, Rigoard P, De Jaeger M, Van Schuerbeek P, Peeters R, Sunaert S, and Moens M. A Regions of Interest Voxel-Based Morphometry Study of the Human Brain During High-Frequency Spinal Cord Stimulation in Patients With Failed Back Surgery Syndrome. Pain Practice. 2020 Nov; 20:878–88. DOI: 10.1111/papr.12922. Available from: https://onlinelibrary.wiley.com/doi/10.1111/papr.12922
78. De Groote S, Goudman L, Peeters R, Linderoth B, Vanschuerbeek P, Sunaert S, De Jaeger M, De Smedt A, and Moens M. Magnetic Resonance Imaging Exploration of the Human Brain During 10 kHz Spinal Cord Stimulation for Failed Back Surgery Syndrome: A Resting State Functional Magnetic Resonance Imaging

Study. Neuromodulation: Technology at the Neural Interface. 2020 Jan; 23:46–55. DOI: 10.1111/ner.12954. Available from: https://linkinghub.elsevier.com/retrieve/pii/S1094715921020675

79. Liao WT, Tseng CC, Chia WT, and Lin CR. High-frequency spinal cord stimulation treatment attenuates the increase in spinal glutamate release and spinal miniature excitatory postsynaptic currents in rats with spared nerve injury-induced neuropathic pain. Brain Research Bulletin. 2020 Nov; 164:307–13. DOI: 10.1016/j.brainresbull.2020.09.005. Available from: https://linkinghub.elsevier.com/retrieve/pii/S0361923020306274
80. Liao WT, Tseng CC, Wu CH, and Lin CR. Early high-frequency spinal cord stimulation treatment inhibited the activation of spinal mitogen-activated protein kinases and ameliorated spared nerve injury-induced neuropathic pain in rats. Neuroscience Letters. 2020 Mar; 721:134763. DOI: 10.1016/j.neulet.2020.134763. Available from: https://linkinghub.elsevier.com/retrieve/pii/S0304394020300331
81. Wang ZB, Liu YD, Wang S, and Zhao P. High-frequency spinal cord stimulation produces long-lasting analgesic effects by restoring lysosomal function and autophagic flux in the spinal dorsal horn. Neural Regeneration Research. 2022; 17:370. DOI: 10.4103/1673-5374.317989. Available from: https://journals.lww.com/10.4103/1673-5374.317989
82. Kogias SS, O'Brien JA, Robertson RV, Peng A, Tinoco-Mendoza FA, Ramachandran A, Henderson LA, and Austin PJ. 10-kHz High-Frequency Spinal Cord Stimulation Significantly Reduces Proinflammatory Cytokines and Distinct Populations of T Lymphocytes in Patients With Persistent Spinal Pain Syndrome Type 2. Neuromodulation: Technology at the Neural Interface. 2025 Aug; 28:937–51. DOI: 10.1016/j.neurom.2025.02.010. Available from: https://linkinghub.elsevier.com/retrieve/pii/S109471592500056X
83. Zhai FJ, Han SP, Song TJ, Huo R, Lan XY, Zhang R, and Han JS. Involvement of Opioid Peptides in the Analgesic Effect of Spinal Cord Stimulation in a Rat Model of Neuropathic Pain. Neuroscience Bulletin. 2022 Apr; 38:403–16. DOI: 10.1007/s12264-022-00844-7. Available from: https://link.springer.com/10.1007/s12264-022-00844-7
84. Cedeño DL, Kelley CA, and Vallejo R. Effect of stimulation intensity of a differential target multiplexed ¡span style="font-variant:small-caps;"¿SCS¡/span¿ program in an animal model of neuropathic pain. Pain Practice. 2023 Jul; 23:639–46. DOI: 10.1111/papr.13235. Available from: https://onlinelibrary.wiley.com/doi/10.1111/papr.13235
85. Cedeño DL, Vallejo R, Platt DC, Williams JM, Litvak LM, Dinsmoor DA, and Siorek M. Evolution of spinal evoked compound action potential thresholds, visual motor thresholds, and impedances in a rodent spared nerve injury model. Frontiers in Neuroscience. 2025 Jun 30; 19:1577059. DOI: 10.3389/fnins.2025.1577059. Available from: https://www.frontiersin.org/articles/10.3389/fnins.2025.1577059/full
86. Rogers ER, Zander HJ, and Lempka SF. Neural Recruitment During Conventional, Burst, and 10-kHz Spinal Cord Stimulation for Pain. The Journal of Pain. 2022 Mar; 23:434–49. DOI: 10.1016/j.jpain.2021.09.005. Available from: https://linkinghub.elsevier.com/retrieve/pii/S1526590021003382
87. Campbell JN and Meyer RA. Mechanisms of Neuropathic Pain. Neuron 2006 Oct; 52:77–92. DOI: 10.1016/j.neuron.2006.09.021
88. Devarajan J, Mena S, and Cheng J. Mechanisms of Complex Regional Pain Syndrome. Frontiers in Pain Research 2024; Volume 5 - 2024. DOI: 10.3389/fpain.2024.1385889
89. Bruehl S. Complex Regional Pain Syndrome. BMJ (Clinical research ed.) 2015; 351. DOI: 10.1136/bmj.h2730. eprint: https://www.bmj.com/content/351/bmj.h2730.full.pdf
90. Rajchgot T, Thomas SC, Wang JC, Ahmadi M, Balood M, Crosson T, Dias JP, Couture R, Claing A, and Talbot S. Neurons and Microglia; a Sickly-Sweet Duo in Diabetic Pain Neuropathy. Frontiers in Neuroscience 2019; Volume 13 - 2019. DOI: 10.3389/fnins.2019.00025
91. Zhu J, Hu Z, Luo Y, Liu Y, Luo W, Du X, Luo Z, Hu J, and Peng S. Diabetic Peripheral Neuropathy: Pathogenetic Mechanisms and Treatment. Frontiers in endocrinology 2023; 14:1265372. DOI: 10.3389/fendo.2023.1265372
92. Bu C, Ren H, Lv Q, Bu H, Gao X, Zheng R, Huang H, Wang W, Wei Y, Cheng J, and Zhang Y. Alteration of static and dynamic intrinsic brain activity induced by short-term spinal cord stimulation in postherpetic neuralgia patients. Frontiers in Neuroscience. 2023 Oct 9; 17:1254514. DOI: 10.3389/fnins.2023.1254514. Available from: https://www.frontiersin.org/articles/10.3389/fnins.2023.1254514/full
93. Cui X, Liu J, Uniyal A, Xu Q, Zhang C, Zhu G, Yang F, Sivanesan E, Linderoth B, Raja SN, and Guan Y. Enhancing spinal cord stimulation-induced pain inhibition by augmenting endogenous adenosine signalling after nerve injury in rats. British Journal of Anaesthesia. 2024 Apr; 132:746–57. DOI: 10.1016/j.bja.2024.01.005. Available from: https://linkinghub.elsevier.com/retrieve/pii/S0007091224000084

94. Gmel GE, Santos Escapa R, Benkohen TE, Mugan D, Parker JL, and Palmisani S. Postsynaptic dorsal column pathway activation during spinal cord stimulation in patients with chronic pain. Frontiers in Neuroscience. 2023 Dec 21; 17:1297814. DOI: 10.3389/fnins.2023.1297814. Available from: https://www.frontiersin.org/articles/10.3389/fnins.2023.1297814/full
95. Koyama S, Xia J, Leblanc BW, Gu JW, and Saab CY. Sub-paresthesia spinal cord stimulation reverses thermal hyperalgesia and modulates low frequency EEG in a rat model of neuropathic pain. Scientific Reports. 2018 May 8; 8:7181. DOI: 10.1038/s41598-018-25420-w. Available from: https://www.nature.com/articles/s41598-018-25420-w
96. Sharma P, Rampersaud H, and Shah PK. Repeated epidural stimulation modulates cervical spinal cord excitability in healthy adult rats. Experimental Brain Research. 2025 Jan; 243:22. DOI: 10.1007/s00221-024-06965-x. Available from: https://link.springer.com/10.1007/s00221-024-06965-x
97. Song Z, Ultenius C, Meyerson BA, and Linderoth B. Pain relief by spinal cord stimulation involves serotonergic mechanisms: An experimental study in a rat model of mononeuropathy. Pain. 2009 Dec; 147:241–8. DOI: 10.1016/j.pain.2009.09.020. Available from: https://journals.lww.com/00006396-200912150-00038
98. Witjes B, Baillet S, Roy M, Oostenveld R, Huygen FJ, and De Vos CC. Heterogeneous Cortical Effects of Spinal Cord Stimulation. Neuromodulation: Technology at the Neural Interface. 2023 Jul; 26:950–60. DOI: 10.1016/j.neurom.2022.12.005. Available from: https://linkinghub.elsevier.com/retrieve/pii/S1094715922014052
99. Yang F, Carteret A, Wacnik P, Chung CY, Xing L, Dong X, Meyer R, Raja S, and Guan Y. Bipolar spinal cord stimulation attenuates mechanical hypersensitivity at an intensity that activates a small portion of A-fiber afferents in spinal nerve-injured rats. Neuroscience. 2011 Dec; 199:470–80. DOI: 10.1016/j.neuroscience.2011.09.049. Available from: https://linkinghub.elsevier.com/retrieve/pii/S0306452211011353
100. Yearwood T, De Ridder D, Yoo HB, Falowski S, Venkatesan L, Ting To W, and Vanneste S. Comparison of Neural Activity in Chronic Pain Patients During Tonic and Burst Spinal Cord Stimulation Using Fluorodeoxyglucose Positron Emission Tomography. Neuromodulation: Technology at the Neural Interface. 2020 Jan; 23:56–63. DOI: 10.1111/ner.12960. Available from: https://linkinghub.elsevier.com/retrieve/pii/S1094715921020687
101. Royds J, Conroy MJ, Dunne MR, Cassidy H, Matallanas D, Lysaght J, and McCrory C. Examination and characterisation of burst spinal cord stimulation on cerebrospinal fluid cellular and protein constituents in patient responders with chronic neuropathic pain - A Pilot Study. Journal of Neuroimmunology. 2020 Jul; 344:577249. DOI: 10.1016/j.jneuroim.2020.577249. Available from: https://linkinghub.elsevier.com/retrieve/pii/S0165572819306216
102. Yang CT, Guan Y, Chen CC, Lin WT, Lu KH, Lin CR, Shyu BC, and Wen YR. Novel Pulsed Ultrahigh-frequency Spinal Cord Stimulation Inhibits Mechanical Hypersensitivity and Brain Neuronal Activity in Rats after Nerve Injury. Anesthesiology. 2023; 139:646–63. Available from: http://dx.doi.org/10.1097/aln.0000000000004680http://www.ncbi.nlm.nih.gov/entrez/query.fcgi?holding=inleurlib_fft&cmd=Retrieve&db=PubMed&dopt=Citation&list_uids=37428715https://ovidsp.ovid.com/ovidweb.cgi?T=JS&CSC=Y&NEWS=N&PAGE=fulltext&D=medp&DO=10.1097%
103. Amirdelfan K and Provenzano D. Effects of Kilohertz Frequency on Paresthesia Perception Thresholds in Spinal Cord Stimulation. Pain physician.
104. Yang F, Duan W, Huang Q, Chen Z, Ford N, Gao X, Sivanesan E, Sarma SV, Vera-Portocarrero LP, Linderoth B, Raja SN, and Guan Y. Modulation of Spinal Nociceptive Transmission by Sub-Sensory Threshold Spinal Cord Stimulation in Rats After Nerve Injury. Neuromodulation: Technology at the Neural Interface. 2020 Jan; 23:36–45. DOI: 10.1111/ner.12975. Available from: https://linkinghub.elsevier.com/retrieve/pii/S1094715921020742

A Appendix A. Search String

Medline:

(Spinal Cord Stimulation/ OR ((spinal* ADJ3 stimulat*) OR SCS).ab,ti,kw.) AND (Paresthesia/ OR Spectrum Analysis/ OR Sensory Thresholds/ OR ((differential* ADJ3 target* ADJ3 multiplexed*) OR dtm OR tonic* OR burst* OR fast* OR contour* OR ((paresthesia* OR paraesthesia*) ADJ3 (free*)) OR conventional* OR subthreshold* OR subperception* OR (high* ADJ3 (densit* OR dose*)) OR 10-kHz OR paradigm* OR ((high* OR low*) ADJ3 frequenc*)).ab,ti,kw.) AND (Neurophysiology/ OR Physical Phenomena/ OR (mechanism* OR moa OR ((physical*) ADJ3 (effect* OR process* OR phenomena*)) OR ((fundamental* OR basic* OR mechanis*) ADJ3 (research* OR stud*)) OR neurophysio*).ab,ti,kw.) NOT (news OR congres* OR abstract* OR book* OR chapter* OR dissertation abstract*).pt.

Embase:

('spinal cord stimulation'/de OR 'spinal cord stimulator'/exp OR ((spinal* NEAR/3 stimulat*) OR SCS):ab,ti,kw) AND ('paresthesia'/de OR 'waveform'/de OR 'high frequency spinal cord stimulation'/de OR 'burst spinal cord stimulation'/de OR 'paradigm'/de OR 'perceptive threshold'/de OR ((differential* NEAR/3 target* NEAR/3 multiplexed*) OR dtm OR tonic* OR burst* OR fast* OR contour* OR ((paresthesia* OR paraesthesia*) NEAR/3 (free*)) OR conventional* OR subthreshold* OR subperception* OR (high* NEAR/3 (densit* OR dose*)) OR 10-kHz OR paradigm* OR ((high* OR low*) NEAR/3 frequenc*)):ab,ti,kw) AND ('mechanism of action'/de OR 'mechanism'/de OR 'neurophysiology'/de OR 'physical phenomena'/de OR 'basic research'/exp OR 'mechanistic study'/de OR (mechanism* OR moa OR ((physical*) NEAR/3 (effect* OR process* OR phenomena*)) OR ((fundamental* OR basic* OR mechanis*) NEAR/3 (research* OR stud*)) OR neurophysio*):ab,ti,kw) NOT ([Conference Abstract]/lim OR [Conference Review]/lim OR [preprint]/lim OR 'clinical trial':it)

Web of Science:

(TS=((spinal* NEAR/2 stimulat*))) AND (TS=((differential* NEAR/2 target* NEAR/2 multiplexed*) OR dtm OR tonic* OR burst* OR fast* OR contour* OR ((paresthesia* OR paraesthesia*) NEAR/2 (free*)) OR conventional* OR subthreshold* OR subperception* OR (high* NEAR/2 (densit* OR dose*)) OR 10-kHz OR paradigm* OR ((high* OR low*) NEAR/2 frequenc*))) AND (TS=(mechanism* OR moa OR ((physical*) NEAR/2 (effect* OR process* OR phenomena*)) OR ((fundamental* OR basic* OR mechanis*) NEAR/2 (research* OR stud*)) OR neurophysio*)) NOT DT=(Meeting Abstract OR Meeting Summary)

Cochrane:

(((spinal* NEAR/3 stimulat*) OR SCS):ab,ti,kw) AND (((differential* NEAR/3 target* NEAR/3 multiplexed*) OR dtm OR tonic* OR burst* OR fast* OR contour* OR ((paresthesia* OR paraesthesia*) NEAR/3 (free*)) OR conventional* OR subthreshold* OR subperception* OR (high* NEAR/3 (densit* OR dose*)) OR ("10" NEXT/1 kHz) OR paradigm* OR ((high* OR low*) NEAR/3 frequenc*)):ab,ti,kw) AND ((mechanism* OR moa OR ((physical*) NEAR/3 (effect* OR process* OR phenomena*)) OR ((fundamental* OR basic* OR mechanis*) NEAR/3 (research* OR stud*)) OR neurophysio*):ab,ti,kw)

("conference abstract":kw OR Trial registry record:pt)

#1 NOT #2

B Appendix C. Included studies on Tonic SCS

Table 3: Included studies investigating mechanistic effects of Tonic SCS.

First Author	Year	Model	Pain model	Freq. (Hz)	PW (μs)	Intensity	Level	Core mechanistic finding
Arle[19]	2014	Computational	Neuropathic/ Nociceptive	50-150	210	–	Spinal	Retrograde dorsal column stimulation involving predominantly large diameter Aβ fibers is sufficient to inhibit WDR cells sending neuropathic pain signals via interneuronal pools and sensitized neuronal populations, without affecting nociceptive pain signals.
Arle[31]	2020	Computational	No	80	200	1-5mA	Spinal	The computational fiber threshold accommodation model predicts that traditional low-frequency stimulation does not produce inversion of thresholds across fiber diameters because the long charge-balancing phase allows accommodation to decay back to initial threshold levels.
Bocci[35]	2018	Human	PSPS	10-200	1-1000	0,1-18mA	Supraspinal	Low-frequency SCS slightly reduced nociceptive laser evoked potential amplitudes and reduced subjective pain scores, but did not significantly alter resting motor threshold, short intracortical inhibition, or cortical silent period duration compared to baseline.
Bu[92]	2023	Human	PHN	30-60	210-480	0-10,5V	Supraspinal	Short-term SCS alters static and dynamic intrinsic neural activity (ALFF/dALFF) in key cortical regions, correlating with the alleviation of pain, sleep, and mood symptoms.
Buonocore[9]	2016	Human	PSPS	60	250	6	Supraspinal	Classical 60 Hz SCS completely inhibits the cortical responses of Somatosensory Evoked Potentials (SEPs), demonstrating a strong, immediate, and reversible conduction block within the lemniscal system. All tested SCS modalities completely inhibited the SEPs cortical responses; Inhibition recovered immediately upon turning stimulation off.
Crosby[61]	2015	Animal	Cervical Radiculopathy	40-50	250-300	80-90% MT	Spinal	Tonic SCS-induced spinal inhibition is mediated by GABAB receptor activation, as the suppression of dorsal horn neuronal firing is completely abolished by a GABAB receptor antagonist, and tonic SCS restores decreased serum GABA concentrations.
Crosby[17]	2017	Animal	SNI	50	200	0,082	Spinal	Conventional 50-Hz SCS evokes action potentials in dorsal column axons characterized by periodic and near-perfect phase synchrony with the stimulation waveform, distinguishing its effect from kilohertz-frequency stimulation.

Continued on next page

First Author	Year	Model	Pain model	Freq. (Hz)	PW (μs)	Intensity	Level	Core mechanistic finding
Cui[93]	2024	Animal	SNI	50	0,2	50%/100% MT	Spinal	Spinal A1R and A3R signaling contribute to SCS-induced inhibition of spinal nociceptive transmission (C-LFP) after nerve injury, and this analgesia can be enhanced by inhibiting adenosine deaminase to augment endogenous adenosine signaling.
de Geus[49]	2023	Animal	PDPN	50	150	50% MT	Spinal, Molecular	Con-SCS significantly reduces mechanical hypersensitivity but simultaneously shifts the spinal inflammatory balance towards a pro-inflammatory state by significantly increasing Tnf- a RNA expression in the dorsal horn.
de Geus 1[42]	2024	Animal	PDPN	50	150	50% MT	Spinal, Molecular	Conventional SCS provides pain relief and decreases the expression levels of specific lipids, including diacylglycerophosphocholines and diacylglycerophosphoserines, in the spinal dorsal horn laminae 1-3 of painful diabetic polyneuropathy animals, suggesting a complex molecular modulation of spinal cord physiology.
de Geus 2[54]	2024	Animal	PDPN	50	210	67% MT	Spinal	Long-term conventional SCS induces structural changes in the nociceptive system, specifically increasing PGP9.5 intraepidermal nerve fiber density peripherally and significantly decreasing pro-BDNF (18 kDa) protein expression centrally in the spinal dorsal horn.
De Groote[32]	2018	Human	PSPS	4 + 60	–	0,2-7V	Supraspinal	Suprathreshold conventional SCS (60 Hz) modulates cerebral function by increasing activation in sensory and frontal regions (e.g., thalamus, frontal gyrus) while causing bilateral deactivation of limbic structures (e.g., parahippocampus).
De Ridder[7]	2016	Human	PSPS	40	330	–	Supraspinal	Burst and tonic SCS commonly modulate the descending pain inhibitory (pgACC) and contextual aversive memory systems. Tonic stimulation modulates the descending pain inhibitory system via the pregenual anterior cingulate cortex (pgACC) and affects the self-referential contextual aversive memory system via the posterior cingulate cortex (PCC) and parahippocampus.
Fabregat-Cid[43]	2023	Human	PSPS	40	300-450	–	Molecular	Conventional tonic SCS modulates the serum protein profile, significantly decreasing proteins related to immune responses and inflammation while increasing proteins related to iron metabolism, synaptic sprouting containment, and restorative processes.

Continued on next page

First Author	Year	Model	Pain model	Freq. (Hz)	PW (μs)	Intensity	Level	Core mechanistic finding
Gao[53]	2010	Animal	No	50	200	30%, 60%, 90% MT	Spinal	Conventional SCS increases peripheral blood flow through both attenuation of sympathetic outflow and antidromic activation of transient receptor potential vanilloid receptor (TRPV1)-containing fibers which release calcitonin gene-related peptide (CGRP).
Gmel[27]	2021	Human	PSPS	2-455	30, 100, 240	3,2-37mA	Spinal, Supraspinal	Increasing SCS frequency results in an inverse relationship where the ECAP amplitude decreases while the perceived paraesthesia strength increases, supporting that SCS-induced paraesthesia is conveyed through both frequency coding and population coding mechanisms.
Gmel[94]	2023	Human	Chronic neuropathic pain	12, 20, 30, 33	30, 50, 100, 240, 400	–	Spinal	Post-synaptic dorsal column (PSDC) fibers can be activated in humans during SCS both synaptically by primary afferents and axonically by the stimulus pulses directly, with activation dependent on the vertebral level of stimulation.
Goudman[37]	2020	Human	PSPS	60	210	–	Supraspinal	Conventional SCS results in the lowest mean power spectrum compared to no SCS and HD SCS in delta, theta, and beta frequency bands, suggesting an inhibitory effect on global cortical electrical changes. In HD, average power spectrum was significantly higher than con SCS in delta, theta, and beta frequency bands; Increased strength of information flow (FC3-TP9).
Hewitt[67]	2023	Human	Neuropathic leg pain	30-60	–	33%, 66%, 100% therapeutic	Supraspinal	Attenuated brushing-related cortical event-related desynchronization (ERD) observed with tonic SCS suggests a gating of cortical activation by afferent impulses in the dorsal column system.
Kishima[34]	2010	Human	Neuropathic pain	10-85Hz	210-450	max 10V	Supraspinal	Tonic SCS modulates supraspinal neuronal activities by increasing regional cerebral blood flow in the contralateral thalamus, bilateral parietal association areas, the anterior cingulate cortex (ACC), and prefrontal areas.
Koyama[95]	2018	Animal	Neuropathic/ CCI	50	200	0,44mA	Supraspinal	Sub-paresthesia conventional SCS reverses thermal hyperalgesia and significantly reduces EEG power in the 3-4 Hz range over S1, suggesting modulation of the pain-related theta biosignature at a cortical level.
Kriek[55]	2018	Human	CRPS	40	–	–	Molecular	Conventional SCS (40 Hz standard frequency) attenuates T-cell activation and significantly reduces IP-10, VEGF, and PDGFbb levels bilaterally, suggesting an immunomodulatory mechanism resulting in diminished endothelial dysfunction and improved peripheral blood flow.

Continued on next page

First Author	Year	Model	Pain model	Freq. (Hz)	PW (μs)	Intensity	Level	Core mechanistic finding
Kuo[20]	2023	Animal	SNI	50	200	40% + 80% MT	Spinal	Conventional 50 Hz SCS, comparable in overall effect to kilohertz frequency stimulation, operates via a local spinal mechanism in the superficial dorsal horn where spontaneously active low-threshold units (putative inhibitory interneurons) are preferentially facilitated, resulting in suppression of other unit types, with effects amplified by increased stimulation duration.
Ladner[28]	2025	Animal	No	50, 200	40	–	Spinal	Conventional SCS (50 Hz) maintains synchronous activation of large, myelinated Dorsal Column Ab fibers by stimulating during the late subnormal phase of the axonal recovery cycle, which is reflected by stable ECAP morphology and CV.
Lee[24]	2022	Animal	No	40	100	70% MT	Spinal	Rostral 40 Hz SCS increases the median firing rate of putatively excitatory interneurons (13 spikes/s) more than putatively inhibitory interneurons (8.7 spikes/s) in the superficial dorsal horn.
Lee[75]	2025	Animal	SCI	50	200	40% + 80% MT	Molecular	Low-frequency (50 Hz) spinal cord stimulation, specifically at high intensity (80% MT), effectively alleviates SCI-induced neuropathic pain and spasticity by significantly reducing the proportion of activated microglia in the spinal dorsal and ventral horns.
Lim[64]	2025	Animal	No	50	300	–	Spinal	Traditional SCS produced minimal significant hemodynamic activation in the dorsal horn; its activation probability was low, and its hyperemia magnitude, area, and depth were generally not significantly greater than control.
Maeda[25]	2009	Animal	SNI	60	250	0,16mA	Spinal	Conventional (60 Hz) SCS activates spinal mechanisms, evidenced by a significant bilateral increase in c-fos protein expression in the dorsal horn at the electrode site and cervical enlargement 2 hours after stimulation in nerve-injured animals.
Meuwissen 1[66]	2020	Animal	SNL	50	200	66%	Spinal	The analgesic effect of tonic SCS is mediated via spinal GABAergic mechanisms, as demonstrated by the ablation of pain relief following intrathecal administration of GABAA or GABAB antagonists.
Meuwissen 2[33]	2020	Animal	SNL	50	200	66%	Supraspinal	Tonic SCS modulates supraspinal activity, inducing significant BOLD signal increases in brain regions associated with both objective and cognitive-emotional aspects of pain.
Niso[70]	2021	Human	PSPS	30-120	250-500	1-17mA	Supraspinal	Conventional tonic SCS reduced P300 brain activity in the unattended condition. Burst SCS reduced P300 brain activity in both attended and unattended conditions.

Continued on next page

First Author	Year	Model	Pain model	Freq. (Hz)	PW (μs)	Intensity	Level	Core mechanistic finding
Qin[26]	2009	Animal	No	1, 10, 20, 50	200	–	Spinal	SCS using conventional frequency (50 Hz) significantly modulates the activity of DCN neurons, suggesting these nuclei serve as a critical neural relay for effects transmitted rostrally via activated dorsal column fibers, potentially mediating beneficial effects on cerebral disorders.
Reinders[68]	2025	Human	PSPS	30	200	1,5mA	Supraspinal	Tonic SCS reduces the cortical evoked response amplitude elitabcited by painful stimuli in the primary somatosensory cortex (S1) and anterior cingulate cortex (ACC) compared to sham, suggesting inhibition of nociceptive input and modulation of cortical capacity to attend to painful stimuli.
Rogers[29]	2021	Computational	No	50	300	–	Spinal	Conventional SCS directly recruits primary afferent fibers at lower stimulation amplitudes than local cells in the dorsal horn.
Rogers[30]	2023	Computational	No	50	300	–	Spinal	Conventional SCS, like other tested waveforms, preferentially polarizes the axons of superficial dorsal horn neurons to a stronger extent than the soma or dendrites, suggesting that SCS-induced modulation of local cells is likely presynaptic.
Rogers[22]	2024	Computational	No	2, 10, 50, 100	200	–	Spinal	Low-frequency stimulation produces synchronous dorsal column fiber firing that generates paresthesia and activates dorsal horn inhibition (gate control). Pain relief varies because different fiber activation patterns lead to variable dorsal horn network responses.
Sharma[23]	2023	Animal	No	50	40-200	–	Spinal	Conventional 50 Hz SCS evokes the Evoked Synaptic Activity Potential (ESAP) which reflects AMPA receptor-mediated glutamatergic synaptic activity in the dorsal horn and distinctively dampens in amplitude during tonic stimulation.
Sharma[96]	2025	Animal	No	0.2, 0.5, 1, 5, 10, 30	200	100-800uA	Spinal	Repeated exposure to cervical ES protocols, even during routine testing, significantly increases spinal cord excitability, prominently facilitating the mono-synaptic (MR) and polysynaptic (LR) components of the Spinal Evoked Motor Responses (SEMR), which translates functionally into increased forelimb muscle activation during motor tasks
Shechter[18]	2013	Animal	SNL	50	240	20%, 40%, 80% MT	Spinal	Conventional 50-Hz SCS inhibits windup in wide-dynamic-range (WDR) neurons within the dorsal horn, supporting the underlying mechanism of the gate-control theory.
Shinoda[21]	2020	Animal	SNI	60	240	80% MT	Spinal, Supraspinal, Molecular	SCS suppresses SNI-induced mechanical hypersensitivity via inhibition of microglial activation (Iba1-IR cells) in the spinal L4 dorsal horn, leading to the suppression of WDR neuronal hyperexcitability and a significant decrease in the activated area of the somatosensory cortex.

Continued on next page

First Author	Year	Model	Pain model	Freq. (Hz)	PW (μs)	Intensity	Level	Core mechanistic finding
Shu[48]	2020	Animal	CCI	50	200	80% MT	Molecular	Conventional SCS transiently attenuates mechanical hypersensitivity while paradoxically increasing spinal M1-like microglial activation (e.g., OX-42, iNOS, CD16 mRNA) and decreasing BDNF protein, suggesting this glial activation compromises the analgesic action.
Smith[46]	2021	Animal	SNI	50	150	0,03-0,09 mA	Molecular	Low Rate Programming (LRP) modulates microglial activation transcriptomes, resulting in weak correlations with healthy control expression profiles and recovering a significantly lower percentage of microglial genes toward naive levels across resting, post-injury, and neuroprotective transcriptomes compared to differential target multiplexed programming (DTMP).
Song[97]	2009	Animal	Neuropathic	50	200	80% MT	Spinal	The spinal serotonergic system plays a crucial role in the conventional SCS-induced pain relief by increasing 5-HT content and immunoreactivity in the dorsal horn of responding rats, suggesting activation of descending serotonergic pathways that inhibit spinal nociceptive processing partially via a GABAB? receptor link.
Stephens[44]	2018	Animal	CCI	50	200	80% MT	Molecular	Repetitive conventional SCS modulates the spinal transcriptome by downregulating key synaptic signaling genes that encode scaffold proteins in the postsynaptic density, suggesting a mechanism involving destabilization of the PSD to attenuate central sensitization and excitatory synaptic transmission.
Sun[51]	2017	Animal	SNL	10, 25	500	60% MT	Spinal	Repetitive low-frequency SCS induces long-lasting and incremental reversal of hyperalgesia primarily through the endocannabinoid system acting on CB1 receptors and attenuates spinal phosphorylation of the central sensitization biomarker GluN2B.
Tang[59]	2019	Animal	No	20, 40	–	–	Spinal	Low-frequency EES (20-40 Hz) shows a positive correlation between spinal cord hemodynamic changes and neuronal activity (EMG response), suggesting a frequency-dependent coupling linked to modulation of the spinal circuitry, with significantly higher and faster responses localized to the dorsal regions.
Tang[39]	2014	Animal	No	40	300	60%, 90% MT	Spinal, Supraspinal	Tonic SCS significantly increases the spontaneous activity of gracile nucleus neurons at 90% MT, which may correlate with paresthesia, while suppressing lumbosacral neuronal responses to noxious visceral and somatic stimuli.

Continued on next page

First Author	Year	Model	Pain model	Freq. (Hz)	PW (μs)	Intensity	Level	Core mechanistic finding
Telkes[38]	2020	Human	PSPS	60	300	0,6-2,5mA	Supraspinal	Conventional tonic stimulation maintains slower theta activity and does not induce significant enhancement of relative alpha power or shifts in the alpha/theta peak power ratio in the somatosensory and frontal cortical regions compared to baseline.
Tilley[41]	2021	Animal	SNI	50	20	70% MT	Molecular	Conventional SCS reverses the injury-induced proteomic state in the dorsal spinal cord by significantly modulating 155 proteins, notably upregulating those related to Extracellular Matrix organization and downregulating metabolic and stress response proteins.
Tilley[47]	2023	Animal	SNI	50	150	70% MT	Molecular	Conventional LR-SCS modulates the spinal matrisome (ECM proteins and associated phosphorylated isoforms), reversing the injury-induced expression changes in 67% of affected ECM proteins and 58% of phosphoproteins, suggesting a mechanism involving molecular modulation of neuroglial components and subsequent partial restoration of homeostasis.
Tilley[40]	2022	Animal	SNI	50	150	70% MT	Spinal, Molecular	LR-SCS partially reverses injury-induced neuroinflammation via modulation of the spinal mTOR pathway, affecting protein expression and phosphorylation states.
Urasaki[36]	2022	Human	PSPS, Parkinson's	30-50	200-500	–	Supraspinal	Tonic SCS induces a dose-dependent reduction in cortical P40/N50 SEP amplitude, demonstrating interference with the ascending somatosensory volley via sufficient activation of the dorsal column pathway.
Vallejo 1[45]	2020	Animal	SNI	50	50	66% MT	Spinal	Symmetric biphasic stimulation differentially modulates spinal transcriptional pathways, significantly downregulating the expression of immune-related genes like Tspo, Cd74, and Aif1, and restoring correlations among genes (e.g., C1qb and Aif1) that were lost post-injury.
Vallejo 2[10]	2020	Animal	SNI	50	150	70% MT	Molecular	Low Rate (conventional) SCS significantly improved mechanical hypersensitivity while modulating the spinal transcriptome, specifically leading to an increased expression of immune-related genes (like Tlr2, Itgam, and Ccl2) relative to untreated injured animals, suggesting a molecular modulation of neuroglial interactions.

Continued on next page

First Author	Year	Model	Pain model	Freq. (Hz)	PW (μs)	Intensity	Level	Core mechanistic finding
Witjes[98]	2023	Human	Chronic Pain		–	–	Supraspinal	Tonic SCS did not produce statistically significant differences in resting-state cortical spectral features (alpha peak frequency, power ratio, or power in theta, alpha, beta, or low-gamma bands) compared to sham stimulation in group analysis, suggesting high heterogeneity in individual cortical responses.
Wu[52]	2007	Animal	No	50	200	30-300% MT	Molecular	Conventional SCS-induced vasodilation is highly dependent on the antidromic activation of TRPV1-containing sensory fibers, triggering the release of Calcitonin Gene-Related Peptide (CGRP) from peripheral nerve terminals.
Xu[58]	2025	Animal	SNI	50	150	20-80% MT	Spinal	Both 10-minute high-intensity conventional SCS (50 Hz, 80% MoT) and 30-minute moderate-intensity conventional SCS (50 Hz, 50% MoT) inhibit the activation of superficial Neurokinin 1 receptor-positive neurons, potentially attenuating spinal nociceptive transmission.
Yang[99]	2011	Animal	SNL	50	200	80-90% MT	Spinal	Tonic SCS attenuates mechanical hypersensitivity by recruiting only a small fraction of the A-fiber population at the utilized stimulus intensity, and efficient dorsal column structure activation correlates with responsiveness.
Yearwood[100]	2020	Human	Chronic intractable pain	30-100	100-500	–	Supraspinal	Tonic SCS modulates supraspinal activity by increasing metabolic rate in the premotor cortex compared to baseline, while pain suppression correlates with decreased metabolic activity in the retrosplenial, motor, and supplementary motor cortices.
Yu[50]	2024	Animal	SNI	40	20	80% MT	Molecular	Conventional SCS provides short-lived analgesia but fails to suppress the pathological Kaiso-P2X7R axis in spinal microglia, leading to rapid pain relapse and increased expression of disease-associated microglial genes.
Zhai[83]	2022	Animal	SNI	50/100	200	up to 80% MT	Molecular	The analgesic effect of 100-Hz SCS is mediated by the kappa-opioid receptor (KOR), likely via the activation of inhibitory dynorphinergic interneurons.

Table 3: SNI = Spinal Cord Injury, SNL = Spinal Nerve Ligation, SNI = Sciatic Nerve Injury, CCI = Chronic Constriction Injury, PSPS = Persistant Spinal Pain Syndrome, PDPN = Painful Diabetic Peripheral Neuropathy, CRPS = Complex Regional Pain Syndrome, PHN = Postherpetic Neuralgia, MT = Motorthreshold

C Appendix C. Included studies on High-Density (High-Dose) SCS

Table 4: Included studies investigating mechanistic effects of High-Density (High-Dose) SCS.

First Author	Year	Model	Pain model	Freq. (Hz)	PW (μs)	Intensity	Level	Core mechanistic finding
Buonocore[9]	2016	Human	PSPS	200, 500	1000, 500	3,5mA	Supraspinal	All tested SCS modalities completely inhibited the SEPs cortical responses; Inhibition recovered immediately upon turning stimulation off.
De Groote[32]	2018	Human	PSPS	500	20	–	Supraspinal	For subthreshold stimulation at a frequency of 500 Hz, activation in the unilateral superior and inferior frontal gyri was investigated. The only significant deactivation was found in the corpus callosum and interhemispheric fissure/PCG.
De Groote[60]	2019	Human	PSPS	500	500	–	Supraspinal	Significant increases in FC strength (mFG left - mFG right, mFG left - RVM, mFG right - AI left); Significant decrease in FC strength (ACC - AI right).
Falowski[56]	2019	Human	PSPS, CRPS	1000	90	–	Spinal, Supraspinal	High-dose programming did not generate any observable EMG responses or change in sensory signals via SSEP collision testing.
Goudman[37]	2020	Human	PSPS	500	500	–	Supraspinal	In HD, average power spectrum was significantly higher than con SCS in delta, theta, and beta frequency bands; Increased strength of information flow (FC3-TP9).
Kriek[55]	2018	Human	CRPS	500	–	–	Molecular	SCS resulted in decreased expression of both pro- and anti-inflammatory cytokines over time; IP-10 (CXCL10), VEGF, and PDGFbb were significantly reduced bilaterally; The pro-inflammatory cytokine IL-15 was significantly reduced over time (p=0.001).
Ladner[28]	2025	Animal	No	500	40	–	Spinal	SCS at increasing frequencies (200, 500, and 1000 Hz) altered DC axon responses, reducing ECAP amplitude and increasing latencies/width. This suggests that DC axon activation depends on the recovery stage of the electrically stimulated fibers, potentially through mechanisms like desynchronization or demyelination.

Continued on next page

FirstAuthor	Year	Model	Pain model	Freq. (Hz)	PW (μs)	Intensity	Level	Core mechanistic finding
Rogers[22]	2024	Computational	No	100, 500, 900, 1000	200	–	Spinal	Low-frequency stimulation produces synchronous dorsal column fiber firing that generates paresthesia and activates dorsal horn inhibition (gate control). Pain relief varies because different fiber activation patterns lead to variable dorsal horn network responses. HD SCS reduces DC fiber activation thresholds, accurately predicting clinical paresthesia perception thresholds, while collateral conduction failure at high rates is essential for producing antinociceptive effects in the dorsal horn.
Solanes[57]	2021	Computational	Chronic pain treatment	350, 600, 800, 1000	100, 300, 500	–	Spinal	Frequencies above 350 Hz significantly reduce or override the firing rate of large sensory A? fibers (e.g., 1000 Hz overrides activity), a phenomenon limited by the recovery dynamics of the sodium h gate.
Tang[59]	2019	Animal	No	200, 500	–	–	Spinal	High stimulation frequencies (200 Hz and 500 Hz) resulted in uncoupling between the spinal cord hemodynamic response (?SCBV) and the EMG response, supporting that modulation parameters activate different mechanisms in the spinal circuitry.
Urasaki[36]	2022	Human	PSPS, Parkinson's	1000, 1200	90-200	–	Supraspinal	High-dose stimulations could not reduce the SEP amplitude; SEP amplitude reduction was significantly smaller than tonic stimulation. Tonic SCS induced dose-dependent somatosensory evoked potential (SEP) reduction, but burst and high-dose SCSs did not, indicating that the latter modalities utilize different, non-dorsal column sites of action.
Xu[58]	2025	Animal	SNI	900	–	50% MT	Spinal	900 Hz SCS applied at moderate intensity significantly inhibited neuronal responses in superficial NK1R+ neurons in SNI-t mice.

Table 4: SNI = Spinal Cord Injury, SNL = Spinal Nerve Ligation, SNI = Sciatic Nerve Injury, CCI = Chronic Constriction Injury, PSPS = Persistant Spinal Pain Syndrome, PDPN = Painful Diabetic Peripheral Neuropathy, CRPS = Complex Regional Pain Syndrome, PHN = Postherpetic Neuralgia, MT = Motorthreshold

D Appendix D. Included studies on Burst SCS

Table 5: Included studies investigating mechanistic effects of Burst SCS.

First Author	Year	Model	Pain model	Freq. (Hz)	PW (μs)	Intensity	Level	Core mechanistic finding
Bocci[35]	2018	Human	PSPS	40 + 5 pulses 500	1000	–	Supraspinal	Burst modulates medial and lateral pain pathways via simultaneous modulation of intracortical GABA(b)ergic and glutamatergic networks.
Crosby[61]	2015	Animal	Cervical Radiculopathy	40 + 5 pulses 500	1000	90% MT	Spinal	Burst SCS attenuates spinal dorsal horn neuronal hyperexcitability and allodynia independent of GABAB? receptor activation and without increasing serum GABA levels.
De Ridder[7]	2016	Human	PSPS	40 + 5 pulses 500	1000	90% MT	Supraspinal	Burst and tonic SCS commonly modulate the descending pain inhibitory (pgACC) and contextual aversive memory systems, but burst uniquely normalizes the pain supporting/suppressing balance via the dACC/pgACC ratio.
Falowski[56]	2019	Human	PSPS, CRPS	40 + 5 pulses 500	1000	90% MT	Spinal, Supraspinal	The core mechanism of the Abbott BurstDR waveform is defined by its superior energy efficiency, generating a propagated EMG signal, uniquely recruiting distal muscle fibers prior to proximal ones, and inducing a transient hyperexcitable state that lowers the threshold for subsequent tonic stimulation. Conversely, Boston Scientific burst stimulation operates as a more efficient iteration of traditional tonic stimulation, exhibiting non-propagating EMG responses, typical proximal muscle recruitment, and reliance on amplitudes that precede the onset of paresthesias
Hewitt[67]	2023	Human	Neuropathic leg pain	40 + 5 pulses 500	1000	33%, 66%, 100% MT	Supraspinal	Burst SCS modulates cortical tactile processing by showing greater event-related desynchronization (ERD) in theta and alpha bands, suggesting involvement of the spinothalamic tract distinct from the dorsal column system.
Kent[63]	2020	Animal	Cervical Radiculopathy	40 + 5 pulses 500	1000	90% MT	Spinal	Burst SCS with passive recharge was the only mode to significantly reduce both evoked and spontaneous spinal neuronal firing rates after noxious pinch, indicating a reduction in neuropathic pain transmission
Kinfe[71]	2017	Human	PSPS	40 + 5 pulses 500	1000	0,15-1,6mA	Molecular	Burst SCS significantly increases systemic circulating anti-inflammatory Interleukin 10 (IL-10) plasma levels, suggesting a burst-evoked modulation of peripheral neuro-inflammation related to chronic back pain reduction and improved sleep quality.

Continued on next page

First Author	Year	Model	Pain model	Freq. (Hz)	PW (μs)	Intensity	Level	Core mechanistic finding
Kriek[55]	2018	Human	CRPS		–	–	Molecular	Spinal cord stimulation attenuates T-cell activation and bilaterally reduces inflammatory mediators (cytokines, IP-10, VEGF, PDGFbb) in blister fluid, suggesting improved peripheral tissue oxygenation.
Lee[65]	2021	Animal	No	40 + 5 pulses 500	1000	30% MT	Spinal	Burst SCS strategies activated non-adapting (inhibitory) and adapting (excitatory) dorsal horn neurons more equally, suggesting a non-selective modulation unlike 10 kHz SCS.
Lim[64]	2025	Animal	No	40 + 5 pulses 500	1000	–	Spinal	Burst SCS significantly activates the Superficial Dorsal Horn (SDH) with a magnitude comparable to other therapies, but provides significantly less area coverage and shallower depth of response than Multiphase SCS.
Meuwissen[62]	2018	Animal	SNI	40 + 5 pulses 449	1000	33%, 50%, 66% MT	Spinal	Burst-SCS efficacy exhibits a non-monotonic relation with amplitude, requiring significantly more mean charge per second than conventional SCS to normalize mechanical hypersensitivity.
Meuwissen 1[66]	2020	Animal	SNL	40 + 5 pulses 449	1000	33%, 50%, 66% MT	Spinal	The analgesic effect of burst SCS is mediated via spinal GABAergic mechanisms, evidenced by decreased intracellular GABA levels and ablation of pain relief by GABAA? or GABAB? receptor antagonists.
Meuwissen 2[33]	2020	Animal	SNL	40 + 5 pulses 449	1000	66% MT	Supraspinal	Active recharge burst SCS profoundly increases BOLD signals in brain areas associated with pain location, cognitive-emotional aspects, raphe nuclei, and reward circuitry (nucleus accumbens and caudate putamen).
Niso[70]	2021	Human	PSPS	40 + 5 pulses 500	1000	0,5-4,5mA	Supraspinal	Burst spinal cord stimulation for the treatment of chronic pain seems to reduce cortical attention that is or can be directed to somatosensory stimuli to a larger extent than conventional spinal cord stimulation treatment.
Reinders[68]	2025	Human	PSPS	40 + 5 pulses 500	1000	0,6mA	Supraspinal	Burst SCS strongly inhibits cortical evoked response amplitudes in the primary somatosensory cortex and anterior cingulate cortex, suggesting the greatest reduction in cortical capacity to attend to painful stimuli compared to tonic SCS.
Rogers[29]	2021	Computational	No	40 + 5 pulses 500	1000	–	Spinal	Burst SCS consistently exhibits the lowest computational activation thresholds for both primary afferent fibers and local dorsal horn cells compared to 50 Hz and 10 kHz paradigms, with primary afferent fibers recruited preferentially.
Rogers[30]	2023	Computational	No	40 + 5 pulses 500	1000	–	Spinal	Burst has the lowest C-fiber activation threshold and produces the strongest polarization (largest in the axon and smallest in the soma).

Continued on next page

First Author	Year	Model	Pain model	Freq. (Hz)	PW (μs)	Intensity	Level	Core mechanistic finding
Royds[101]	2020	Human	Chronic Neuropathic Pain	40 + 5 pulses 500	1000	0,55-0,6mA	Molecular	Burst SCS alters the cerebrospinal fluid proteome, with changes primarily linked to the positive regulation of synapse assembly and the downregulation of specific neuropeptides, indicating a modulation of CNS cellular function and potential supraspinal mechanisms.
Tang[39]	2014	Animal	No	40 + 5 pulses 500	1000	–	Spinal, Supraspinal	Burst SCS is more efficacious in suppressing visceral nociception and noxious somatic response at low intensity (60% MT) than tonic SCS, and uniquely avoids increasing spontaneous activity in gracile nucleus neurons.
Urasaki[36]	2022	Human	PSPS, Parkinson's	40 + 5 pulses 500	1000	–	Supraspinal	Tonic SCS induced dose-dependent somatosensory evoked potential (SEP) reduction, but burst and high-dose SCSs did not, indicating that the latter modalities utilize different, non-dorsal column sites of action.
Vanneste[69]	2023	Human	PSPS	40 + 5 pulses 500	1000	–	Supraspinal	BurstDR SCS normalizes the chronic pain imbalance by decreasing pathological theta/gamma activity in the SSC and alfa/beta activity in the dACC, while increasing effective information flow from the inhibitory pgACC to the SSC and dACC.
Witjes[98]	2023	Human	Chronic Pain		–	–	Supraspinal	Burst SCS significantly increases magnetoencephalography sensor signal power below 3 Hz compared with tonic and sham stimulation.
Yearwood[100]	2020	Human	Chronic intractable pain of the trunk and/or limbs	40 + 5 pulses 500	1000	–	Supraspinal	Burst stimulation selectively modulates the dorsal anterior cingulate cortex (dACC), exhibiting a significant increase in metabolic rate in this medial pain pathway structure compared to tonic stimulation.

Table 5: SNI = Spinal Cord Injury, SNL = Spinal Nerve Ligation, SNI = Sciatic Nerve Injury, CCI = Chronic Constriction Injury, PSPS = Persistant Spinal Pain Syndrome, PDPN = Painful Diabetic Peripheral Neuropathy, CRPS = Complex Regional Pain Syndrome, PHN = Postherpetic Neuralgia, MT = Motorthreshold

E Appendix E. Included studies on High-Frequency SCS

Table 6: Included studies investigating mechanistic effects of high-frequency spinal cord stimulation (HF-SCS).

First Author	Year	Model	Pain model	Freq. (Hz)	PW (μs)	Intensity	Level	Core mechanistic finding
Arle [72]	2016	Computational	Neuropathic Pain	0-10,000	–	–	Spinal	HFS preferentially blocks AP generation in larger diameter fibers (¿9 or 10μm) and concomitantly recruits medium and smaller fibers; The AP blockade is achieved through the interaction of ion channel gate dynamics (specifically the recovery time of the h-gate) and the electrical effects of the AF virtual anode.
Crosby [17]	2017	Animal	SNI	1000, 5000	24	up to 6mA	Spinal	KHF-SCS produces asynchronous and transient onset firing in DC axons, which differs significantly from the periodic activation by conventional 50-Hz SCS, and conduction block is unlikely to contribute to analgesia as it occurs primarily only above motor threshold.
de Geus [49]	2023	Animal	PDPN	1200	50	50% MT	Spinal, Molecular	HF-SCS (1200 Hz) significantly reduced mechanical hypersensitivity after 48 hours and shifted the spinal inflammatory balance towards an anti-inflammatory state (increased IL-10), suggesting a distinct underlying mechanism compared to Conventional SCS.
De Groote [32]	2018	Human	PSPS	1000	75	–	Supraspinal	Suprathreshold 1 kHz stimulation resulted in the highest overall charge delivered and produced extensive activation of frontal, limbic, and sensory cortices, whereas subthreshold 1 kHz stimulation specifically deactivated pain-related regions like the precuneus and PCG.
Kent [63]	2020	Animal	Cervical Radiculopathy	1200	200	90% MT	Spinal	HF SCS modes (10 kHz and 1.2 kHz) and burst SCS modes exhibited different motor thresholds and effects on spinal neuronal firing rates in response to noxious pinch, suggesting they operate via different mechanisms.
Kriek [55]	2018	Human	CRPS	1200	–	–	Molecular	Although high frequencies (500 Hz, 1200 Hz) were investigated in the crossover period and chosen by some patients as their preferred setting, the limited sample size prevented the drawing of conclusions regarding whether different frequencies could have differential immunomodulatory effects.
Kuo [20]	2023	Animal	SNI	1200	130	40%, 80% MT	Spinal	HF-SCS (1.2 kHz and 10 kHz) generated comparable overall effects to 50 Hz SCS at 40% MT, suggesting a local mechanism in the SDH where unit responses depend on the cell type and integrated stimulation dose (intensity/duration), rather than frequency alone.

Continued on next page

First Author	Year	Model	Pain model	Freq. (Hz)	PW (μs)	Intensity	Level	Core mechanistic finding
Ladner [28]	2025	Animal	No	1000	40	–	Spinal	SCS at increasing frequencies (200, 500, and 1000 Hz) altered DC axon responses, reducing ECAP amplitude and increasing latencies/width. This suggests that DC axon activation depends on the recovery stage of the electrically stimulated fibers, potentially through mechanisms like desynchronization or demyelination.
Lee [74]	2020	Animal	Neuropathic pain	1000, 5000	30	10%, 30%, 60%, 80% MT	Spinal	1 kHz or 5 kHz SCS do not selectively activates inhibitory interneurons in the spinal DH.
Lee [75]	2025	Animal	SCI	1000	200	40%, 80% MT	Molecular	HF with 80% MT intensity effectively alleviates neuropathic pain and spasticity by reducing spinal microglial activation in the dorsal horn.
Lim [64]	2025	Animal	No	8333	30	–	Spinal	High kHz SCS (8333 Hz) produced strong hemodynamic responses (hyperemia) in the dorsal spinal cord, but its area of coverage and depth (0.7 mm at 130% eCAPT) were significantly less than those observed for Multiphase therapy.
Rogers [30]	2023	Computational	No	1000	200	–	Spinal	SCS-induced modulation of dorsal horn neurons (including 10 kHz) is likely presynaptic in nature, as axons were preferentially polarized, and 10 kHz SCS did not activate C-fibers or modulate C-fiber spike timing.
Shechter [18]	2013	Animal	SNL	1000	24	20%, 40%, 80% MT	Spinal	High-intensity kilohertz-level SCS (1-kHz and 10-kHz) provided earlier inhibition of mechanical hypersensitivity than conventional 50-Hz SCS, potentially involving different peripheral (A-fiber conduction change) and spinal segmental mechanisms (failed inhibition of WDR windup).
Smith [46]	2021	Animal	SNI	1200	50	70% MT	Molecular	High Rate Programming (HRP, 1,200 Hz) modulates microglial activation transcriptomes by reversing gene expression changes induced by neuropathic pain toward naïve levels, although it is less effective than DTMP.
Wang [73]	2024	Animal	No	1000, 3000, 5000, 8000	30	6 mA	Spinal	Increasing kilohertz frequency (1 to 10 kHz) resulted in a monotonic escalation of dorsal horn neuron activation, with 10 kHz and 8 kHz eliciting the strongest responses, particularly in deeper neurons.
Yang [102]	2023	Animal	SNI		–	–	Supraspinal	Novel pUHF-SCS produces long-lasting inhibitions of mechanical and cold allodynia in a duration-dependent manner and attenuated the C-component of local field potentials in the primary somatosensory and anterior cingulate cortices.

Continued on next page

First Author	Year	Model	Pain model	Freq. (Hz)	PW (μs)	Intensity	Level	Core mechanistic finding

Table 6: SNI = Spinal Cord Injury, SNL = Spinal Nerve Ligation, SNI = Sciatic Nerve Injury, CCI = Chronic Constriction Injury, PSPS = Persistant Spinal Pain Syndrome, PDPN = Painful Diabetic Peripheral Neuropathy, CRPS = Complex Regional Pain Syndrome, PHN = Postherpetic Neuralgia, MT = Motorthreshold

F Appendix F. Included studies on 10-kHz SCS

Table 7: Included studies investigating mechanistic effects of 10-kHz SCS.

First Author	Year	Model	Pain model	Freq. (Hz)	PW (μs)	Intensity	Level	Core mechanistic finding
Amirdelfan[103]	2025	Human	PSPS	10.000Hz	30 æs	2.4 mA	Spinal	Therapeutic 10-kHz SCS utilizes stimulation amplitudes far below the PPT, indicating non-activation of dorsal column axons, and the PPT decreases as kilohertz frequency increases.
Arle [72]	2016	Computational	Neuropathic Pain	10.000Hz	–	–	Spinal	10kHz preferentially blocks AP generation in larger diameter fibers (¿9 or 10μm) and concomitantly recruits medium and smaller fibers; The AP blockade is achieved through the interaction of ion channel gate dynamics (specifically the recovery time of the h-gate) and the electrical effects of the AF virtual anode.
Buonocore[9]	2016	Human	PSPS	10.000Hz	20	3,5mA	Supraspinal	The 10 kHz SCS modality completely inhibited the SEPs cortical responses, suggesting a probable mechanism acting at the stimulation site independent of action potential generation, similar to paresthesia mediated stimulation. All tested SCS modalities completely inhibited the SEPs cortical responses; Inhibition recovered immediately upon turning stimulation off.
Crosby[17]	2017	Animal	SNI	10.000Hz	24	up to 6mA	Spinal	10kHz SCS produces asynchronous and transient onset firing in DC axons, which differs significantly from the periodic activation by conventional 50-Hz SCS, and conduction block is unlikely to contribute to analgesia as it occurs primarily only above motor threshold.
De Groote 1[78]	2020	Human	PSPS	10.000Hz	30	1,5-2,5mA	Supraspinal	HF-10 SCS influences supraspinal mechanisms over time, causing a bilateral decrease in hippocampal grey matter volume that is positively correlated with back pain intensity, alongside increased functional connectivity between the anterior insula and frontoparietal/central executive networks, where the strength between the left dorsolateral prefrontal cortex and the right anterior insula correlated significantly with improved sleep quality (PSQI MCID).
De Groote 2[77]	2020	Human	PSPS	10.000Hz	30	1,5-2,5mA	Supraspinal	HF-10 SCS modulates supraspinal functional connectivity by significantly strengthening the interaction between the anterior insula (affective Salience Network) and the Central Executive and Frontoparietal Networks, suggesting a mechanism that alters the emotional awareness of pain rather than solely sensory transmission

Continued on next page

First Author	Year	Model	Pain model	Freq. (Hz)	PW (μs)	Intensity	Level	Core mechanistic finding
Kent[63]	2020	Animal	Cervical Radiculopathy	10.000Hz	30	90% MT	Spinal	HF SCS modes (10 kHz and 1.2 kHz) and burst SCS modes exhibited different motor thresholds and effects on spinal neuronal firing rates in response to noxious pinch, suggesting they operate via different mechanisms.
Kogias[82]	2025	Human	PSPS	10.000Hz	30	1-5mA	Molecular	10-kHz HF SCS significantly reduces proinflammatory cytokines and distinct populations of T lymphocytes.
Kuo[20]	2023	Animal	SNI	10.000Hz	24	40%, 80% MT	Spinal	HF-SCS (1.2 kHz and 10 kHz) generated comparable overall effects to 50 Hz SCS at 40% MT, suggesting a local mechanism in the SDH where unit responses depend on the cell type and integrated stimulation dose (intensity/duration), rather than frequency alone.
Lee[65]	2021	Animal	No	10.000Hz	30	30% MT	Spinal	Low-intensity 10 kHz SCS selectively activates inhibitory interneurons in the spinal dorsal horn, suggesting it inhibits pain-sensory processing without activating dorsal column fibers, resulting in paresthesia-free pain relief.
Lee[74]	2020	Animal	Neuropathic pain	10.000Hz	30	10%, 30%, 60%, 90% MT	Spinal	Low-intensity 10 kHz SCS selectively activates inhibitory interneurons in the spinal dorsal horn, which may inhibit pain sensory processing without activating dorsal column fibers, resulting in paresthesia-free pain relief.
Lee[24]	2022	Animal	No	10.000Hz	–	–	Spinal	Simultaneous 10 kHz and 40 Hz spinal cord stimulation increases dorsal horn inhibitory interneuron activity.
Lempka[76]	2015	Computational	Neuropathic pain	10.000Hz	30	0,5-5mA	Spinal	10kHz SCS used at clinical intensities likely does not cause the direct activation or conduction block of dorsal column or dorsal root fibers; therefore, alternative sites such as synaptic terminals, cell bodies, and dendrites should be explored.
Liao 1[80]	2020	Animal	SNI	10.000Hz	30	–	Molecular	10kHz SCS significantly attenuated SNI-induced neuropathic pain by counteracting the activation of spinal and DRG MAPKs (ERK, JNK, p38) and by enhancing spinal glutamate uptake, which resulted in reduced spinal glutamate release and a partial reversal of increased miniature excitatory postsynaptic currents (mEPSCs) in lamina II neurons.
Liao 2[79]	2020	Animal	SNI	10.000Hz	30	–	Molecular	10 kHz SCS mitigates neuropathic pain by enhancing spinal glutamate transporter activity to lower pathologically elevated extracellular glutamate levels, thereby disrupting the mGluR5-mediated positive feedback loop responsible for excessive presynaptic excitatory transmission
Rogers[86]	2022	Computational	No	10.000Hz	–	–	Spinal	Provides insight into unknown mechanisms of action by investigating neural recruitment during 10-kilohertz SCS within a single modeling framework.

Continued on next page

First Author	Year	Model	Pain model	Freq. (Hz)	PW (μs)	Intensity	Level	Core mechanistic finding
Rogers[30]	2023	Computational	No	10.000Hz	30	–	Spinal	SCS-induced modulation of dorsal horn neurons (including 10 kHz) is likely presynaptic in nature, as axons were preferentially polarized, and 10 kHz SCS did not activate C-fibers or modulate C-fiber spike timing.
Shechter[18]	2013	Animal	SNL	10.000Hz	24	20%, 40%, 80% MT	Spinal	High-intensity kilohertz-level SCS (1-kHz and 10-kHz) provided earlier inhibition of mechanical hypersensitivity than conventional 50-Hz SCS, potentially involving different peripheral (A-fiber conduction change) and spinal segmental mechanisms (failed inhibition of WDR windup).
Telkes[38]	2020	Human	PSPS	10.000Hz	30	0,6-2,5mA	Supraspinal	HFS (10 kHz) creates dynamic spectral changes characterized by enhanced relative alpha power and a frequency shift toward alpha rhythms in frontal and somatosensory cortices, serving as an objective neural signature correlating with clinical pain relief (ODI score improvement).
Wang[81]	2022	Animal	SNL	10.000Hz	24	50% MT	Molecular	HF-SCS produces long-lasting analgesic effects on neuropathic pain by restoring lysosomal function and alleviating the impairment of autophagic flux in spinal dorsal horn neurons.
Wang[73]	2024	Animal	No	10.000Hz	30	6mA	Spinal	Increasing kilohertz frequency (1 to 10 kHz) resulted in a monotonic escalation of dorsal horn neuron activation, with 10 kHz and 8 kHz eliciting the strongest responses, particularly in deeper neurons.
Yang[104]	2020	Animal	SNL	10.000Hz	24	90% MT	Spinal	Subthreshold 10,000 Hz SCS did not significantly inhibit spinal nociceptive transmission, as quantified by C-LFP, regardless of electrode placement (T13-L1 or L2-L3).
Yu[50]	2024	Animal	SNI	10.000Hz	20	0,13mA	Molecular	HF10 SCS produces long-lasting pain relief by suppressing neuroinflammation and modulating microglia activity through the repression of the Kaiso-P2X7R pathological axis in the spinal dorsal horn.
Zhai[83]	2022	Animal	SNI	10.000Hz	30	80% MT	Molecular	The analgesic effect of 10 kHz SCS is mediated by all three major opioid receptors (μ, δ, κ)

Table 7: SNI = Spinal Cord Injury, SNL = Spinal Nerve Ligation, SNI = Sciatic Nerve Injury, CCI = Chronic Constriction Injury, PSPS = Persistant Spinal Pain Syndrome, PDPN = Painful Diabetic Peripheral Neuropathy, CRPS = Complex Regional Pain Syndrome, PHN = Postherpetic Neuralgia, MT = Motorthreshold

G Appendix G. Included studies on Differential Target Multiplexed SCS

Table 8: Included studies investigating mechanistic effects of Differential Target Multiplexed SCS.

First Author	Year	Model	Pain model	Freq. (Hz)	PW (μs)	Intensity	Level	Core mechanistic finding
Cedeno[84]	2023	Animal	SNI	50 + 3x 300	150 + 50	40%, 70% MT	Molecular	DTM provided similar reduction of pain-like behavior and similar effects on cell-specific transcriptomes when applied at either 40% MT or 70% MT.
Cede¤o[85]	2025	Animal	SNI	50 + 3x 300	150 + 50	50% MT	Spinal	Continuous DTM does not appear to alter the electrophysiology of the dorsal column Aβ fibers (from which ECAPs originate) based on stable ECAPT:vMT ratios post-stimulation.
de Geus[49]	2023	Animal	PDPN	50 + 1200	150 + 50	50% MT	Spinal, Molecular	DTM significantly decreased mechanical hypersensitivity and shifted the inflammatory balance towards an anti-inflammatory state in PDPN animals.
de Geus 1[42]	2024	Animal	PDPN	50 + 1200	150 + 50	50% MT	Spinal, Molecular	DTM provides pain relief and decreases the spinal dorsal horn lipid expression in PDPN animals, although the behavioral effect (reduction of mechanical hypersensitivity) was not significantly different from Con-SCS.
Smith[46]	2021	Animal	SNI	50 + 1200	150 + 50	70% MT	Molecular	DTM is more effective than HRP and LRP at modulating microglial transcriptomes, recovering resting, post-injury, and neuroprotective/repopulating transcriptomes toward nave levels.
Tilley[47]	2023	Animal	SNI	50 + 1200	150 + 50	70% MT	Molecular	Of the 186 proteins identified as extracellular-matrix-related, DTM reversed expression levels of 83% of them back to levels seen in uninjured animals, whereas LR-SCS reversed 67%. Protein phosphorylation is indicative of activation/deactivation of signaling pathways. Phosphorylation can occur at multiple locations on a protein and multiple times as well. There were 883 unique phosphorylated states found among 93 ECM-related proteins. Relative to the pain model, DTM had a reversal effect on 76% versus 58% by LR-SCS on phosphorylated proteins.
Tilley[40]	2022	Animal	SNI	50 + 1200	150 + 50	70% MT	Spinal, Molecular	DTM modulates the Extracellular Matrix (ECM) by reversing most injury-induced protein expression and phosphorylation changes to a greater degree than LR-SCS.
Vallejo 2[45]	2020	Animal	SNI	50 + 1200	150 + 50	70% MT	Molecular	DTM significantly modulated 11 out of 23 affected gene modules (48%) back toward the expression pattern of nave animals, providing a more effective way of modulating gene expression associated with neuroglial interactions.

Continued on next page

First Author	Year	Model	Pain model	Freq. (Hz)	PW (μs)	Intensity	Level	Core mechanistic finding

Table 8: SNI = Spinal Cord Injury, SNL = Spinal Nerve Ligation, SNI = Sciatic Nerve Injury, CCI = Chronic Constriction Injury, PSPS = Persistant Spinal Pain Syndrome, PDPN = Painful Diabetic Peripheral Neuropathy, CRPS = Complex Regional Pain Syndrome, PHN = Postherpetic Neuralgia, MT = Motorthreshold